

Control of Frequency in Future Power Systems



ZEYAD ASSI OBAID AL-OBAIDI

School of Engineering

Cardiff University

A thesis submitted for the degree of

Doctor of Philosophy

April 2018

ABSTRACT

Future power systems will face a significant challenge due to the reduced stability of frequency. The reduction of inertia drives this challenge due to the increasing level of power electronics connected to renewable energy sources. In this thesis, new control techniques, such as a new secondary frequency control, a control of a population of water heaters (WHs), and a control of a population of battery energy storage systems (BESSs), are studied.

A fuzzy logic-based secondary frequency controller was developed to supplement the conventional frequency control in large synchronous generators. This controller is suitable for the provision of mandatory frequency response in the Great Britain (GB) power system, where an additional 10% power output for primary response and 10% for secondary response are required within ten seconds and thirty seconds respectively. The controller was demonstrated using a simplified GB power system and a multi-machine benchmark power system. The results showed that, following a disturbance, the controller improved frequency deviation and error compared to the conventional PI controller. Thus, the controller provides a stable frequency control in future power systems.

A hierarchical control of a population of WHs and BESSs was used to provide frequency response services. This was based on two decision layers. The aggregator layer receives the states of WHs/BESSs and sends a command signal to each WH/BESS control layer. The hierarchical control enables the aggregator to choose the number of controllable WHs/BESSs and set the desired amount of responses to offer different frequency response services. As a result, it reduces the uncertainty associated with the response of the population during a frequency event. The WH/BESS controller provides a response based on the last command signal from the aggregator, the value of frequency deviation (ΔF) and the level of the water temperature or BESS state of charge (SoC). The WH/BESS controller provides a response even when a failure occurs in the communication with the aggregator control layer.

The WH/BESS controller handles both negative and positive ΔF . Hence, the aggregated loads participate in both low and high frequency responses. The response of the population of BESSs goes from the highest to lowest SoC when the frequency falls and from the lowest to highest SoC when it rises. The response from WHs is from highest to lowest water temperature when the frequency drops. Thus, this reduces the risk of a

simultaneous power change in a large number of controllable loads at the same time, which, in turn, reduces the impact.

The dynamic behaviour of a population of WHs/BESSs was modelled based on the Markov chain to allow the aggregator to offer different frequency response services. A Markov-based model was also used to evaluate the effective capacity of aggregated WHs/BESSs during the frequency event. The Markov-based model was demonstrated on a simplified GB power system and the South-East Australian power system, considering different aggregation case studies.

DEDICATION

To the soul of my Father

Who took my hand and guided me to the right way

To my blessed Mother

The priceless woman who is lighting my life

To my Beloved Wife and Children

The beauty, happiness, and shiny part of my life

To my Brothers, Sisters, and family

The great and blessed persons who accompanying my success

To my beloved Country ..'Iraq'

To all others who love me

ACKNOWLEDGEMENTS

I am deeply thankful to God for the amazing graces, then to the following people, without whom this endeavour would not have been possible.

I am eternally grateful for the financial support from the Higher Committee for Education Development in Iraq (HCED Iraq) through all my years of PhD study.

I would like to express my immense gratitude to my supervisors, Dr Liana Cipcigan and Professor Nick Jenkins, for providing me with the opportunity to carry out this highly interesting and relevant research, as well as for their continued supervision and support. Their vision and understanding of the key research challenges in this area have been invaluable for guiding my work.

A great thank my colleague Dr Saif S. Sami for the help he provided and the time he spent discussing and purifying my work.

My thanks also go out to all my colleagues in the Centre for Integrated Renewable Energy Generation and Supply (CIREGS) for their support, encouragement and fruitful discussions during meetings and seminars, especially Mr Mazin T. Muhssin.

My thanks to Mr Ben Marshall, a Technical Specialist, System Performance at National Grid for his feedback and multiple discussions regarding my work.

TABLE OF CONTENTS

	Page
ABSTRACT	i
DECLARATION	iii
DEDICATION	iii
ACKNOWLEDGEMENTS	v
TABLE OF CONTENTS	vi
LIST OF FIGURES	x
LIST OF TABLES	xiv
LIST OF ABBREVIATIONS	xvi
CHAPTER 1	1
INTRODUCTION	1
1.1 Background	1
1.2 Control of frequency in the GB power system	4
1.3 Scope of work and thesis layout	7
1.4 Research objectives	7
1.5 Contributions	9
1.5.1 Chapter 3: The development of new secondary frequency control	9
1.5.2 Chapters 4 and 5: Control of a population of WHs and BESSs for frequency response	9
1.6 Applications	10
1.6.1 The development of new secondary frequency control	10
1.6.2 Control of a population of WHs and BESSs for frequency response	11
1.7 Publications	11
1.7.1 Author publications	11
1.7.2 Author unpublished work	12
1.7.3 Collaborative published work	12
CHAPTER 2	14
Literature Review	14
2.1 Inertia in the GB power system	14

2.1.1 Source of inertia in the GB power system	14
2.1.2 The challenges of an inertia reduction	15
2.2 Demand side frequency response	18
2.2.1 Demand-side integration	18
2.2.2 Control methods of loads for frequency response	19
2.2.3 Thermostatically based controllable loads	21
2.2.4 Water Heaters	22
2.2.5 Electric vehicles	24
2.3 Battery energy storage systems	25
2.4 Control of distributed energy resources	27
2.5 Low-frequency oscillations in power systems	29
2.6 Monitored oscillations in the GB power system	33
2.7 Benchmark power systems for control and stability analysis	35
2.7.1 IEEE 4-machine 2-area power system	36
2.7.2 IEEE 10-machine New England power system	36
2.7.3 IEEE 14-machine South-East Australian power system	37
2.8 Summary of the review	37
2.8.1 Review summary of the large signal stability and control	37
2.8.2 Review summary of the small signal stability and control	39
CHAPTER 3	41
Developing a Secondary Frequency Control for Synchronous Generators	41
3.1 Introduction	41
3.2 Generalised model of the GB power system	41
3.3 Proposed control and optimisation method	42
3.3.1 Structure of fuzzy logic controller	43
3.3.2 Optimisation method	46
3.4 Performance comparison of controllers	48
3.4.1 Using two-inputs fuzzy controller and 49 Rules	48
3.4.2 Using three-inputs fuzzy controller and 49 Rules	49
3.4.3 Using fuzzy inference system with 9 Rules	50
3.4.4 Robustness analysis against parameters uncertainties	51
3.5 Demonstration of the proposed control on a multi-machine power system	56
3.5.1 Integrate the controller in Generator 9 with sudden load rise	56

3.5.2 Integrate the controller in generator 9 with three-phase fault	58
3.5.3 Integrate the controller in generator 10 with sudden load rise	58
3.5.4 Integrate the controller in generator 10 with three-phase fault	59
3.6 Summary	61
CHAPTER 4	62
Control of a Population of Water Heater Devices for Frequency Response	62
4.1 Introduction	62
4.2 Hierarchical control of water heaters	63
4.3 Structure of the proposed device controller	65
4.3.1 Measurements of frequency deviation	66
4.3.2 Measurements of water temperature	67
4.3.3 Structure of logic circuit and logic control output	68
4.4 Modelling of a population of controllable water heaters	70
4.4.1 Modelling the dynamic behaviour of WHs population	71
4.4.2 Modelling the dynamic switching of devices during a frequency event	72
4.5 Demonstration of the proposed control of WHs	76
4.5.1 Simplified GB power system	76
4.5.2 The South-East Australian power system	78
4.6 Summary	82
Chapter 5	83
Control of a Population of BESSs for Frequency Response	83
5.1 Introduction	83
5.2 Hierarchical control of BESSs	83
5.3 Structure of the proposed BESS controller	85
5.3.1 Measurements of SoC level	86
5.3.2 Measurements of frequency deviation	87
5.3.3 Structure of logic gates and logic control output	88
5.4 Modelling of a population of controllable BESSs	91
5.4.1 Modelling the dynamic behaviour of the BESSs population	91
5.4.2 Modelling the dynamic switching of BESSs during a frequency event	93
5.5 Demonstration of the proposed control of BESSs	96
5.5.1 Simplified GB power system	97
5.5.2 The South-Est Australian power system	98

5.6 Summary	102
Chapter 6	103
Conclusions and Future Work	103
6.1 Conclusions	103
6.1.1 The development of a new secondary frequency control	103
6.1.2 Control of a population of water heaters and BESSs for frequency response	103
6.2 Recommendations for future work	105
REFERENCES	107
Appendix	117

LIST OF FIGURES

Figure	Page
Figure 1.1. A progress of UK energy from RESs in 2015 [2].	2
Figure 1.2. Primary and secondary frequency response in the GB power system defined by the MFR [8].	6
Figure 1.3. The timescale of MFR and EFR in the GB power system [8].	7
Figure 1.4. Flowchart of the thesis layout.	8
Figure 2.1. Frequency simulation of 600 MW generation loss in the GB power system showing the impact of inertia reduction [8].	16
Figure 2.2. Dynamic variation of frequencies measured shows different deviation values at different generator terminals in the GB power system [19].	17
Figure 2.3. A typical temperature control of a thermostat-based heating device.	21
Figure 2.4. Types of WHs, (a) HPWH, (b) ERWH [58].	23
Figure 2.5. Element Power's 12.5 MWh battery storage project, which secured one of the most remunerated contracts in last year's EFR tender by National Grid [75].	26
Figure 2.6. The general layout of a microgrid [82].	28
Figure 2.7. An example of basic elements in a VPP [86].	29
Figure 2.8. Block diagram of the control of excitation system [94].	30
Figure 2.9. Generator rotor speed oscillations after the disturbance in GB power system with different generation units. The graph displays various generators across England and Scotland, further details in [110].	34
Figure 2.10. Power flow oscillation over the simulated AC line between generators Harker and Hutton in England followed a disturbance [110].	34
Figure 2.11. IEEE 4- machine 2-area test system [126].	36
Figure 3.1. A simplified model of GB power system with primary and secondary frequency loops.	42
Figure 3.2. The structure of the proposed supplementary control.	43
Figure 3.3. Structure of a typical two-inputs fuzzy logic controller showing the inputs scaling gain and the FIS.	44
Figure 3.4. Parallel structure of a three inputs PIDFLC.	44
Figure 3.5. The version I of FIS, (a) inputs MSF, (b) output MSF.	45

Figure 3.6. Input/outputs MSF of version II FIS.	45
Figure 3.7. Simulation results of the frequency deviation in the GB power system using two-inputs PDFLC and 49 rules.....	49
Figure 3.8. The frequency deviation using three-inputs PIDFLC and 49 rules.	50
Figure 3.9. Simulation results of the frequency deviation in the GB power system using fuzzy controllers with 9 rules.....	51
Figure 3.10. The frequency response of GB power system with parameters uncertainty comparison of case 1 and 2 without secondary frequency control.	53
Figure 3.11. Comparison of controllers using case 1 parameters uncertainties and 49 fuzzy rules.	53
Figure 3.12. Comparison of controllers using case 2 parameters uncertainties and 49 fuzzy rules.	54
Figure 3.13. A comparison of controllers with case 1 parameters uncertainties and 9 fuzzy rules.	55
Figure 3.14. A comparison of controllers with case 2 parameters uncertainties and 9 fuzzy rules.	55
Figure 3.15. The 39-Bus, 10-machine New England Test System (explained in section 2.7.2 [127, 129])......	57
Figure 3.16. AMV of the frequency responses at generator G9 with and without the proposed controller (a disturbance equal to 200MW).....	57
Figure 3.17. AMV of the frequency responses at generator G9 with and without the proposed controller (three-phase fault).	58
Figure 3.18. AMV of the frequency responses at generator G10 with and without the proposed controller (a disturbance equal to 200 MW).....	59
Figure 3.19. Comparison of power generated from generator G10 following a disturbance at $t = 4s$	60
Figure 3.20. Results for the grid code support tests at the new Severn Power Station (CCGT), near Newport City, Wales, UK, by Siemens AG. The results for the MFR are: (i) Primary response achieved +46 MW (11%) in 10 seconds, (ii) Secondary response achieved +66 MW (15%) in 30 seconds [132].	61
Figure 4.1. Block diagram of the proposed hierarchical control of WHs.	64

Figure 4.2. The desired response of the WHs population, where T_m = Measured temperature and T_u = User defined temperature.	65
Figure 4.3. The block diagram of the proposed WH controller.	66
Figure 4.4. Logic indication groups of the frequency deviation levels.	66
Figure 4.5. The proposed measurements levels for the water temperature.	67
Figure 4.6. The logic circuits and logic control in the proposed WH controller.	69
Figure 4.7. Markov-based state transition diagram of the dynamic load behaviour, (a) A population of ERWHs, (b) A population of HPWHs (adapted from [62]).	71
Figure 4.8. Proposed MSF to represent the dynamic switching conditions in a population of WHs, (a) the switching into ‘ON’ state, (b) the Switching into ‘OFF’ state.	74
Figure 4.9. Flowchart of the modelling process of the control of a population of WHs.	75
Figure 4.10. Simplified GB frequency control model with controllable WHs.	77
Figure 4.11. The frequency response of the simplified GB power system following a disturbance.	77
Figure 4.12. IEEE 14-machine 59-bus, 5-area, the South-East Australian power system [131, 150].	79
Figure 4.13. Frequency response comparison at the power generation unit of busbar 203-area 2.	80
Figure 4.14. Frequency response comparison at the power generation unit of busbar 301-area 3.	80
Figure 4.15. Frequency response comparison at the power generation unit of busbar 404-area 4.	81
Figure 4.16. Frequency response comparison at the power generation unit of busbar 501-area 5.	81
Figure 5.1. The block diagram of the hierarchical control of BESSs.	84
Figure 5.2. The desired response of a population of BESSs during a frequency event.	85
Figure 5.3. The block diagram of the BESS controller.	86
Figure 5.4. Logic bands for measurements of SoC level.	86
Figure 5.5. Six logic frequency bands in the BESS controller.	87
Figure 5.6. Detailed logic Circuits in the proposed BESS controller.	90
Figure 5.7. State diagram representing the dynamic behaviour of the BESSs population according to five levels of SoC (adapted from [78]).	92

Figure 5.8. MSFs for the switching of the BESSs population, (a) switching probabilities into ‘charging’ state, (b) switching probabilities into ‘discharging’ state. 94

Figure 5.9. Flowchart of modelling process of the proposed control of a population of BESSs..... 96

Figure 5.10. Simplified GB power system model for frequency control with controllable BESSs..... 97

Figure 5.11. Frequency deviations of the simplified GB model after the loss of generation. 97

Figure 5.12. Frequency response at power unit (GPS_4) of busbar 404 using different aggregators’ cases in Table 5.4. 100

Figure 5.13. Frequency response at power unit of busbar 404 using a different value of frequency bands in Table 5.6. 101

LIST OF TABLES

Table	Page
Table 1.1. The frequency containment policy of the GB power system [12].	4
Table 2.1. Payments for different frequency response services by National Grid in July 2016 and January 2017 [18].	15
Table 2.2. Frequency response requirements for different values of inertia and generation loss.	16
Table 2.3. The estimated flexible demand in the GB power system during a peak hour of a winter day [33].	20
Table 2.4. Critical review summary of the oscillation modes in power systems.	33
Table 3.1. Fuzzy rule tables of the version I FIS.	46
Table 3.2. Fuzzy rule tables of version II FIS.	46
Table 3.3. The optimal value of the PID controllers' gains	48
Table 3.4. Frequency response performance using two-inputs PDFLC and 49 rules	49
Table 3.5. Frequency response performance using three-inputs PIDFLC and 49 rules	50
Table 3.6. Frequency response performance using fuzzy controllers with 9 rules	51
Table 3.7. Uncertain parameters and the variation range for the simplified GB power system presented in Figure 2.1.	52
Table 3.8. Performances comparison of parameters uncertainties for frequency response using fuzzy controllers with 49 rules	54
Table 3.9. Performances comparison of parameters uncertainties for frequency response using fuzzy controllers with 9 rules	56
Table 3.10. Power generated by generator G10 following a disturbance considering secondary frequency controllers	60
Table 4.1. States conditions of the switching in the device controller (NC= no change) for the negative	70
Table 4.2. The assumption of controllable WHs types for each aggregator.	78
Table 4.3. Study cases for the simulation results.	78

Table 5.1. Truth table of the control output of the charging operation (NC=no change). ... 89

Table 5.2. Truth table of the control output of the discharging operation (NC=no change).
..... 89

Table 5.3. Aggregators and their assumption of BESSs' population..... 98

Table 5.4. Study cases for the South-East Australian power system (similar to the cases of capacities presented in Table 4.3). 99

Table 5.5. Assumptions of initial conditions of the population of BESSs according to the level of SoC..... 99

Table 5.6. Different values of frequency bands parameters..... 99

LIST OF ABBREVIATIONS

UK	United Kingdom
RESs	Renewable Energy Sources
LFOs	Low Frequency Oscillations
GB	Great Britain
WHs	Water Heaters
BESSs	Battery Energy Storage Systems
SoC	State of Charge
LFC	Load Frequency Control
AGC	Automatic Generation Control
V2G	Vehicle to Grid
RoCoF	Rate of Change of Frequency
DSI	Demand Side Integration
TCLs	Thermostatic-controlled loads
CO ₂	Carbon dioxide
ERWH	Electric Resistance Water Heater
HPWH	Heat Pump Water Heater
USA	United States of America
EVs	Electric Vehicles
DERs	Distributed Energy Resources
DG	Distributed Generation
VPP	Virtual Power Plant
AVR	Automatic Voltage Regulator
PSS	Power System Stabiliser
POD	Power Oscillation Damping Controller
rpm	Revolution per minute
AC	Alternating Current
DC	Direct Current
HVDC	High Voltage DC
SVC	Static Var Compensator
DSR	Demand-Side Response
FFR	Firm Frequency Response
EFR	Enhanced Frequency Response

MFR	Mandatory Frequency Response
PV	Photovoltaics
Kv	Kilo volt
MVA	Mega Volt Ampere
MW	Mega Wat
GW	Giga Wat
IEEE	Institute of Electrical and Electronics Engineering
km	Kilo metre
PSO	Particle Swarm Optimisation
PID	Proportional-Integral-Derivative
PI	Proportional-Integral
PD	Proportional- Derivative
FIS	Fuzzy Inference System
MSF	Membership Function
PDFLC	PD Fuzzy Logic Controller
PIDFLC	PID Fuzzy Logic Controller
H	Inertia Constant
D	Damping Factor
Tg	Governor time constant
R	Droop speed constant
p.u	Per unit
AMV	Absolute Mean Value
CCGT	Combined Cycle Gas Turbine
PMUs	Phasor Measurement Units
FACTS	Flexible AC Transmission Systems
TCSC	Thyroster Controlled Static Compensator
NB	Negative Big
NM	Negative Medium
NS	Negative Small
Z	Zero
P	Positive
N	Negative
PS	Positive Small
PM	Positive Medium
PB	Positive Big

CHAPTER 1

INTRODUCTION

1.1 Background

By 2050, in the United Kingdom (UK), it is anticipated that 65% of the total system power generation will be located behind the metre or on the distribution network. A large part of this installed capacity is by an intermittent power generation. Most of this capacity is provided by renewable energy sources (RESs¹), which is 63 GW of solar and 65 GW of wind generation [1]. The National Grid, which is the UK system operator, has proposed four different energy scenarios for the future possibilities of energy sources. The 2017 future scenarios are as follows [1]:

1. **Two Degrees:** In this scenario, policy interventions alongside innovations are effectively implemented to reduce greenhouse gas emissions. A higher level of growth for achieving carbon reduction is guaranteed with a top priority on environmental sustainability.
2. **Slow Progression:** This scenario considers the economic conditions which are limiting the ability of transitions to a low carbon world. It also restricts the choices of low carbon technologies. Hence, the progress toward decarbonisation is slower than the ambitions of society.
3. **Steady State:** In this scenario, electricity supply is dominated by the traditional sources of energy which are implemented with limited innovations in energy uses.

¹ 'Energy is renewable if it is derived from natural processes and replenished more rapidly than expended', such as: (i) wind, solar and hydro energy, (ii) bioenergy (energy from combustion of plant and animal matter), (iii) waste energy, such as landfill gas, (iv) aerothermal, geothermal and hydrothermal energy (heat from the air, ground and water, respectively).

4. **Consumer Power:** This scenario is a wealthy and market-driven world with a high level of growth for a higher level of investment and innovation. Predominantly, new technologies will be adopted with a focus on the consumers' desires to reduce greenhouse gas emissions.

In 2015, the UK announced that it was three-quarters of the way towards its sub-target of producing 30% of electricity supply from RESs. As shown in Figure 1.1, in 2015, as 22.31% of electricity, 5.64% of heat and 4.23% of transport fuel consumption were produced from RESs.

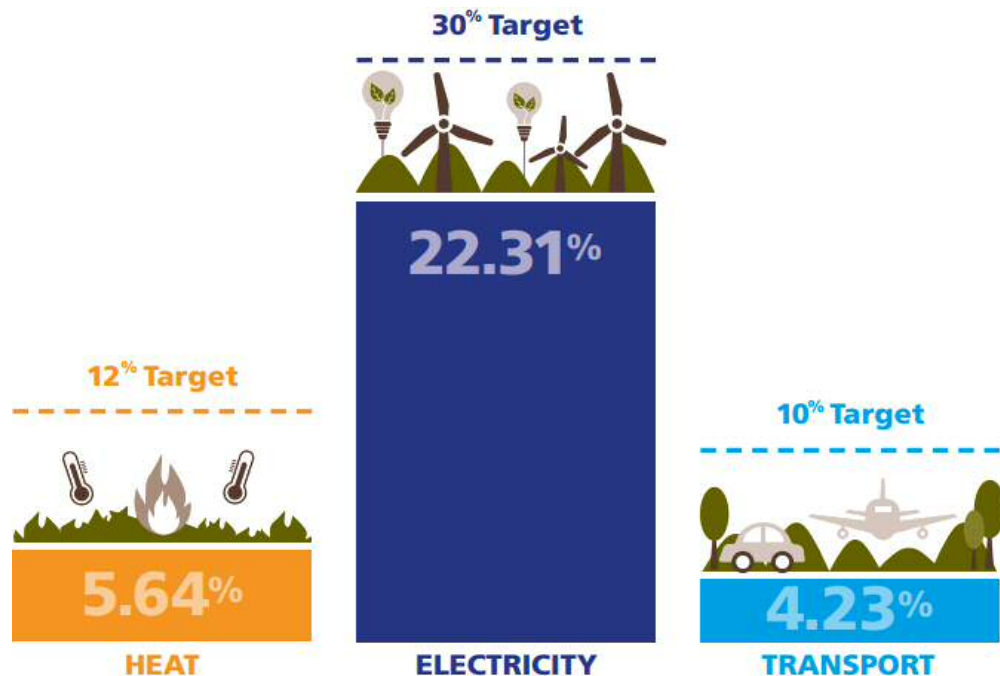


Figure 1.1. A progress of UK energy from RESs in 2015 [2].

At lunchtime on Wednesday 7th June 2017, 50.7% of the UK's electricity was produced from RESs, such as wind, solar, hydro and biomass. Adding nuclear power units, by 2 pm on the same day, 72.1% of electricity in Great Britain (GB) was produced from low carbon sources [3, 4].

There are two main types of renewable energy generators: large-capacity units connected to transmission systems and small-capacity units connected to distribution networks. However, increasing the level of RESs in the generation introduces serious

challenges. For example, there are fluctuations of power output in some RESs, such as wind and solar, due to environmental conditions. Hence, it introduces a challenge for the operation and planning of power system [5]. Another challenge is reducing the total inertia²[6] of the power system due to the power electronics connected to RESs. As a result, the system's ability to maintain the frequency deviation within acceptable limits is decreased. In addition, the rate-of-change-of-frequency is increased when the system is subjected to sudden disturbances, such as loss or increase in the demand or generation [6, 7].

The frequency of a power system is balanced by the active power generated and the load demand. Hence, the system frequency deviation remains within the acceptable limits, i.e. $\pm 1\%$ of the nominal system frequency (50.00 Hz) [6, 7]. In the GB power system, the primary response is the dynamic power generation that reaches its maximum in ten seconds, while the secondary response reaches full operation in thirty seconds. Frequency reserve services are divided into dynamic and non-dynamic; the former responds automatically to any change in the frequency, while the latter is triggered by load frequency relays [6, 7].

Performing primary frequency control using the only generation becomes not only expensive but also technically difficult due to the increasing needs of RESs. The combination of high wind and solar output along with a low demand means that a significant number of interventions by the GB system operator should be taken for balancing and operability reasons [8].

Therefore, there are opportunities to further develop demand-side services during both periods of low and high demand. Demand-side frequency control presents a novel way to mitigate the increasing need for conventional power generators [9-11]. Further details of these concepts will be provided in Chapter 2 of this thesis.

² Inertia comes from rotating masses of large synchronous generators. The inertia response measures how the power system will act to overcome the sudden imbalance between the power generation and the electric demand.

1.2 Control of frequency in the GB power system

Frequency in a power system is a real-time changing variable that indicates the balance between generation and demand. In GB, the National Grid is the system operator that is responsible for maintaining the frequency response of the power system within acceptable limits. Two main levels define these limits: the operational limit, which is equal to ± 0.2 Hz (i.e. 49.8 Hz to 50.2 Hz), and the statutory limit, which is equal to ± 0.5 Hz (i.e. 49.5 Hz and 50.5 Hz). Under a significant drop in the frequency (i.e. below 49.2 Hz), a disconnection by low-frequency relays is provided for frequency control of both the generators and demand. Table 1.1 describes the frequency containment policy in the GB power system [8, 12-15].

Table 1.1. The frequency containment policy of the GB power system [12].

Frequency limits	Case description
± 0.2 Hz	System frequency under normal operating conditions and the maximum frequency deviation for a loss of generation or a connection of demand up to ± 300 MW
± 0.5 Hz	Maximum frequency deviation for a loss of generation bigger than 300 MW and less than or equal to 1,320 MW
-0.8 Hz	Maximum frequency deviation for a loss of generation bigger than 1,320 MW and less than or equal to 1,800 MW. The frequency must be restored to at least 49.5 Hz within 1 minute

Many of the interventions of the GB system operator should be adopted for balancing the frequency. This can be carried out by integrating different balancing services, such as (i) reserve services, (ii) system security services and (iii) frequency response services. These services aim to maintain the frequency within the acceptable limits and restore the frequency after sudden changes in the demand or generation. The services involve both generation and demand. The frequency response services include firm frequency response

(FFR), mandatory frequency response (MFR) and enhanced frequency response (EFR), as indicated below [13]:

- **Firm frequency response**

This provides a dynamic or non-dynamic response to the changes in the frequency. This service is acquired from generators, except for in generators that provide MFR. In addition, it is provided from the demand through a competitive process of tenders. These tenders can be assigned for a low or high-frequency event or both [13].

- **Mandatory frequency response**

This refers to an automatic change in the output of the active power of a generator in response to a pre-set value of frequency deviation. The grid code in the GB power system requires the availability of this service in all large-capacity generators connected to the transmission system. Large generators can be defined as all generators with a capacity equal to or larger than 100 MW in England and Wales and equal to or larger than 10 MW in Scotland. These generators work at under an 80% load and must provide a primary response, a secondary response and a high-frequency response (see Figure 1.2), as stated below [8, 13]:

1. The primary frequency response is an automatic 10% increase in the output of a generator in response to a frequency drop within ten seconds and can be sustained for a further twenty seconds.
2. The secondary frequency response is an automatic 10% increase in the output of a generator in response to a frequency drop within thirty seconds and can be sustained for up to thirty minutes.
3. The high-frequency response is an automatic reduction in the output of a generator in response to a frequency rise within ten seconds and can be sustained indefinitely.

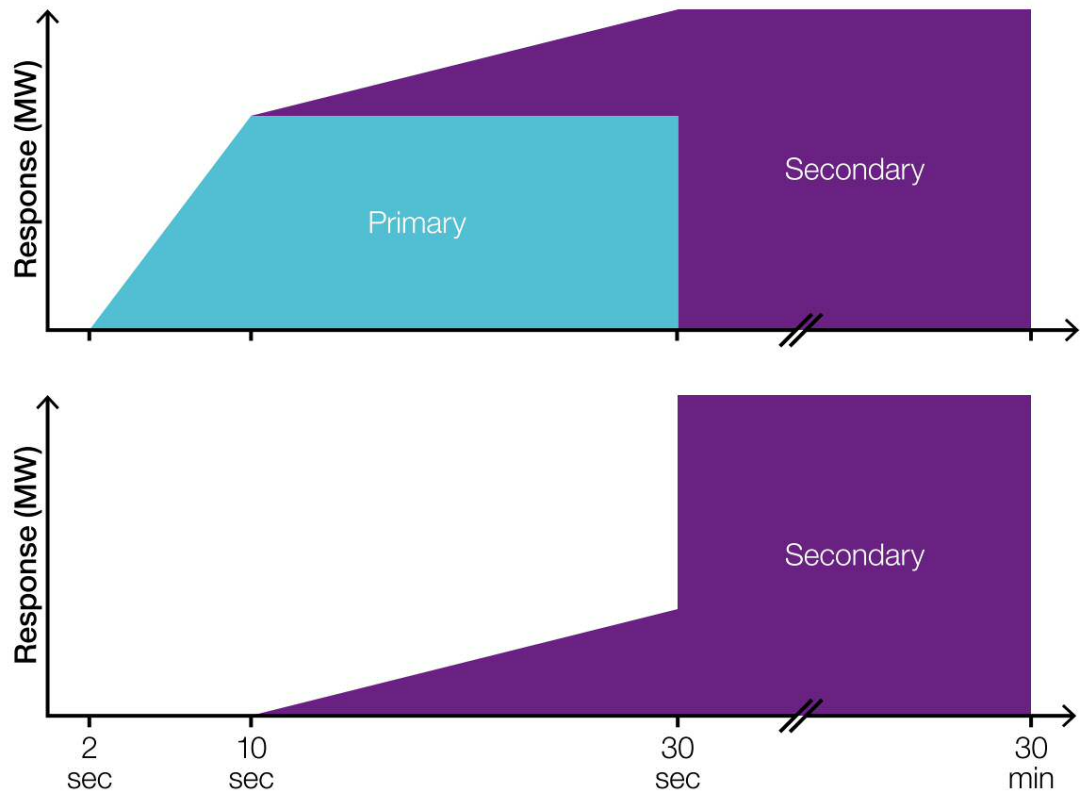


Figure 1.2. Primary and secondary frequency response in the GB power system defined by the MFR [8].

- **Enhanced frequency response**

The provision of 100% of the output of the active power within one second following a pre-set value of a measured frequency deviation and can be sustained for up to fifteen minutes [8]. Recently, the National Grid contracted a total of 201 MW of EFR services from energy storage systems through different providers. Most of these providers are expected to provide their services by the end of 2017. Figure 1.3 shows the timescale for the MFR and EFR services in the GB power system [8].

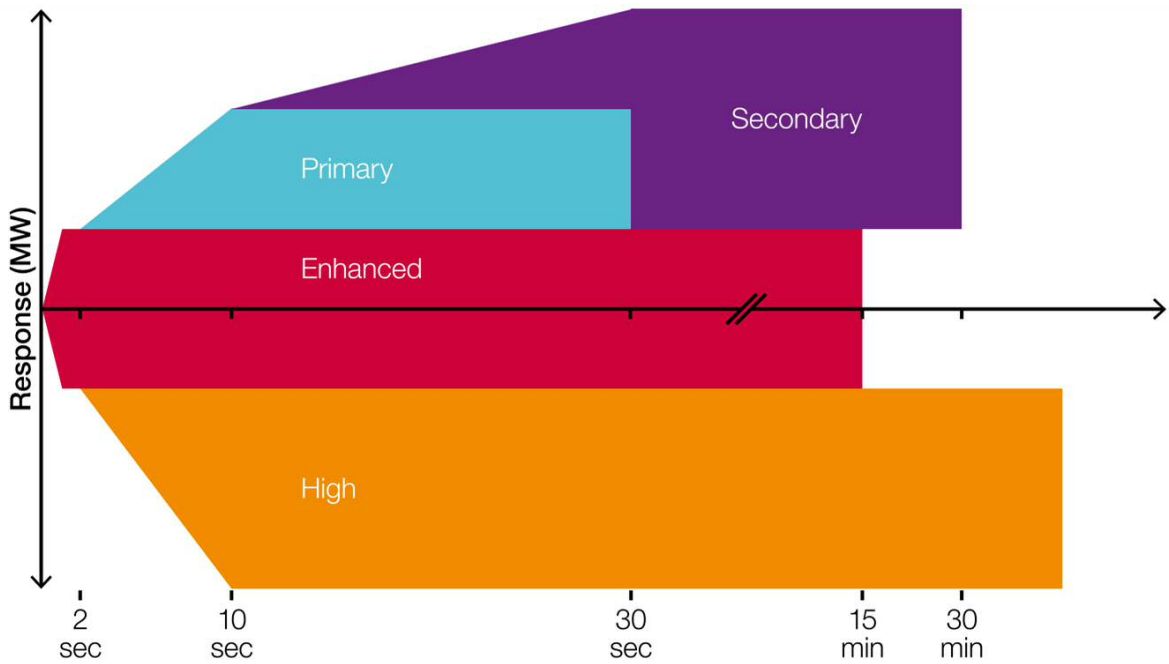


Figure 1.3. The timescale of MFR and EFR in the GB power system [8].

1.3 Scope of work and thesis layout

The flowchart shown in Figure 1.4 provides the layout and the main scope of each chapter in this thesis.

1.4 Research objectives

This work aims to introduce and develop new control techniques to face the challenge of a reduced frequency stability in future power systems due to the large amount of RESs. To achieve this aim, the following points are addressed:

1. To design an optimal fuzzy-based secondary frequency controller for power generators with a structure that can supplement the conventional control rather than replace it.
2. To design and model a hierarchical control of a population of water heaters (WHs) to provide frequency response services.
3. To design and model a hierarchical control of a population of battery energy storage systems (BESSs) to provide frequency response services.
4. To demonstrate the work on the simplified GB power system and a larger multi-machine power system considering different case studies.

Control of Frequency in Future Power Systems

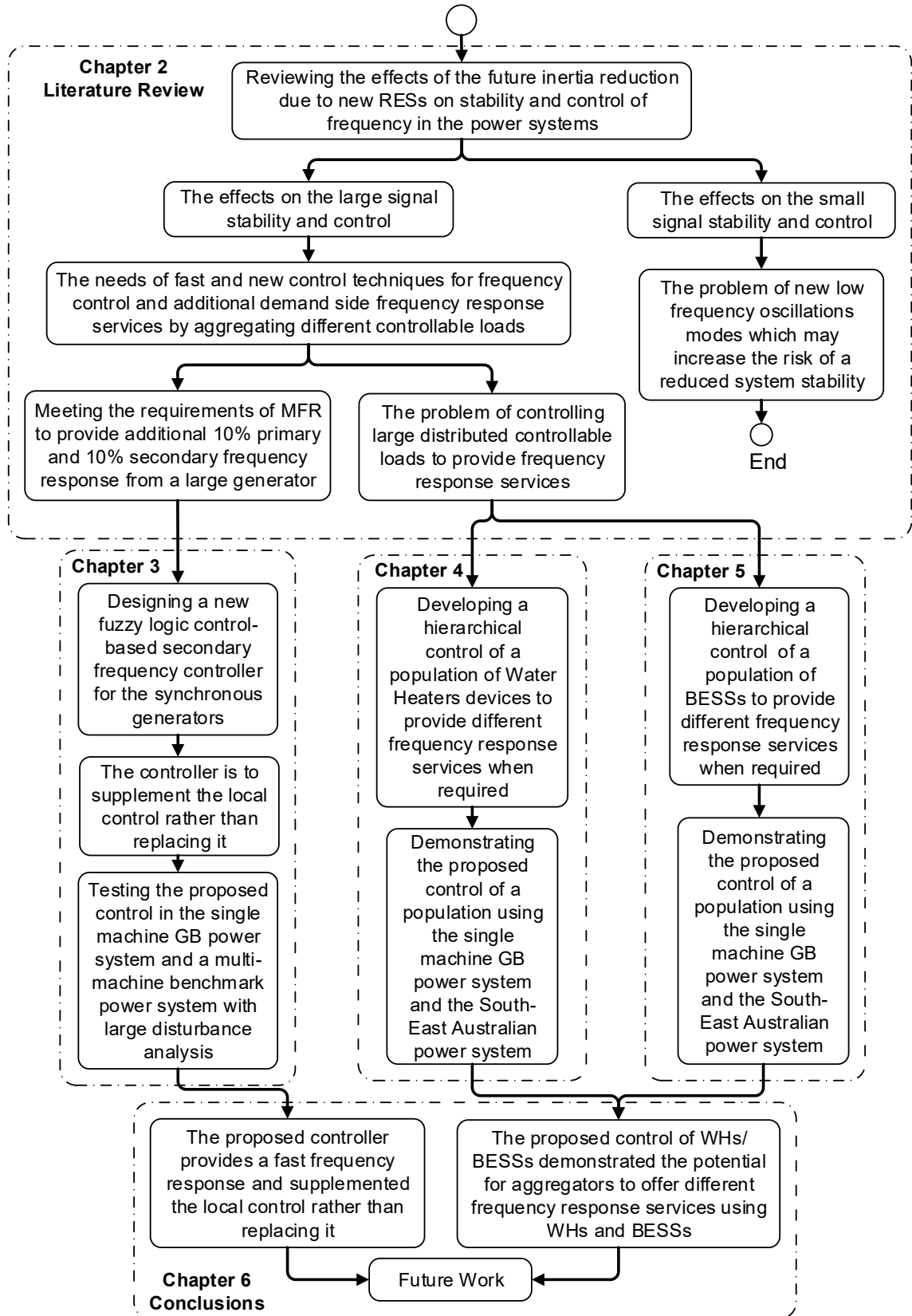


Figure 1.4. Flowchart of the thesis layout.

1.5 Contributions

1.5.1 Chapter 3: The development of new secondary frequency control

The proposed fuzzy-based secondary frequency controller improved the power system frequency response against the frequency collapse and parameters uncertainties than the conventional PI controller. The proposed controller could be used by a system operator to supplement the local frequency control rather than replacing it. In addition, it can be used in a broad range of real-time applications in both centralised and decentralised frequency control methods in future power systems.

1.5.2 Chapters 4 and 5: Control of a population of WHs and BESSs for frequency response

These chapters present a control of a population of WHs/BESSs to provide frequency response services when required. The contributions are:

1. The proposed hierarchical control is based on two decision layers. The aggregator layer receives the states of WHs/BESSs and sends a command signal to each WHs/BESSs control layer. The proposed hierarchical control enables the aggregator to choose the number of controllable WHs/BESSs and set the desired amount of responses to offer different frequency response services. As a result, this reduces the uncertainty associated with the response of the population during a frequency event.
2. The WHs/BESSs controller provides a response based on the last command signal from the aggregator, the value of frequency deviation () and the level of the water temperature or the level of state of charge (SoC) of the BESS. Hence, the WHs/BESSs controller provides a response, even when a failure occurs in the communication with the aggregator. Therefore, the proposed method is not fully decentralised nor fully centralised in controlling large distributed controllable WHs/BESSs
3. The measurements in the BESS controller are based on six levels of and five levels of BESS's SoC. The response from BESSs is from the highest to lowest SoC when the

frequency falls and from the lowest to highest SoC when it rises. Furthermore, the measurements in the WHs' controller is based on four levels of and four levels of water temperature. The response from WHs is from the highest to lowest water temperature when the frequency drops. Thus, it reduces the risk of a simultaneous power change of a large number of controllable loads at the same time, and the impact on the power system and the end users will be reduced. The WHs/BESSs controller handles both negative and positive . Hence, the population participates in both low and high frequency response services.

4. The dynamic behaviour of a population of controllable WHs/BESSs was modelled based on the Markov-chain to demonstrate the potential for an aggregator to offer frequency response services. The dynamic switching behaviour of the population of WHs/BESSs during the frequency event was also modelled. The effective capacity of aggregated WHs/BESSs during the frequency event was evaluated using the Markov-based model by considering different aggregation case studies in a multi-machine power system.

1.6 Applications

This section presents a summary of the interests of the industry of each chapter in the thesis, as follows:

1.6.1 The development of new secondary frequency control

The fuzzy-based secondary frequency control was designed for the frequency controller in large synchronous generators to meet the requirements of Mandatory Frequency Response in the GB power system. Moreover, the proposed design applies to the application of the load frequency control (LFC)/Automatic generation control (AGC) and to supplement conventional frequency control rather than replacing it in future power systems.

1.6.2 Control of a population of WHs and BESSs for frequency response

A model of a population of WHs/BESSs was developed based on the Markov-chain, and it can be used to demonstrate the potential for an aggregator to offer different frequency response services, and to evaluate the effective population capacity during a frequency event.

The proposed hierarchical control is applicable for the aggregation of WHs/BESSs in future power systems. The WHs/BESSs controller was developed to offer the capabilities of different frequency response services. Therefore, aggregators can use it to offer primary, secondary and high-frequency response services or to offer a steady state frequency regulation. The proposed hierarchical control enables aggregators to choose a number of their controllable loads. Therefore, it can be used in such applications as Virtual Power Plants. In addition, the proposed control can be applied for the aggregation of (i) Residential and non-residential WHs, (ii) Residential and non-residential BESSs, and (iii) Vehicle-to-grid (V2G) as storage.

1.7 Publications

1.7.1 Author publications

This section presents the publications related to the work by the author presented in the thesis chapters.

1. **Z. A. Obaid**, L. M. Cipcigan, and M. T. Muhssin, 'Fuzzy Hierarchical Approach-Based Optimal Frequency Control in the Great Britain Power System', Elsevier Electric Power Systems Research, Volume 141, December 2016, Pages 529–537.
2. **Z. A. Obaid**, L. M. Cipcigan, and M. T. Muhssin, 'Power System Oscillations and Control: Classifications and PSSs' Design Methods: A review', Elsevier Renewable & Sustainable Energy Reviews, Vol. 79, P: 839–849, 2017.

3. **Z. A. Obaid**, L. M. Cipcigan, and M. T. Muhssin, 'Frequency Control of Future Power Systems: Reviewing and Evaluating the Challenges and New Control Methods', Accepted in Springer Journal of Modern Power Systems and Clean Energy.
4. **Z. A. Obaid**, L. M. Cipcigan, and M. T. Muhssin, 'Design of a Hybrid Fuzzy/Markov Chain-based Hierarchical Demand-side Frequency Control', the 2017 IEEE Power and Energy Society General Meeting, Chicago, USA, 17-20 July 2017.
5. **Z. A. Obaid**, L. M. Cipcigan, M. T. Muhssin, and S. S. Sami, 'Development of a Water Heater Population Control for the Demand-side Frequency Control', IEEE PES Innovative Smart Grid Technologies, Europe (ISGT Europe), 26-29 September 2017, Turin, Italy.
6. **Z. A. Obaid**, L. M. Cipcigan, and M. T. Muhssin, 'Analysis of the Great Britain's Power System with Electric Vehicles and Storage Systems', IEEE 18th International Conference on Intelligent System Application to Power Systems (ISAP), 11-16 Sept. 2015, Porto, Portugal.

1.7.2 Author unpublished work

The section presents the remaining unpublished work in this thesis which is submitted to peer-review.

7. **Z. A. Obaid**, L. M. Cipcigan, N. Jenkins, S. S. Sami, and M. T. Muhssin, 'Control of a Population of Battery Energy Storage Systems for Frequency Response', Journal paper Progressing.

1.7.3 Collaborative published work

The section presents the published work with other colleagues but not included in the thesis chapters.

8. M. T. Muhssin, L. M. Cipcigan, N. Jenkins, S. Slater, M. Cheng, and **Z. A. Obaid**, 'Dynamic Frequency Response from Controlled Domestic Heat Pumps', IEEE Transactions on Power Systems, Vol. PP, Issue: 99.

9. M. T. Muhssin, L. M. Cipcigan, N. Jenkins, S. S. Sami and **Z. A. Obaid**, 'Potential of Aggregated Load Control for the Stabilization of the Grid Frequency', Journal of Applied Energy, Vol. 220, 15 June 2018, P. 643–656.
10. M. T. Muhssin, L. M. Cipcigan, **Z. A. Obaid**, W. F. AL-Ansari, 'A novel adaptive deadbeat- based control for load frequency control of low inertia system in interconnected zones north and south of Scotland', Elsevier International Journal of Electrical Power & Energy Systems, Vol. 89, 2017, Pages 52-61.
11. M. T. Muhssin, L. M. Cipcigan, N. Jenkins, M. Cheng, and **Z. A. Obaid**, 'Potential of a Population of Domestic Heat Pumps to Provide Balancing Service', Journal Tehnički vjesnik/Technical Gazette, vol. 25, pp. 709-717, 2018.
12. M. T. Muhssin, L. M. Cipcigan, **Z. A. Obaid**, 'Small Microgrid Stability and Performance Analysis in Isolated Island', IEEE conference proceedings, UPEC2015, Staffordshire., UK, 2015.
13. M. T. Muhssin, L. M. Cipcigan, N. Jenkins, M. Cheng, and **Z. A. Obaid**, 'Modelling of a population of Heat Pumps as a Source of load in the Great Britain power system', IEEE International Conference on Smart Systems and Technologies (SST), 2016, pp. 109-113.
14. M. T. Muhssin, L. M. Cipcigan, N. Jenkins, M. Cheng, and **Z. A. Obaid**, 'Load Aggregation over a Time of Day to Provide Frequency Response in the Great Britain Power System', Presented at 9th International Conference on Applied Energy (ICAE), 2017.

CHAPTER 2

Literature Review

2.1 Inertia in the GB power system

2.1.1 Source of inertia in the GB power system

System inertia can be defined by the availability of the energy in the rotating mass of generators that are directly coupled to the power system [6]. System inertia determines the response of a power system to a frequency disturbance, such as a sudden loss of generation or load. In the GB power system, large-capacity synchronous generators provide about 70% of the system inertia. The rest is provided by smaller synchronous generators and synchronous demand [8].

The National Grid is currently instructing conventional generators to run continuously, even if there are no economic profits since they are part-loaded. This creates a minimum level of available inertia to secure a capacity for frequency response [8]. This capacity is expected to be 30-40% more than the current capacity in the next five years [16]. However, these generators are expensive to operate and produce large amounts of greenhouse gas emissions.

For example, the required capacity for the FFR service in the summer is higher than other seasons due to low demand. Hence, fewer synchronous generators are committed to supplying that demand. This capacity varies from 400 MW to 700 MW for the primary response, 1,200 MW to 1,450 MW for the secondary response and 0 MW to 150 MW for the high-frequency response [17]. As a result, the payments for frequency response services vary as well. Table 2.1 shows an example of the payments for July 2016 (summer) and January 2017 (winter) [18].

Table 2.1. Payments for different frequency response services by National Grid in July 2016 and January 2017 [18].

Service type	Payment cost	
	July 2016	January 2017
MFR	£2.4 million	£2.33 million
FFR plus frequency control by demand management	£8.86 million	£7.71 million

2.1.2 The challenges of an inertia reduction

The absence of direct coupling between the machine and the power system in some RESs, e.g. wind generators due to their power electronics, prevent their rotating mass from contributing to system inertia [6]. Therefore, RESs reduce the total system inertia, and hence, lead to reduced power system stability and increase the difficulties of the operation and control of the power system. RESs have power fluctuations due to the change of the wind speed and solar, causing a significant impact on the stability of the frequency deviation.

Figure 2.1 shows the frequency drop and the required frequency response capacity of a simulated GB power system done by National Grid. The simulations were performed for the system with 20 GW of demand during a generation loss of 600 MW and different values of the system inertia [6]. When the system inertia decreases, the frequency response services procured are increased to maintain an acceptable level of security, as shown in Figure 2.1 [6]. Table 2.2 shows some examples of the requirements of the frequency response for different values of inertia and generation loss. In addition, the inertia reduction across the entire power system will not have the same reduction levels; areas with high RESs have a higher frequency deviation than other areas [19, 20] (see Figure 2.2).

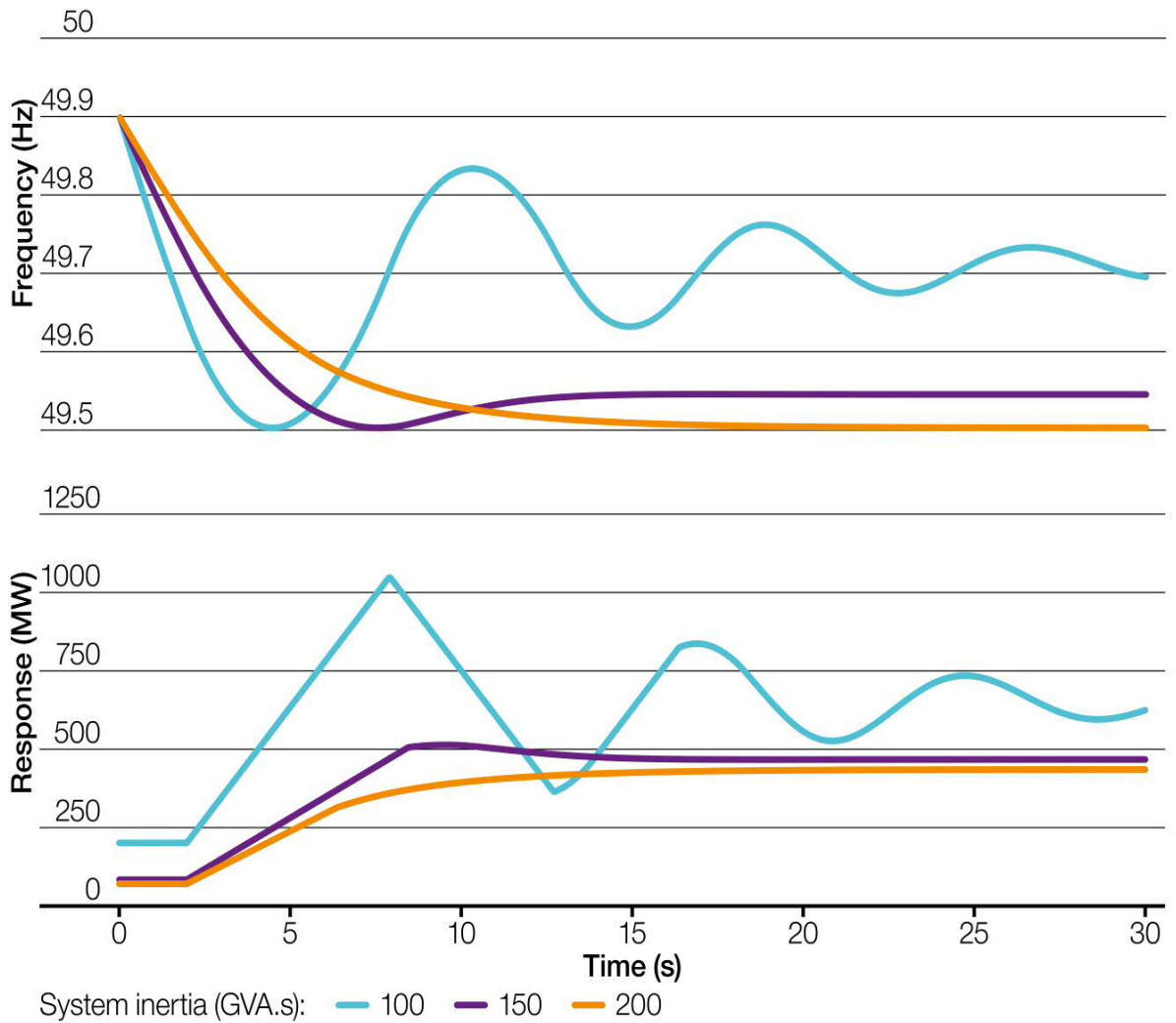


Figure 2.1. Frequency simulation of 600 MW generation loss in the GB power system showing the impact of inertia reduction [8].

Table 2.2. Frequency response requirements for different values of inertia and generation loss.

System inertia (GVA.s)	Generation loss (MW)	
	500	600
	Response requirement (MW)	
100	590	1,285
150	365	575
200	365	365

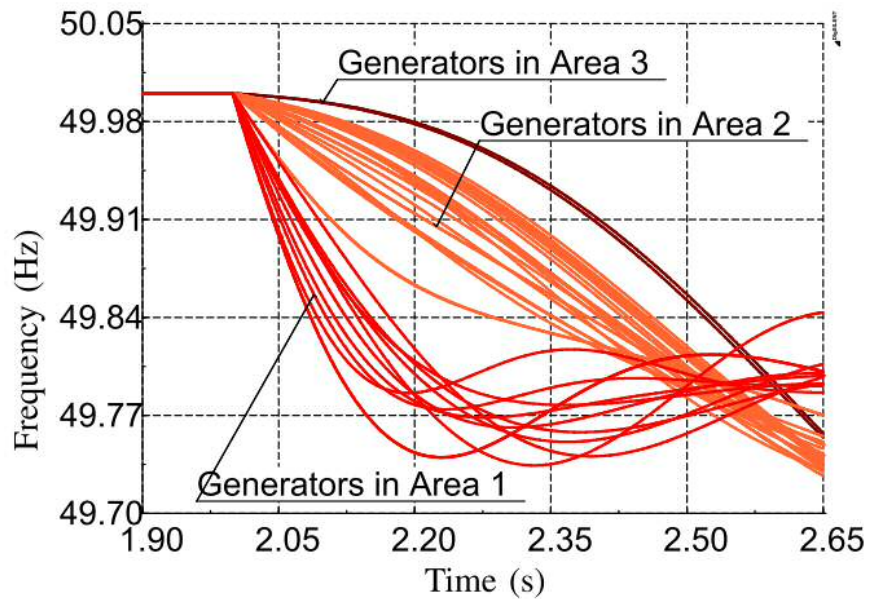


Figure 2.2. Dynamic variation of frequencies measured shows different deviation values at different generator terminals in the GB power system [19].

A reduction in the system inertia will increase the rate of change of frequency (RoCoF) when the system is subjected to sudden disturbances such as loss or increase in the demand or generation. In this situations, it is highly recommended to minimise the settling time during the disturbance period [6, 7]. Therefore, the need for additional frequency control is increased [6, 7]. A fast frequency response from the generation side is one of the recommended solutions to mitigate the increased frequency deviation issue. Also, the RESs alongside with the classical generators have potential to provide frequency control as ancillary service [21, 22].

The control system, which is responsible for controlling the frequency, must provide a fast and stable response [9], [23]. A rapid response to a high RoCoF is strongly recommended; however, a very quick response has a risk of system oscillations [9]. A flexible embedded real-time controller that offers higher flexibility versus low cost is required with the ability of event detection and response algorithm to any disturbance. The designed controller is preferable to have scalable parameters and fast controller latency to create a new adaptive protection system that is capable of standing against frequency collapse in

future energy networks. This scheme is intended to supplement local control, rather than replace it. Existing load shedding and governor-frequency control processes continue to be in place, but new forms of frequency control will reduce the extent to which the conventional response would be called on. This stage will allow the control scheme to be fine-tuned based on real-time measurements [6, 7].

2.2 Demand side frequency response

With the increasing needs of RESs, performing primary frequency control using only the generation side becomes not only expensive but also technically difficult. In addition, the combination of high wind and solar output alongside with a low demand means that a significant number of interventions by the GB system operator should be taken for balancing and operability reasons. Therefore, there are opportunities to further develop demand-side services during both periods of low and high demand [8].

Demand-side frequency response presents a novel way to mitigate the increasing need in the conventional power generators [9-11]. The uses of the emergency power amount from the load side for the frequency reserve services presents a new challenge. The challenge is associated with the control of large distributed loads [24]. Especially, with the electric vehicles, residential BESSs, WHs, and cloth dryers.

2.2.1 Demand-side integration

Demand-Side Integration (DSI) measures how to use the loads and local generations to support system management and to improve power supply. The term DSI refers to the relationship between the power systems, energy supply and end users. This relationship includes demand-side management and demand-side response [27]. The potential of DSI depends on customers, such as the duration and the timing of their demand response, the availability and the timing of the information provided to them, the automation of end-use equipment, metering, pricing/contracts, and the performance of the communications infrastructure [25].

There are two types of programs for the application of DSI: price-based programs and incentive-based programs [26, 27]. In price-based programs, consumers adjust their energy consumption about the changes in electricity market price. In contrast, the latter is provided through curtailment or interruptible contracts where consumers are paid to shift or reduce their energy consumption [26].

In the GB power system, a project estimated that the programs of DSI are more commercially viable for distribution network operators at medium voltage level than lower levels in term of investments [28].

However, it is important to address the challenges associated with the demand side integration, such as changing the natural diversity of loads, which can create more unpredictable and undesirable effects. For example, the amount of recovered energy through the demand side response may be larger than the required load reduction [29].

2.2.2 Control methods of loads for frequency response

A flexible demand in industrial and public buildings, such as water supply companies, steelworks, the wastewater treatment industry, hospitals, factories, food markets and universities, can be controlled to provide frequency response in the GB power system [30-32]. The estimated availability of this flexible demand from commercial and educational buildings is growing, and it was 2.5 GW in 2012 in the GB power system, as shown in Table 2.3 [33]. The loads with a thermal storage showed suitable characteristics to provide a provision of demand-side frequency response than other types of loads [30, 34-36].

Two control methods were used in the literature to control flexible demand units: centralised and decentralised control methods. Centralised control of the demand units relies on the infrastructure of information and communication technology to provide communications between the unit and the centralised control of the aggregator [37]. For example, a centralised frequency controller presented in [38] sends a signal to turn 'ON/OFF' domestic air conditioning units and water heaters after a pre-set value of

frequency rise/dip. The centralised controller reduces the uncertainty in the response of controllable units. However, the establishment of communications in the centralised method presents real challenges, such as cost and latency.

Table 2.3. The estimated flexible demand in the GB power system during a peak hour of a winter day [33].

Sector type	Capacity (GW)
Retail	0.7
Education	0.3
Commercial	0.3
Other non-domestic sectors	1.2
Total capacity	2.5

To overcome these challenges, decentralised frequency controllers were developed. A decentralised controller, presented in [35], regulated the set-points of the temperature of refrigerators according to the variation in frequency deviation and its power consumption was controlled. A dynamic decentralised controller was developed in [34] to change the aggregated power consumption of refrigerators in a linear relationship with a frequency change. The controller aimed to avoid affecting the primary cold supply function of refrigerators. Similar controllers were developed to provide a frequency response from industrial bitumen tanks [30] and melting pots [39].

The required availability of refrigerators to provide frequency response was estimated by work presented in [40]. It was estimated that approximately 1.5 million refrigerators are required to provide 20 MW of response. The total cost of frequency controllers added to each refrigerator was calculated in 2007 at a price of approximately £3 million (£2 of an estimated cost for each controller) [35].

2.2.3 Thermostatically based controllable loads

Recently, the thermostatically-based controllable loads (TCLs) such as refrigerators, air-conditioners, and ceiling heaters have been widely considered in the literature due to the potential short-term modulation of their aggregate power consumption [19, 41-50]. TCLs have an electrical heating/cooling thermostat controlled-based device. It modulates the used power for cooling/heating to maintain the temperature nearly to the desired level (see Figure 2.3). The most common implementation of these loads is that the thermostat takes the advantages of the temperature deadband around the desired level [44].

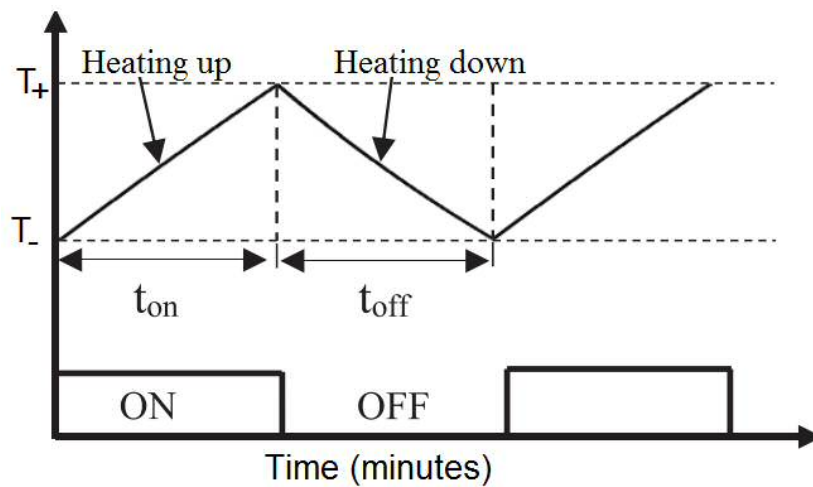


Figure 2.3. A typical temperature control of a thermostat-based heating device.

In GB's power system, the demand-side response was evaluated and considered in the applications of the frequency control [45, 46, 51]. The aggregation of TCLs for the demand side frequency response in the GB power system was investigated in [45, 46]. The demand side response model was used to regulate the dynamic of the TCLs. The model was used to obtain the optimal power consumption and allocated sufficient ancillary services. The model was developed for a multi-stage stochastic unit commitment and integrated into a mixed integer linear programming formulation. It was proposed to deal with the future inertia reduction under future low-carbon scenarios. The study cases were focused on the total system cost and the produced amount of the CO₂ emission [46].

In addition, domestic refrigerators as an example of TCLs demand side frequency response in the GB power system was proposed in [45] to deal with the future inertia reduction. The method presented a non-real-time communication controlled TCLs. The aggregated power of the TCLs was controlled as a linear function of the local frequency change. A technique was developed in [45] for estimating the infeed loss and post-fault in a power system.

Markov chain model was used to represent the aggregated power consumption of the TCLs population for demand side response [9-11, 52]. A hierarchical framework with two layers was presented in [52] for demand side response. The top layer is used to obtain the control gain of the drooping amount. This value was sent to the local layer which involves a population model including different devices. The local layer changed their power consumption of the controllable loads to meet the value of the control gain. The local layer had a Markov chain-based frequency controller to change the power consumption to meet the gain value probabilistically. The TCLs were designed according to three operation states, 'ON', 'OFF', and 'LOCK' [52]. Similarly, the same framework was used in [9, 11] to represent the TCLs but with four operation states, 'ON', 'OFF-Locked', 'OFF', and 'ON-Locked'.

2.2.4 Water Heaters

Electric WHs are ideal home appliances which can be controlled to provide frequency response by turning 'ON/OFF' the device in response to a pre-set value of frequency deviation [53-57]. There are two main types of water heaters: the electric resistance water heater (ERWH) and the heat pump water heater (HPWH), as shown in Figure 2.4. In addition, a hybrid type of water heater has both types incorporated in the same unit [58].

Both types of electric WHs have the same potential of providing different frequency services. The only difference is that HPWH has a compressor so that the response of the device will be different from ERWH regarding the number of responses. For example, when

the compressor becomes 'OFF' during the service, it requires several minutes to be 'ON' again limiting the availability of these devices [56, 57, 59]. In contrast, the ERWH has no compressor so that the device can be switched 'ON/OFF' at any time during the service if the water temperature is still below the user-defined level [53, 60, 61].

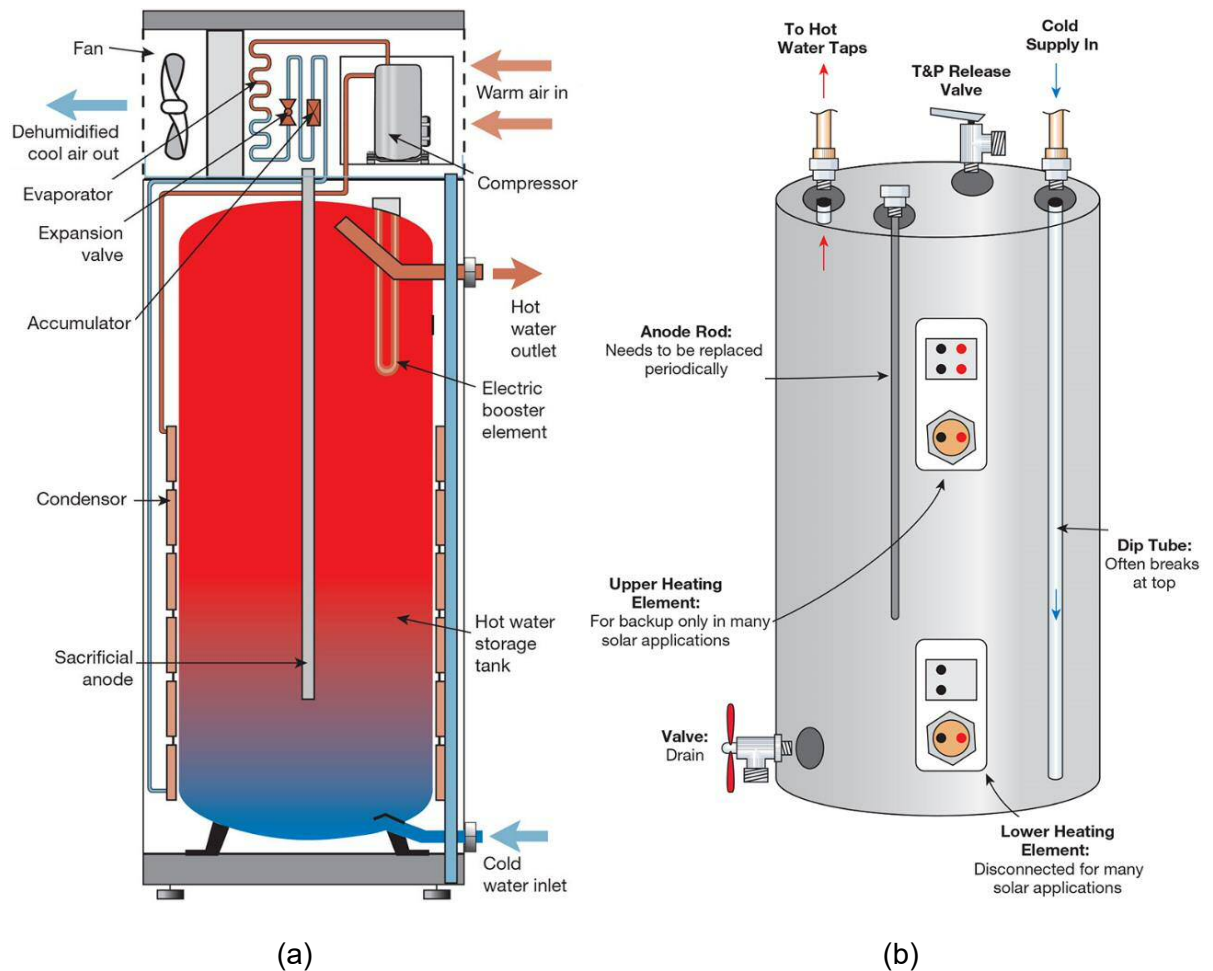


Figure 2.4. Types of WHs, (a) HPWH, (b) ERWH [58].

In general, WHs have advantages [53-57], for example:

1. There is a large population of WHs in the present and future power system. The WH has a power consumption higher than other home appliances, such as dryers, washing machines and refrigerators. For example, in certain areas in the USA, water heaters consume about 30% of the household load, which contributes significantly to the peak load.

2. WHs can be used as energy storage devices by heating up water to a higher temperature than its normal range. Hence, no energy is wasted in providing balancing services, and there is no impact on customers comfort.

The modelling and control of WHs devices are widely covered in the literature to support the frequency in power systems [53, 60, 61]. Markov chain was used to represent the aggregated power for a various controllable population of WHs for demand side frequency control [9-11, 52]. A hierarchical control framework for the demand side frequency control with two decision layers was presented in [62-64]. The top layer is the supervisory control of the aggregator, while the local layer is for the devices population and a frequency controller. The dynamic behaviour of the controllable load was represented by using Markov-based states [62-64]. The ERHW was represented by two states ('ON and OFF') while the HPWH was represented by four states 'ON', 'OFF-Locked', 'OFF', and 'ON-Locked' [62]. Markov chain-based states are representing the dynamic behaviour of the switching in the end-user controllable water heater devices. Hence, it represents the population of those controllable devices. The controller changed the power consumption of controllable loads with an amount according to the gain value sent by the supervisory control layer. The gain value was calculated according to the number of the system loads and the controllable loads (see further details in [62-64]).

2.2.5 Electric vehicles

Recently, an increasingly ambitious target for a high level of electric vehicles (EVs) integration was announced around the world. An internationally high priority target was placed on deploying and developing the technology for EVs [22, 65]. It is assumed that the annual production of EVs would be over 100 million by 2050 [65]. The UK government has declared that EVs are anticipated to play a major role in future transport sectors. The increased interest in EVs leads to a significant impact on power systems [22].

However, the high uptake of EVs introduces a new challenge to the planning and operation of current and future power systems. This challenge relates to the uncontrolled charging of EVs, or so-called 'dumb charging'. This uncontrolled charging may create a new peak load, such as charging when EV owners return home from their last day trip [65].

EVs' load can be controlled to provide frequency response in a power system. However, providing a primary frequency response from EVs in certain cases can introduce a negative impact on power system stability. This impact is due to insufficient load estimation of aggregated EVs [66]. The common approach to provide a demand-side frequency response from EVs is to control the charging/discharging rates of V2G. There are many types of control and management of loads (including EVs), such as reducing users' bills, charging coordination of EVs and charging scheduling [67].

Load control with the integration of EVs and distributed generators was presented in [68] for the power regulation. The load-shifting optimisation problem was solved according to technical and market conditions. This approach is applicable for various distributed energy resources, such as the EVs' smart charging [68].

2.3 Battery energy storage systems

Energy storage systems are among key factors for future power systems [69-71]. BESSs are evaluated and considered in the literature for the frequency regulation [71-73]. Also, the estimated growth of storages in the GB power system by 2050 will be about 10.7 GW based on the 'Consumer Power Scenario' [74]. Also, residential and non-residential BESSs are growing up day by day due to the technical developments and cost reduction as well as high levels of PV integration [73, 74]. A large number of these batteries are connected to distribution networks installed behind the meter [74]. The BESSs present a fast dynamic response to compensate the load variations in distribution networks. In the GB power system, many tenders were taken into consideration by the National Grid to provide

an EFR from BESSs [74, 75]. Figure 2.5 presents one of the most profitable BESSs projects to provide EFR.



Figure 2.5. Element Power’s 12.5 MWh battery storage project, which secured one of the most remunerated contracts in last year’s EFR tender by National Grid [75].

The application of BESSs in direct load control (DLC) is proposed in [76]. The combination of electrical load, the load level in the building, and their controllable devices were considered to investigate the DLC application. The problem of controlling many distributed small-scale BESSs was highlighted as well. The scheme presented in [76] reduced the frequency deviation by controlling SoC of the batteries installed behind the meters [76]. A coordination method of batteries charging was presented in [72] for controlling neighbouring batteries to regulate the frequency and voltage.

Markov-chain was previously used to represent dynamic behaviour of the battery SoC for EVs batteries [77] or PV charging-based batteries [78]. The modelling of the batteries SoC for the power supply availability from PV was presented in [78]. The model was used to improve the availability of photovoltaic generation and to understand the nature

of the charge/discharge rates of the batteries supplied by PV. The dynamic representation of BESS's SoC was designed according to many states transitions, from zero to full charge and vice versa [78]. Various types of batteries and their applications were presented such as behind meter BESSs (home-based) [76], smart charging of EVs (as V2G) [79], and large-scale BESSs (grid-scale BESS) [80]. The aggregation of these types is important in regulating the power system frequency [76, 79, 80].

2.4 Control of distributed energy resources

Distributed energy resources (DERs) include energy storage systems, demand response and distributed generation (DG). Different approaches are presented in the literature to control and coordinate the operation of DERs. Many of these approaches aimed to actively integrate DERs into distribution networks rather than through a conventional passive connection to achieve a more secure and economical operation than with conventional methods.

Breaking the distribution network into smaller areas, such as microgrids, or wider control areas, such as CELLS, is one of the active approaches to manage DERs [25]. Both CELLS and Microgrids are aimed at managing and coordinating the DERs to supply their local demand. Virtual power plant (VPP) is another control approach, which was established to manage DERs. VPP aimed to aggregate different types of DERs to represent a special type of power unit to participate in the energy market [25].

- **Microgrids**

A microgrid is a small area of a distribution network that involves different types of DERs (see Figure 2.6) and can operate in the island or grid-connected mode to supply local energy demand [81]. The control in a microgrid aims to regulate both frequency and voltage. The coordination of DERs within a microgrid presents a novel way to increase the benefits to the overall system performance, such as reducing losses of feeders,

compensating the fluctuation of RESs, improving power quality and supporting local frequency and voltage [25, 81].

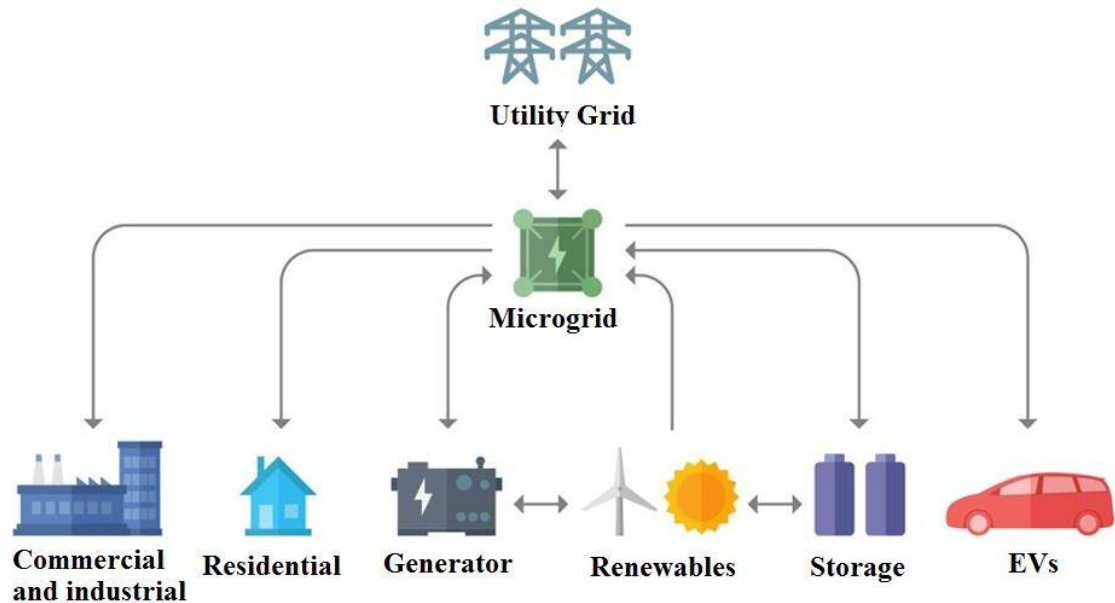


Figure 2.6. The general layout of a microgrid [82].

- **Wider control area (CELLs)**

The 'CELLs' concept was introduced to overcome the challenges when more than 50% of the total generation capacity is from DG. The high penetration of DG introduces a fluctuated impact on the power system, as is the case in the Danish power system [25, 83]. Therefore, a CELL is a wide area in a distribution system with a group of controlled DERs [25].

Like the microgrids, the control in this area covers both frequency and voltage and can work on the island or grid-connected modes. In the normal operation mode, CELL effectively manages its DERs. In the case of a regional emergency, such as a real risk of a blackout, it disconnects itself from the grid and moves to the islanded mode [25, 83].

- **Virtual power plant**

VPP aggregates different types of DERs to make them visible to the system operator as a single controlled unit to participate in the ancillary services [84, 85]. The output of the

aggregated DERs in a VPP is arranged to be as a central generation unit with commercial and technical roles [84]. The commercial role of a VPP is driven by the activity of market participation, such as energy supplier. In contrast, the technical role of a VPP was driven by the activity of the system management and support [85]. Figure 2.7 shows the basic elements in VPP.

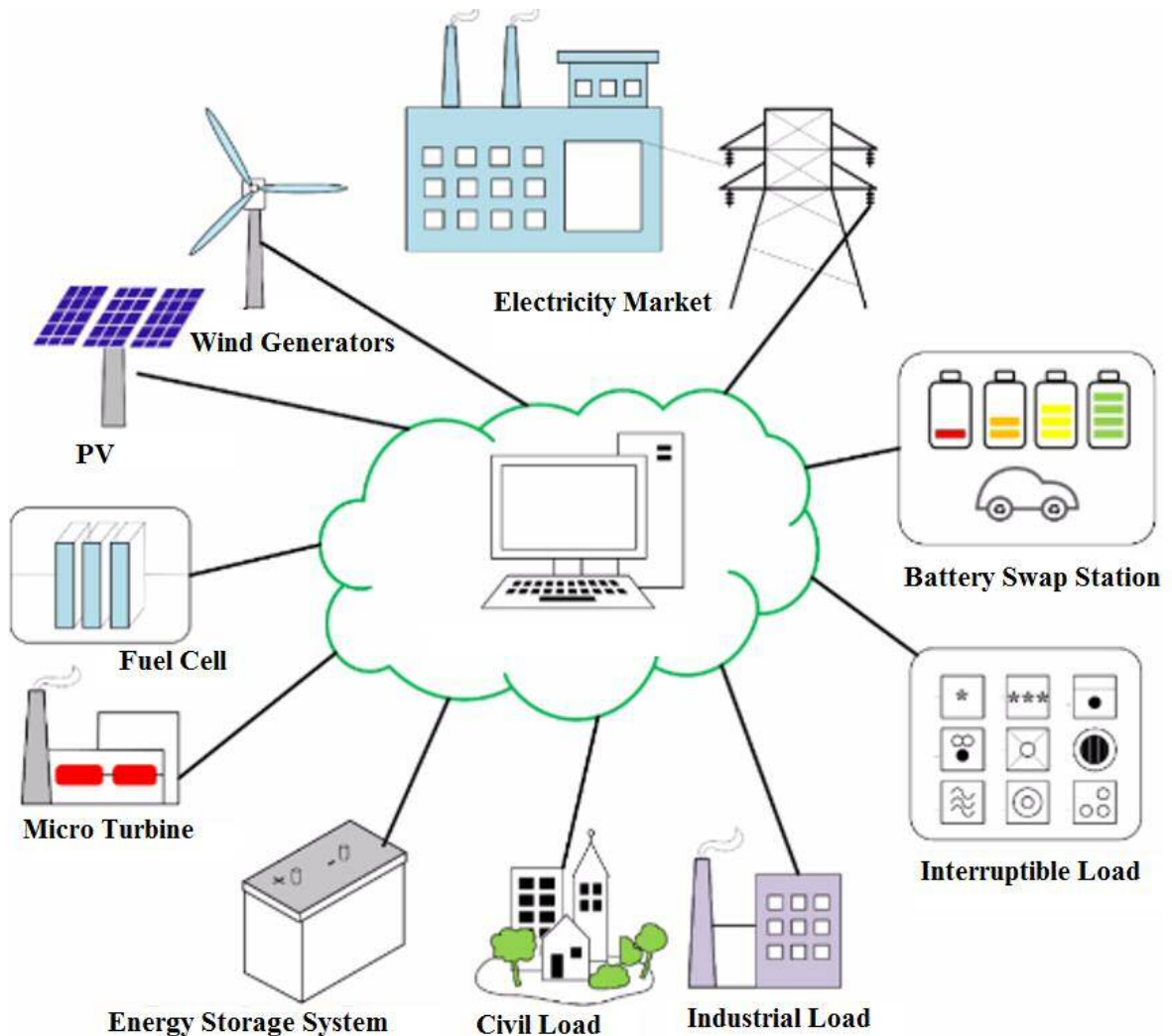


Figure 2.7. An example of basic elements in a VPP [86].

2.5 Low-frequency oscillations in power systems

As explained earlier, frequency response services are used to increase the stability of the frequency in a power system following different disturbances in low inertia system. However, other factors can lead to a reduced system stability such as low-frequency

oscillations. Therefore, due to their importance in multi-machine power systems, transient stability and power system oscillations are considered in the literature [87-93]. The disturbance might have an extreme impact on power system stability regarding large and small signal stability.

The small signal stability is used to describe the oscillation modes related to the control of the excitation system in a synchronous generator. The term 'excitation control system' (see Figure 2.8) is used to distinguish the combined performance of the synchronous machine, power system and excitation system from that of the excitation system alone [94].

The oscillation modes must be damped as much as possible to achieve optimal operating conditions of the excitation system. There is an oscillatory relationship between the synchronous machine and a power system, and between synchronous machines in the power system. This relationship should be carefully considered in the design of an excitation system [94]. Extended research has been conducted on small and large signal stability to study the effect of different types of oscillations [95, 96].

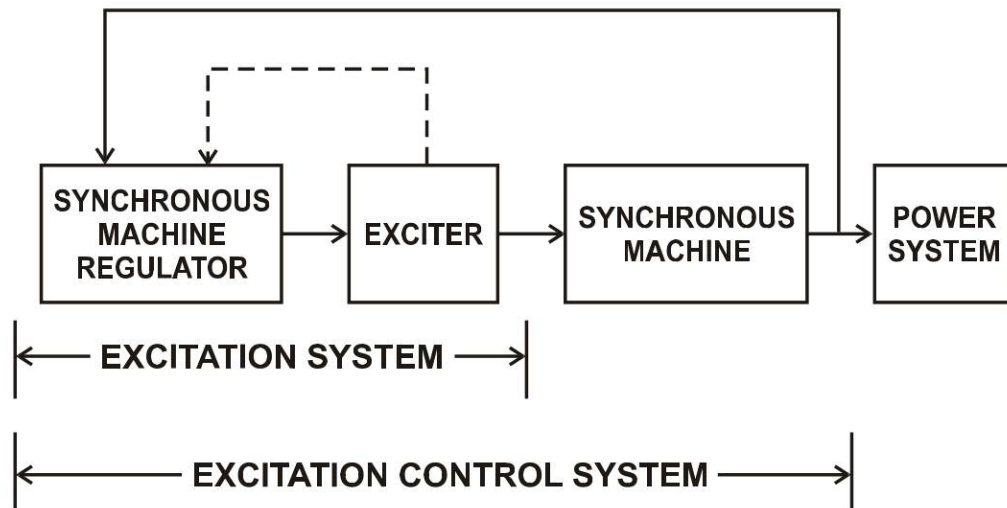


Figure 2.8. Block diagram of the control of excitation system [94].

Various studies have been carried out and focused on the question of to what extent the automatic voltage regulator (AVR) and power system stabiliser (PSS) can play a major

role in the power system's stability [97-107]. Essentially, the AVR and PSS trade off against one other. The high gain fast response of the AVR decreases the stability of low frequency oscillation and increases transient stability, and vice versa. In contrast, the PSS reduces the transient stability by overriding the voltage signal to the exciter and growing the oscillation stability [105].

However, the design of AVR and PSS can be coordinated to provide optimal power stability for both transient and oscillation stability analysis [108]. Moreover, the actions of both devices are dynamically connected [105]. The PSS is a supplementary controller, which provides an additional damping signal to the excitation system in the AVR to damp the low-frequency oscillation [109]. There are four main types of low-frequency oscillation in power systems, as follows:

- **Local machine/unit oscillation mode**

This oscillation type occurs when one or more synchronous generators, in a specific power station, swing together against the whole large power system or load centre. This may become a serious problem in power plants with high load and reactance tie lines. This type of oscillation usually occurs within a frequency ranging from 0.7 Hz to 3.0 Hz [94, 102, 110-115].

- **Inter/Wide-area oscillation mode**

Inter/Wide-Area oscillation has been widely investigated in the literature. Along with the local mode, most authors consider this mode to be the effective power oscillation mode. This mode occurs when a group of generators in one area swing against another group of generators located in another area of a wide-area power system within a range from 0.1 to 0.7 Hz [110]. This impact is related to the generator's location in the network and the PSS connection [94, 110]. Hence, in this mode, it is necessary to apply a reliable control and monitoring system, such as PSSs, to damp this oscillation and guarantee the stability of the wide power system with many generators [94, 110].

- **Inter-unit/plant oscillation mode**

This mode occurs when two or more synchronous generators, in the same power plant or nearby power plant, swing against each other in a frequency ranging between 1.5 to 3 Hz. By adding a PSS, the oscillation might be damped or not depending on the PSS tuning. Therefore, the PSS must be re-tuned to tackle this type of oscillation [94, 116].

- **Torsional oscillations mode**

Torsional oscillation usually occurs in turbo-machines (steam-driven systems). This mode takes place within the rotating elements of the unit, such as synchronous machines, turbine stages, or rotating exciters mounted on the same shaft. The frequency is usually higher than 10 Hz for turbines with 3600 rpm, and about 5 Hz for those with 1800 rpm. It is difficult for the generator's operator to monitor this mode, as it contains frequencies that are higher than the normal PSS frequency range. When dealing with this mode, the excitation system with high gains can lead to shaft damage [94, 102, 117-120]. Therefore, multi-band PSSs, such as PSS2B and PSS4B, are strongly recommended to damp the torsional oscillations [94, 102, 117-120].

Moreover, other elements can affect the damping of torsional oscillations, such as unbalanced faults, HVDC converter control, static VAR converter control, governor control, and transmission series capacitors. These can be named as the control/exciter oscillation mode [94, 116].

Table 2.4 shows the complete summary of various oscillation types. The inter-unit mode has not been mentioned widely because its frequency range is within the local machine mode. Therefore, it was considered by the authors to be within the analysis of the local mode. When two modes occur together (e.g. local mode and inter-area mode), a complex power system oscillation is considered [121].

Table 2.4. Critical review summary of the oscillation modes in power systems.

	Local machine mode	Inter-area mode	Inter-unit mode	Torsional mode
Range of frequency	0.7 to 3 Hz	0.1 to 0.7 Hz	1 to 3 Hz	>10 Hz with 3600 rpm turbine >5 Hz with 1800 rpm turbine
Occurs in	One or more Synchronous Machine	Group of generators in one area	Two or more generators in the same power plant or nearby power plant	Generator-turbine shaft of the unit
Swinging against	The whole power system or load centre	Another group in another area	Each other	Create twisting oscillations in the same unit
Serious effective elements which may increase the mode	1- Generator with high load. 2- High reactance tie lines. 3- A fast-acting or wide bandwidth excitation.	1- Wide area power system. 2- Huge number of the synchronous machine. 3- Generators with PSS and its allocation on the network.	1- Adding a PSS without a good tuning process. 2- A complete eigenvalue analysis must be executed.	1- Turbo system with a long shaft. 2- High gain excitation can lead to shaft damage. 3- Unbalanced faults. 4- HVDC converter control and static converter control. 5- Governor control. 6- Transmission series capacitors.
Application of PSS	1- Classic PSS. 2- Wideband PSS is recommended. 3- Adaptive PSS.	1- Reliable and developed modern control system such as PSS is highly recommended	1- PSS might be used, but the designer should carefully tune its parameters. 2- Adaptive PSS with specific protection limiters can be used.	1- Single input PSS with notch filters. 2- Single input PSS with a wide band exciter. 3- PSS2B is recommended. 4- PSS4B is highly recommended.
References	[94, 102, 110-115]	[94, 110].	[116 ,94]	[94, 102, 117-120]

2.6 Monitored oscillations in the GB power system

A recent study was performed on the GB power's system for monitoring wide inter-area power oscillations [110]. It was found that there are unknown inter-area oscillation

parameters following a significant disturbance. Figure 2.9 shows the response of the generators' rotor speed following a disturbance. The generators in Scotland were swung against generators in England leading to inter-area oscillation modes. Also, local oscillation modes influence the monitored inter-area mode especially in the few seconds following a disturbance. Therefore, that leads to an oscillation in the active power flow over the Harker-Hutton AC line as shown in Figure 2.10 [110].

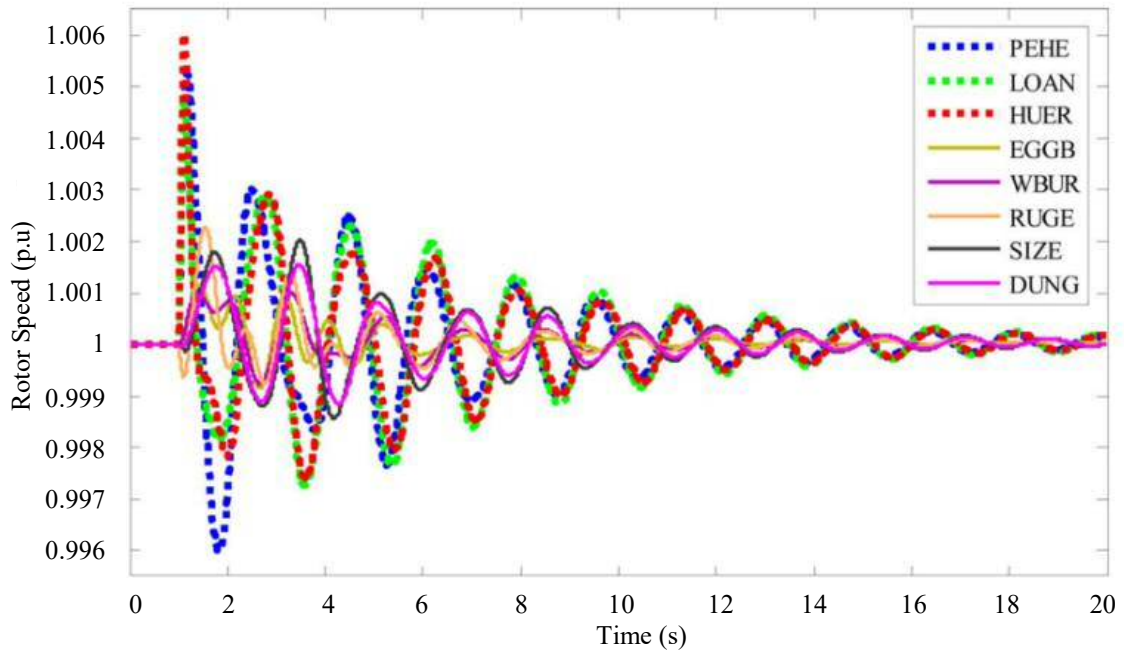


Figure 2.9. Generator rotor speed oscillations after the disturbance in GB power system with different generation units. The graph displays various generators across England and Scotland, further details in [110].

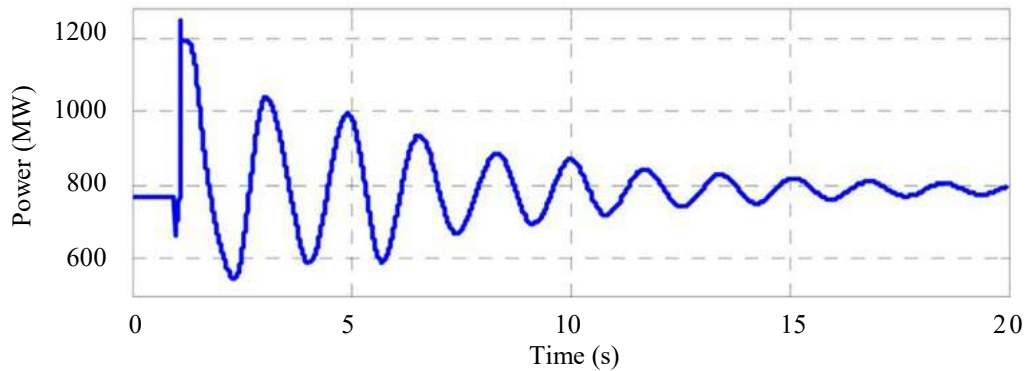


Figure 2.10. Power flow oscillation over the simulated AC line between generators Harker and Hutton in England followed a disturbance [110].

Moreover, the investigation of the oscillation damping control on GB transmission lines was considered in [122]. The classic structure of the PSS and the power oscillation damping controller (POD) were used with HVDC controller and conventional static VAR compensators (SVC). It was demonstrated that for an AC system connected to another DC system, any failure in the AC part will lead to an instantaneous power imbalance in the system and has a negative impact on the transient stability [122].

PSS and POD have a real impact on reducing power oscillations when this situation occurs. It was recommended in [125] to use this method to the real GB power system especially with the integration of the RESs [122, 123]. In [124], it was found that adding a POD to the Western HVDC line of the GB power system could reduce the settling time of the inter-area oscillation from 33s to 12s after a disturbance. The optimal parameters of the POD compensators were obtained using generalised predictive control optimisation method. It was mentioned that a PSS was incorporated in 70% of the machines without further details of the PSS model or the effect of it [124].

However, adding a centralised POD to the wide area GB power system might have drawbacks such as communications delays and the possibility of losing the signal of the remote controller with many machines. Therefore, it is important to design a more decentralised approach on a single machine and perform further analysis for the improvement of the local PSS performances. Although, an old work in the literature presented a little investigation of the frequency oscillation with and without PSS. The study focused on the dynamic instability of the power flow from Scotland to England from a series of tests which were conducted between 1980 and 1985. The results showed that the system damping was improved by adding a PSS on some generators in Scotland [125].

2.7 Benchmark power systems for control and stability analysis

There are many dynamic benchmark models of power systems which were developed for the dynamic stability studies and to evaluate different controller designs [87].

This section presents different benchmark models for multi-machines power systems. These benchmark power systems are: (i) the IEEE 4-machine power system [126], (ii) the IEEE 10-machine New England power system, and (iii) IEEE 14-machine South-East Australian power system. These models were widely used in the analysis of dynamic stability and control of power systems (see [87, 127, 128] for further details). The models were built using MATLAB Simulink and are available for free download at ‘MATLAB File Exchange’.

2.7.1 IEEE 4-machine 2-area power system

The model has 2-area with two generators in each area connected by weak tie-lines. The generators are symmetrical in both areas and have the same rating equal to 900 MVA, 20 kV. The nominal voltage of the tie-lines is 230 kV (see Figure 2.11). The loads are distributed to allow area 2 to import about 413 MW from area 1. The system has a complex power system oscillation. Area 1 and area 2 have local modes equal to 1.12 Hz and 1.16 Hz respectively. The whole system has an inter-area mode at a frequency equal to 0.64 Hz [126].

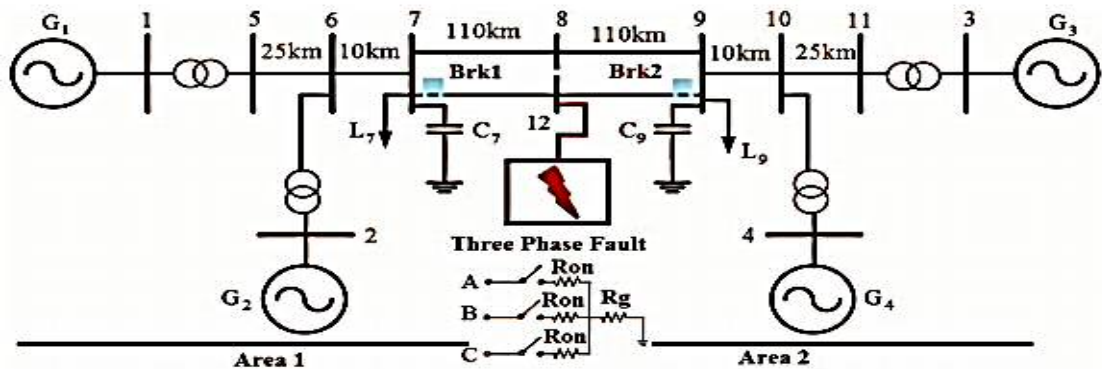


Figure 2.11. IEEE 4- machine 2-area test system [126].

2.7.2 IEEE 10-machine New England power system

This system represents the New England - New York interconnected power system (it will be displayed in chapter 3 in Figure 3.15). The generators from G2 to G10 represent the New England while G1 represents the New York system side (further details in [129]).

2.7.3 IEEE 14-machine South-East Australian power system

This model represents the southern and eastern Australian system (it will be displayed in chapter 4 in Figure 4.12). It extends for some 5000 km from Port Lincoln in South Australia to Cairns in far north Queensland. Four connected regions represented the system [130, 131]. Five SVCs, as well as a series, compensated transmission line, are integrated into this system.

5th or 6th order generator models were used, and two basic types of excitation systems were employed from IEEE Std. 421.5(2005): a static excitation system ST1A and a rotating AC exciter AC1A. The conventional PSS tuning procedure was carried out according to a range of system loading and interconnection power flow conditions. These conditions are represented by six different operating conditions, which are demonstrated in this benchmark model. Therefore, this benchmark system presents a solid basis to test a PSS's tuning and other control techniques [131].

2.8 Summary of the review

Firstly, the impact of future inertia reduction on frequency stability was highlighted. This impact covered the possible challenges related to both large and small signal stability and control. The frequency control in the GB power system, the source of inertia, the challenge of inertia reduction, DSR through different DERs and the challenges of future low-frequency oscillation modes were summarised and highlighted.

2.8.1 Review summary of the large signal stability and control

Large signal stability refers to the transient stability and control of frequency in a power system following a disturbance. The frequency control limits in the GB power system are defined by two main levels: the operational limit, which is equal to ± 0.2 Hz, and the statutory limit, which is equal to ± 0.5 Hz. The frequency response services in the GB power system aim to maintain frequency within the acceptable limits and restore frequency after sudden changes in demand/generation.

Large-capacity synchronous generators provide about 70% of the total system inertia in the GB power system. The rest is provided by smaller synchronous generators and synchronous demand. Conventional generators are continuously run to create a minimum level of available inertia to secure a capacity for frequency response. This capacity is expected to be 30-40% more than current capacity in the next five years. However, these generators are expensive to operate and produce large amounts of greenhouse gas emissions.

The absence of direct coupling between the machine and the power system in some RESs, e.g. wind generators due to the power electronics, prevent their rotating mass from contributing to the system inertia. Therefore, RESs reduce the total system inertia, and hence, increase the difficulties of the power system operation and control. RESs have power fluctuations due to environmental conditions causing a significant impact on the stability of the frequency. A reduction in the system inertia will increase the RoCoF when the system is subjected to sudden disturbances such as loss or increase in the demand or generation. In this situations, it is highly recommended to minimise the settling time during the disturbance period. Therefore, the need for additional frequency control is increased due to an increased level of RESs. A fast frequency response from the generation side is one of the recommended solutions to mitigate the increased frequency deviation issue.

The control system, which is responsible for controlling the frequency, must provide a fast and stable response. A rapid response to a high RoCoF is strongly recommended; however, a very quick response has a risk of system oscillations. A flexible embedded real-time controller that offers higher flexibility versus low cost is required with the ability of event detection and response algorithm to any disturbance. The designed controller is preferable to have scalable parameters and fast controller latency to create a new adaptive protection system that is capable of standing against frequency collapse in future power systems. This scheme is intended to supplement local control, rather than replace it.

With the increasing needs of RESs, there are opportunities to further develop demand-side services during both periods of low and high demand. However, the uses of the emergency power amount from the load side for the frequency reserve services presents a new challenge. The challenge is associated with the control of large distributed loads. Especially, with the EVs, residential BESSs, WHs, and cloth dryers. The estimated level of storage in the GB power system by 2050 will be about 10.7 GW based on 'Consumer Power Scenario'. Also, residential and non-residential BESSs are growing up day by day due to the technical developments and cost reduction as well as high levels of PV integration. A large number of these batteries are in distribution and are connected to the meter. The BESSs present a fast dynamic response to compensate the load variations in distribution networks. In the GB power system, many tenders were taken into consideration by National Grid to provide EFR from BESSs.

2.8.2 Review summary of the small signal stability and control

A critical review of power system oscillation modes for the small signal stability and control has been carried by highlighting types of low-frequency oscillation modes and the serious, effective elements. In summary, it was found that:

Both AVR and PSS can be coordinated to reduce the effects of power oscillations on the power system by using appropriate tuning, design techniques and fine-allocation of the PSSs. The parameters' tuning and the location of the PSS on a generator play a major role in the whole power system stability. The effects of oscillation modes are interlinked with the generator's output, the power flow in tie-lines and the action of the generator's excitation system. The IEEE PSS4B stabiliser provides superior results to older models of PSS.

Integrating more RESs, and therefore, reducing the total system inertia have a severe impact on the system's stability. As a result, the risk of oscillations in future low-inertia networks with the increased numbers of RESs will be magnified. Adaptive PSS was recommended to reach full stability in small and even large-signal stability. Integration of

adaptive techniques with the PSS4B will lead to a robust and modern design of PSS. In the case of power systems, such types of intelligent design can be considered as the key solution to RESs' penetration and the improvement of the power systems' efficiency. In addition, the implementation of PMUs and PSSs reduces the risk of inter-area oscillation.

There were unknown inter-area oscillations in the GB power system following a significant disturbance. PSS and POD have a real impact on reducing power system oscillations during a failure when an AC system is connected to a DC system. Therefore, the damping of this oscillation can be improved by adding a centralised POD or by adding PSSs to particular generators. However, other solutions are recommended, for example, integrating a new POD with FACTS devices, such as SVC or TCSC.

CHAPTER 3

Developing a Secondary Frequency Control for Synchronous Generators

3.1 Introduction

Integration of increasing level of power electronics leads to a reduction in the inertia of the power system. This reduction of inertia leads to a reduced system stability and increases the frequency deviation following a disturbance such as a losing generator or load. The grid code of the GB power system requires the provision of MFR so that each large generator working at under 80% output must supply 10% an increase of its rated power for a primary response within 10 seconds in the event of a decreased frequency below a pre-set threshold. Another 10% increase in secondary response within 30 seconds is required [132-134].

This secondary response can be provided by a secondary frequency controller that is connected to the generating unit to the governor's reference load (RL) to provide an additional power output. A conventional PI controller can be used to compensate the required power and to reduce the error in the frequency. However, in this conventional control method, there is a real risk that these controllers may not be effective because of parameters uncertainty [9]. Therefore, the development of a new secondary frequency control is considered in this chapter, and its impact on frequency response is investigated. The proposed design supplements the conventional PI frequency control rather than replacing it to provide a more accurate frequency response than conventional control.

3.2 Generalised model of the GB power system

The model shown in Figure 3.1 represents the power system by the inertia constant ($M=2H$) and the damping factor of the generators (D). Two first order systems, as well as a

controller rather than optimising the fuzzy logic directly.

Classical control algorithms have some limitations in a power system such as dealing with parameter uncertainties or changing the operation point. Intelligent methods such as fuzzy logic have been widely used in research due to its robustness, offering better control performance than classical methods. Fuzzy logic is widely used in real-time industrial applications and embedded systems. Fuzzy was applied widely in power systems, scaling gains are added to the inputs making the fuzzy controller act as a classical form of PD/PI/PID controller [140-142]. This option makes the fuzzy logic controller suitable to supplement the conventional secondary frequency control in the power systems knowing that the conventional PI controller is used in real-time power systems (see Figure 3.2).

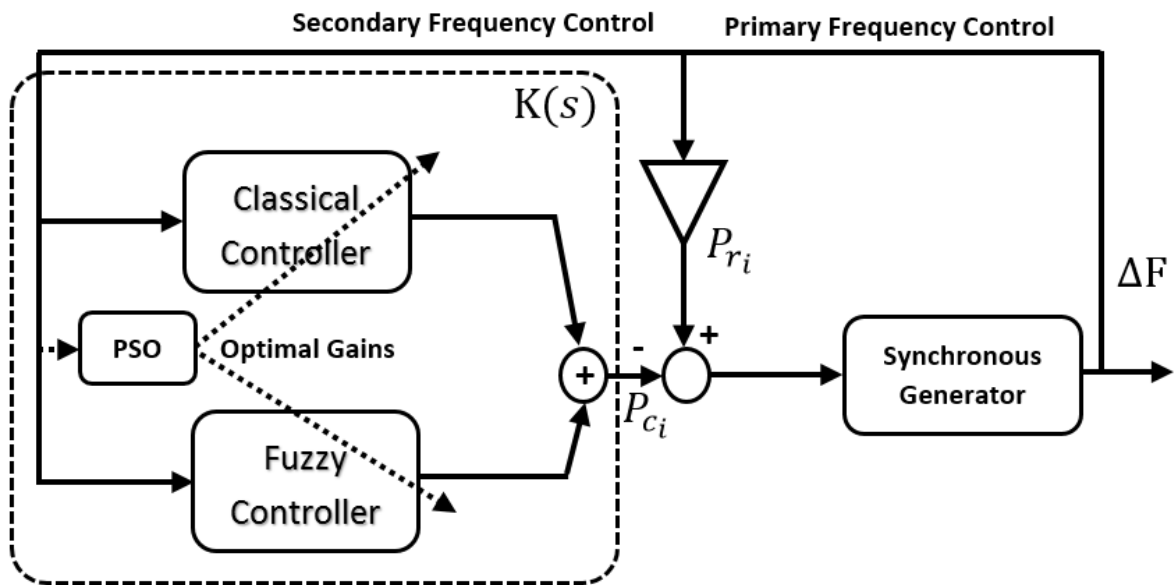


Figure 3.2. The structure of the proposed supplementary control.

3.3.1 Structure of fuzzy logic controller

A typical two-inputs one-output fuzzy logic controller is shown in Figure 3.3. The controller has two main parts: The fuzzy inference system (FIS) and the scaling gains of the inputs. This structure can be modified into different multi-input/multi-output fuzzy controller by adding a membership function (MSF) at each input or output.

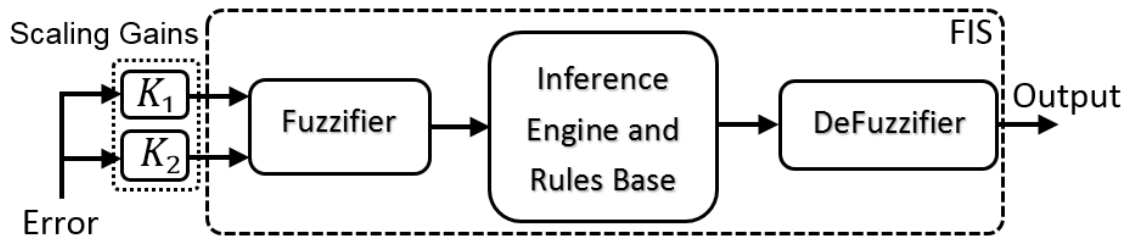


Figure 3.3. Structure of a typical two-inputs fuzzy logic controller showing the inputs scaling gain and the FIS.

As mentioned earlier, the scaling gains were added to the inputs making the fuzzy controller act as a classical form of PD/PI/PID controller. MSF with three linguistic variables is the least number in the application of PID-like fuzzy logic controller. Increasing the number of the linguistic variables in an MSF will increase the accuracy of the control action. However, increasing the number of linguistics variables will increase the number of fuzzy rules. For example, for MSF with seven linguistic variables, the design of three inputs PID-like fuzzy logic controller (PIDFLC) controller has fuzzy rules equal to $7 \times 7 \times 7 = 343$. This high number of fuzzy rules requires higher execution time with the consequence of slowing down the controller action [140, 141, 143]. Therefore, a fuzzy logic controller with the parallel structure of PIDFLC was developed as shown in Figure 3.4 to supplement the classical controller. This design has benefits in reducing the number of fuzzy rules. For example, for MSF with seven linguistic variables, the parallel structure of PIDFLC will reduce that large number to $7 \times 7 + 7 \times 7 = 98$ fuzzy rules instead of 343 (see Figure 3.4).

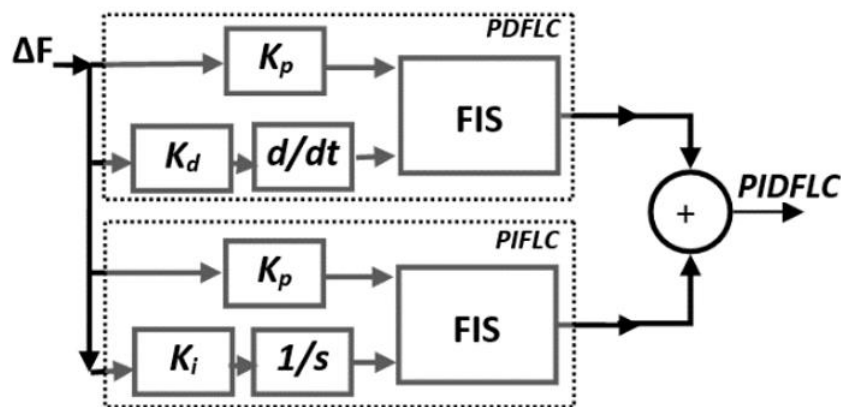


Figure 3.4. Parallel structure of a three inputs PIDFLC.

Two versions of FIS were used in this research. The first design considers seven triangle linguistic variables at each MSF and 49 fuzzy rules (see Figure 3.5 and Table 3.1) while the second one with three triangle linguistic variables and nine fuzzy rules (see Figure 3.6 and Table 3.2). Both versions with their parameters range are widely used with the PI/PID fuzzy logic controller, and they offered good results and fast execution time due to their ramp gradual transitions and simple mathematical representation [140, 141, 143, 144]. Fuzzy toolbox in MATLAB was used to design both versions of FIS (see Appendix A3.1).

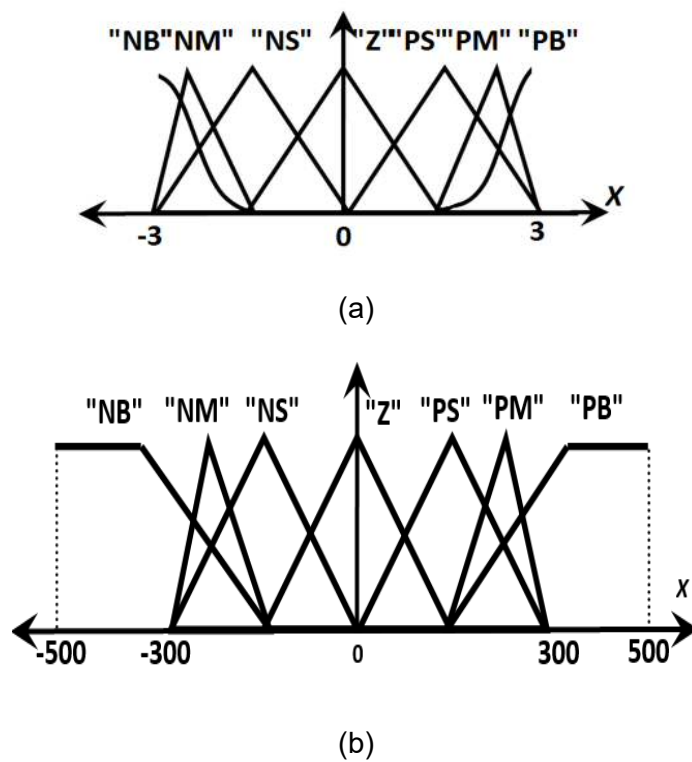


Figure 3.5. The version I of FIS, (a) inputs MSF, (b) output MSF.

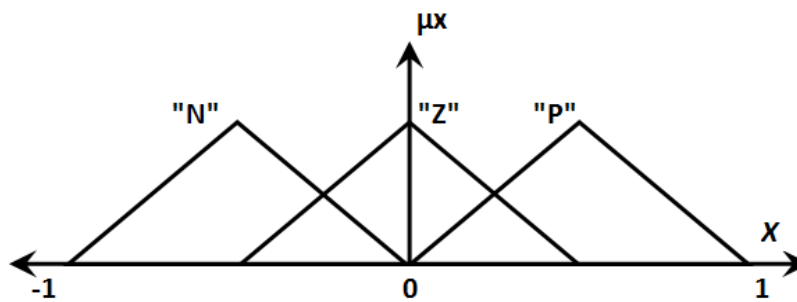


Figure 3.6. Input/outputs MSF of version II FIS.

Table 3.1. Fuzzy rule tables of the version I FIS.

		Input1(Kp)						
		NB	NM	NS	Z	PS	PM	PB
Input2 (Kd/Ki)	NB	NB	NB	NM	NM	NS	NS	Z
	NM	NB	NM	NM	NS	NS	Z	PS
	NS	NM	NM	NS	NS	Z	PS	PS
	Z	NM	NS	NS	Z	PS	PS	PM
	PS	NS	NS	Z	PS	PS	PM	PM
	PM	NS	Z	PS	PS	PM	PM	PB
	PB	Z	PS	PS	PM	PM	PB	PB

Table 3.2. Fuzzy rule tables of version II FIS.

		Input1 (Kp)		
		N	Z	P
Input2 (Kd/Ki)	N	N	N	Z
	Z	N	Z	P
	P	Z	P	P

3.3.2 Optimisation method

The scaling gains of the fuzzy logic controller have a significant impact on tuning the MSF at each input of the controller. Trial and error method can be used to optimise these gains, but not offer an optimal value or good control performance. The benefits of these gains are to re-scale the range of the universe of discourse of the MSF. These values are very important to get better control performance.

The simplest model of the PID controller is presented in equation (3.1) with parallel structure available in the MATLAB Simulink [136]. Where: $P= Kp$, $I= Ki$, $D= Kd$, and N are defined in this equation only as the controller gains and the filter coefficient, respectively.

$$- \quad \frac{\quad}{\quad} \quad (3.1)$$

The built-in tuner of the PID block in the MATLAB Simulink can obtain the optimal

value of the controller's parameters in any closed-loop linear system. However, in the applications of the complex and nonlinear systems, it is difficult to obtain the optimal value using this tuner. Therefore, the PSO was used to get the optimal values of these gains due to the high optimisation capability. The PSO was used along with the PID tuner in the MATLAB Simulink model of the GB power system presented in Section 3.2 to validate the effectiveness of the proposed method, which is using the fuzzy logic controller for controlling the frequency without adding any complexity to the control system.

The primary function of the PSO is to obtain the optimal value of K_p , K_i , and K_d by minimising the fitness function to a minimum possible value. The fitness function was represented by the integral square error (ISE) presented in equation (3.2). The error represents the ΔF as shown in Figure 3.2.

$$ISE = \sum_{t=0}^{Maxiterat...} (e(t))^2 \quad (3.2)$$

The proposed tuning method is looking to tune the existing classical controller to get the optimal values of its gains and to use these gains in the fuzzy supplementary controller (see Figure 3.2). The optimal condition in both Simulink PID tuner and PSO was set to

for avoiding high value of the gains. The optimal controller's gains value of both tuner and PSO were obtained once and were used in simulation results to prove the efficiency of the proposed tuning methods (see Table 3.3). These values were obtained by using the PID controller as a classical secondary frequency control (in Figure 3.2) in the GB power system model of Figure 3.1 to reuse them in the fuzzy controller.

An event of 27th May 2008 was used as the load disturbance, where two generators were lost with a power equal with 1,320 MW of the total generation power of the GB power system [1], [12]. In this study, it was assumed that such disturbance occurs on an average weekday and the estimated loss was approximately 0.03 p.u. A PSO-based optimisation of the PID controller gains was applied for 30s simulation time (iteration) considering the

disturbance (see Appendix A3.2). The values in Table 3.3 are the optimal values which were obtained for a minimum value of ISE.

Table 3.3. The optimal value of the PID controllers' gains

	Classical PID			
	Kp	Ki	Kd	(N) Filter coefficient
Simulink tuner	23.22	10.906	3.48	1.089
PSO	30	14.247	30	100

3.4 Performance comparison of controllers

This section compares the control performance of different structures of the fuzzy controller and their optimal response using the simplified GB power system. Three simulation cases were used to evaluate the fuzzy logic controller as a supplementary secondary frequency controller as shown in Figure 3.2. The optimal gains presented in Table 3.3 were used in all simulation cases.

3.4.1 Using two-inputs fuzzy controller and 49 Rules

The typical PD fuzzy logic controller (PDFLC) shown in Figure 3.3 was used with the aid of the optimal PID gains and Version I FIS shown in Figure 3.5. The simulation results show high speed and improved transient frequency response as presented in Figure 3.7 and Table 3.4. The PSO - based PDFLC controller had the best response with 0.016 deviation value and 5s settling time. The classical PID controller provided a good response as well, but with a critical value of ΔF reaching -0.2 Hz with 9s and 11s settling time for tuner-based PID and PSO-based PID, respectively.

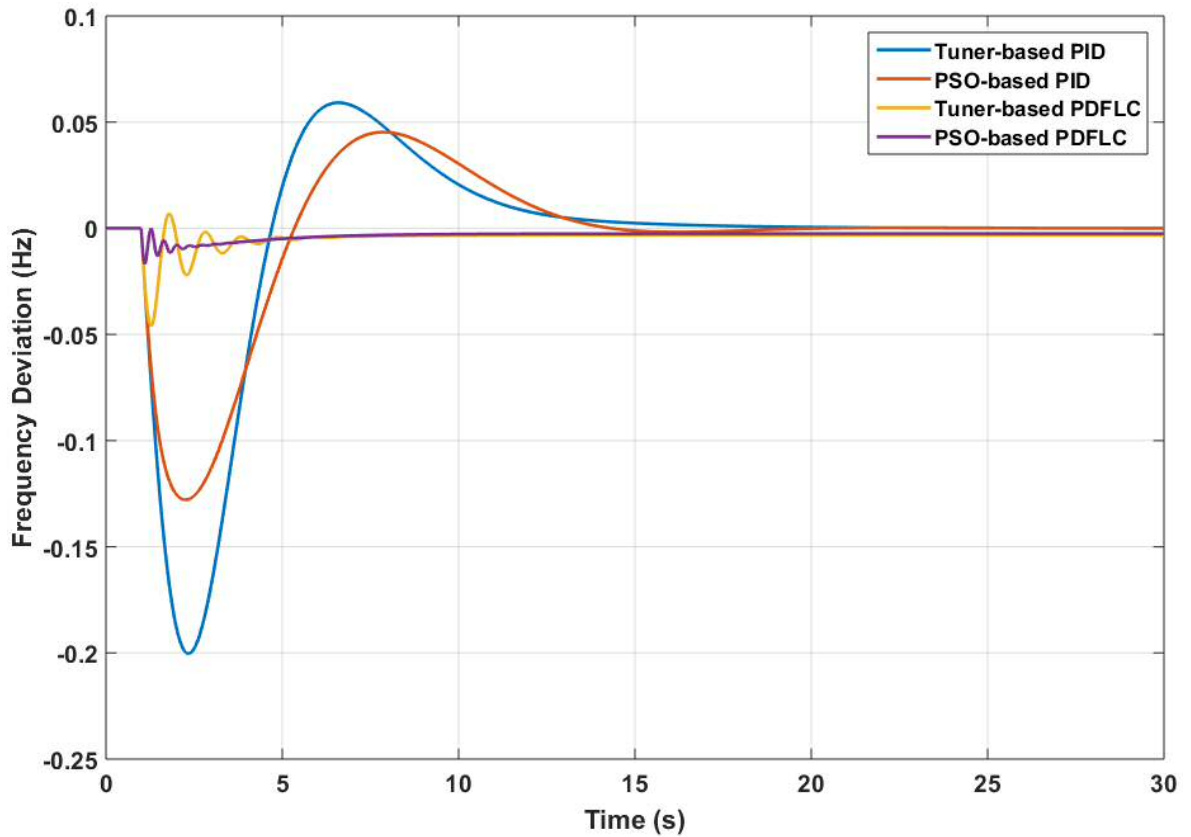


Figure 3.7. Simulation results of the frequency deviation in the GB power system using two-inputs PDFLC and 49 rules.

Table 3.4. Frequency response performance using two-inputs PDFLC and 49 rules

		Max value of ΔF (Hz)	Settling time (s)	Error (Hz)
Controller type	T-PID	-0.2	9	0
	PSO-PID	-0.13	11	0
	T-PDFLC	-0.041	4	-0.0032
	PSO-PDFLC	-0.016	4	-0.0025

3.4.2 Using three-inputs fuzzy controller and 49 Rules

This section presents the PIDFLC with the parallel structure of PIFLC+PDFLC (see Figure 3.4) and the version I FIS (see Figure 3.5). The structure of this controller offers greater stability versus fast response with only 3s settling time and -0.015 ΔF and zero error (see Figure 3.8 and Table 3.5).

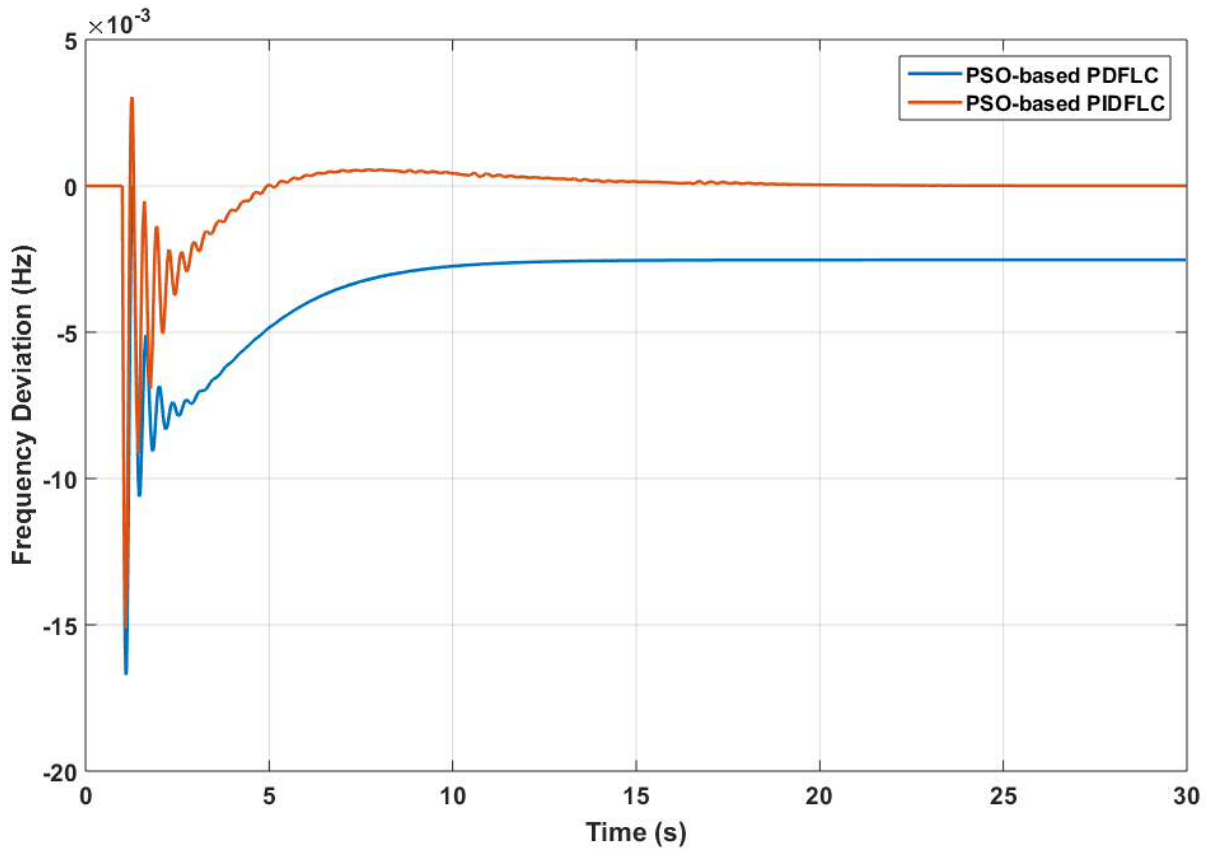


Figure 3.8. The frequency deviation using three-inputs PIDFLC and 49 rules.

Table 3.5. Frequency response performance using three-inputs PIDFLC and 49 rules

Controller type	Max value of ΔF (Hz)	Settling time (s)	Error (Hz)
PSO-PDFLC	-0.017	6	-0.016
PSO-PIDFLC	-0.015	3	00

3.4.3 Using fuzzy inference system with 9 Rules

This section presents a comparison of fuzzy controllers but with version II FIS (see Figure 3.6) for testing the proposed control with the smallest number of fuzzy rules. Version II has a simple MSF of three linguistic variables and nine fuzzy rules. This number is the lowest number of rules used in the control applications of the fuzzy logic controller. PDFLC has an error bigger than other controllers while PIDFLC provides a better response performance than all other controller types with 0.1 deviation value and 9s settling time.

However, PID has a response with zero error but longer settling time (see Figure 3.9 and Table 3.6).

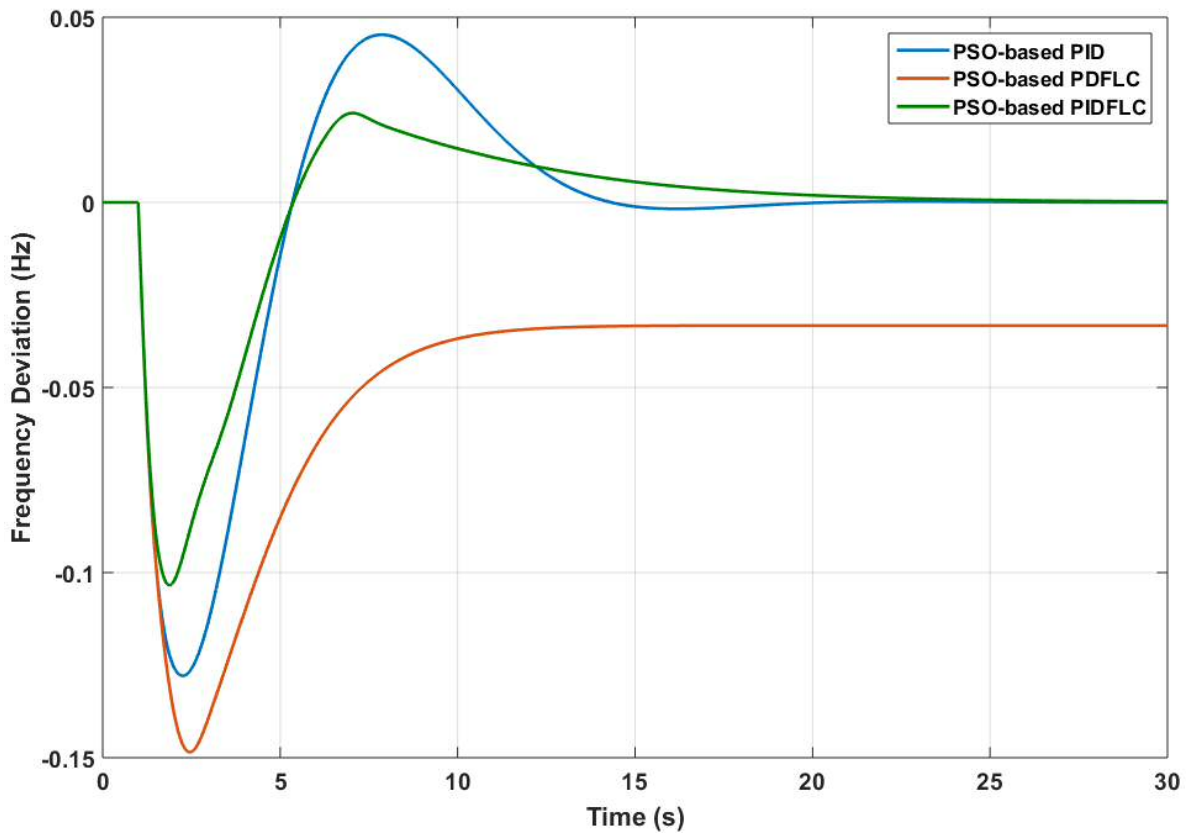


Figure 3.9. Simulation results of the frequency deviation in the GB power system using fuzzy controllers with 9 rules.

Table 3.6. Frequency response performance using fuzzy controllers with 9 rules

Controller type	Max value of ΔF (Hz)	Settling time (s)	Error (Hz)
PSO-PID	-0.13	11	00
PSO-PDFLC	-0.14	7	-0.033
PSO-PIDFLC	-0.1	9	00

3.4.4 Robustness analysis against parameters uncertainties

An analysis of parameter uncertainties of the GB power system was performed by using a different range of values. The simplified GB power system has many parameters that can be changed such as governor time constant (T_g), Damping factor (D), Inertia (H), and the value of the droop constant (R). The changes in each parameter (increase or

decrease) has a different effect on the system stability. For example, increasing D can reduce the frequency deviation of the system while increasing H can slower the system. Furthermore, increasing Tg can increase the frequency deviation resulting in a rise of system's instability. The effect of changing each parameter on the primary frequency response of the simplified GB power system is presented in Appendix A3.3. Two different cases of parameters uncertainties of R , Tg , D and H were considered (see Table 3.7 and Figure 3.10) in the GB power system.

Table 3.7. Uncertain parameters and the variation range for the simplified GB power system presented in Figure 2.1.

Parameters		Base case	Variation range	New value
Case 1	R	0.09	+ 70%	0.123
	Tg	0.2	- 50%	0.1
	D	1	- 70%	0.3
	H	3.42	+ 50%	5.1
Case 2	R	0.09	- 70%	0.027
	Tg	0.2	+ 50%	0.3
	D	1	+ 70%	1.7
	H	3.42	- 50%	1.7

3.4.4.1 Parameters uncertainties using fuzzy controllers with 49 rules

By applying parameter uncertainties of study case 1 and 2 to the classical PID controller only (PSO-based PID), the supplementary PDFLC plus the classical (PSO-based PDFLC), supplementary PIDFLC plus the classical (PSO-based PIDFLC), and the supplementary PIDFLC without the classical (PSO-based:onlyFuzzy). It was found that the classical controller has a critical response to high oscillation and overshoot. In contrast, all the other types of supplementary fuzzy controller improve the frequency response and showed a robustness (see Figure 3.11, Figure 3.12, and Table 3.8). In addition, the response with fuzzy only is nearly identical to the fuzzy plus classical PIDFLC because that the fuzzy controller is the dominant controller as shown in the zoomed areas.

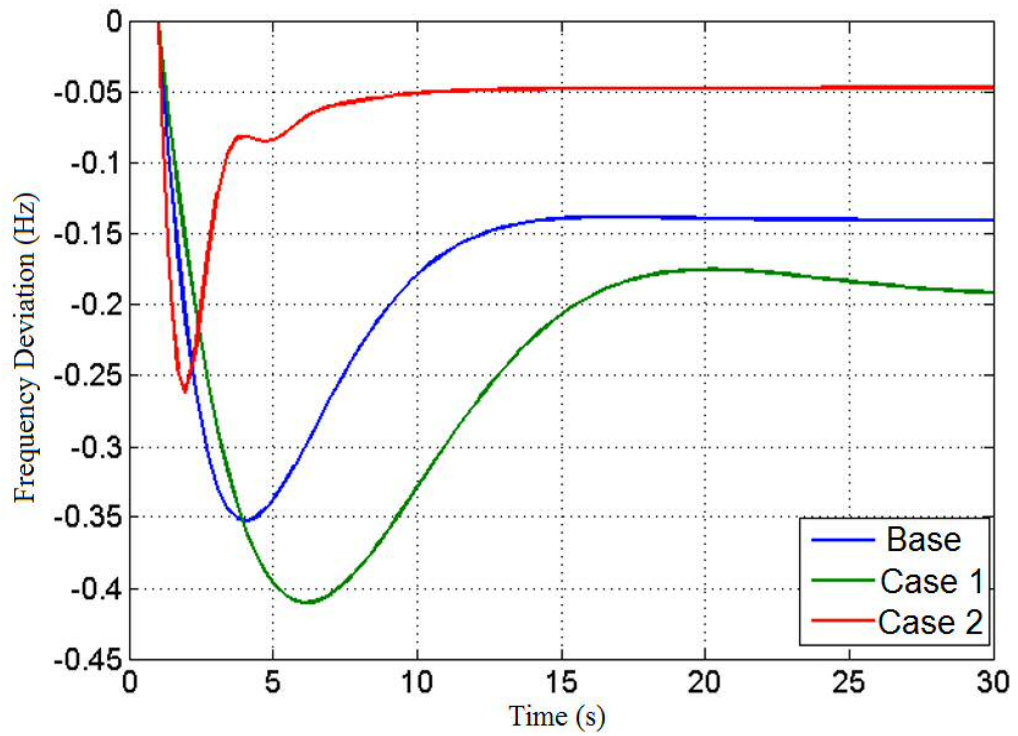


Figure 3.10. The frequency response of GB power system with parameters uncertainty comparison of case 1 and 2 without secondary frequency control.

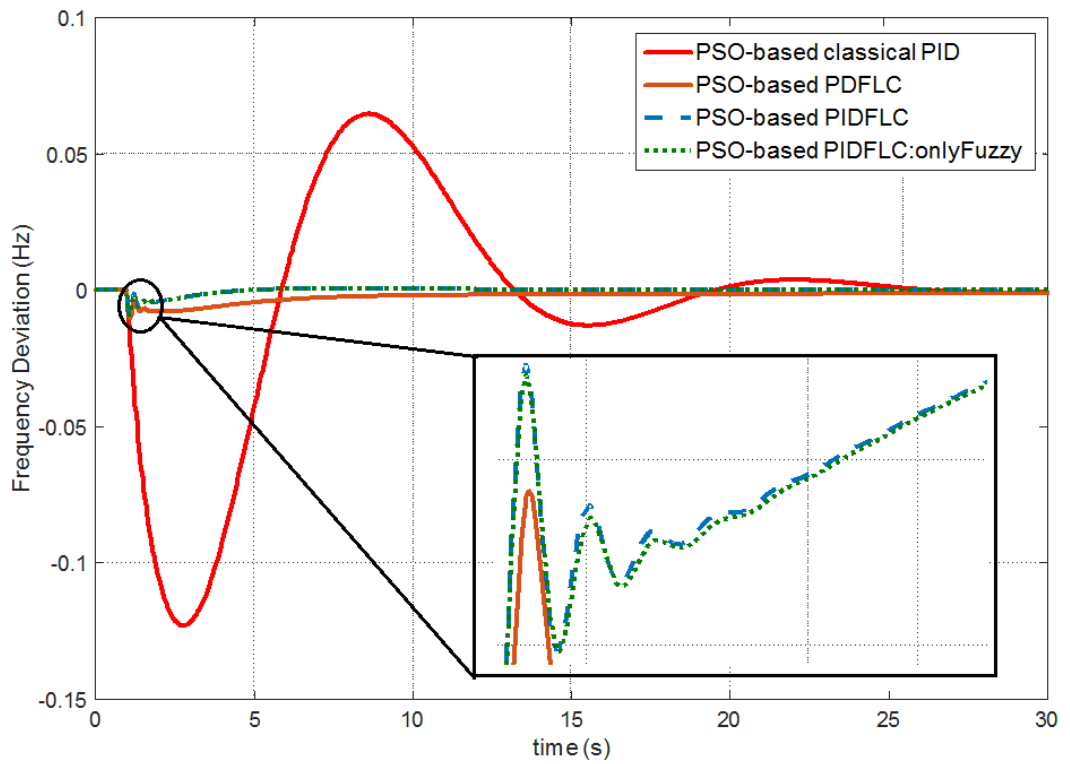


Figure 3.11. Comparison of controllers using case 1 parameters uncertainties and 49 fuzzy rules.

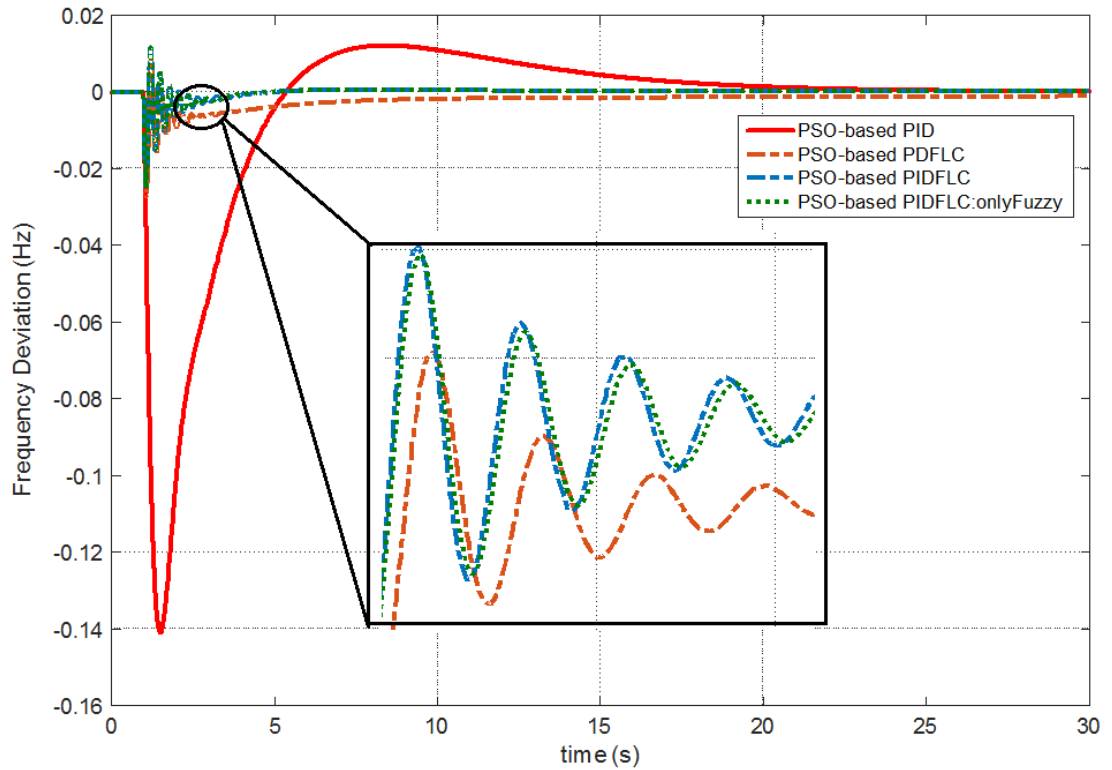


Figure 3.12. Comparison of controllers using case 2 parameters uncertainties and 49 fuzzy rules.

Table 3.8. Performances comparison of parameters uncertainties for frequency response using fuzzy controllers with 49 rules

	ΔF (Hz)		Settling time (s)		Error (Hz)	
	Case1	Case2	Case1	Case2	Case1	Case2
PSO-PID	-0.13	-0.14	15	9	00	00
PSO-PDFLC	-0.01	-0.028	9	5	-0.003	-0.0025
PSO-PIDFLC	-0.009	-0.023	8	3	00	00

3.4.4.2 Parameters uncertainties using fuzzy controllers with 9 rules

This section uses the version II FIS, having the simplest fuzzy MSF and rules for evaluating the behaviour of the three fuzzy controllers considering parameters uncertainties. The PIDFLC controller provides a better response than other controllers with high robustness. However, PID controller had also zero error but with higher frequency deviation (see Figure 3.13, Figure 3.14, and Table 3.9).

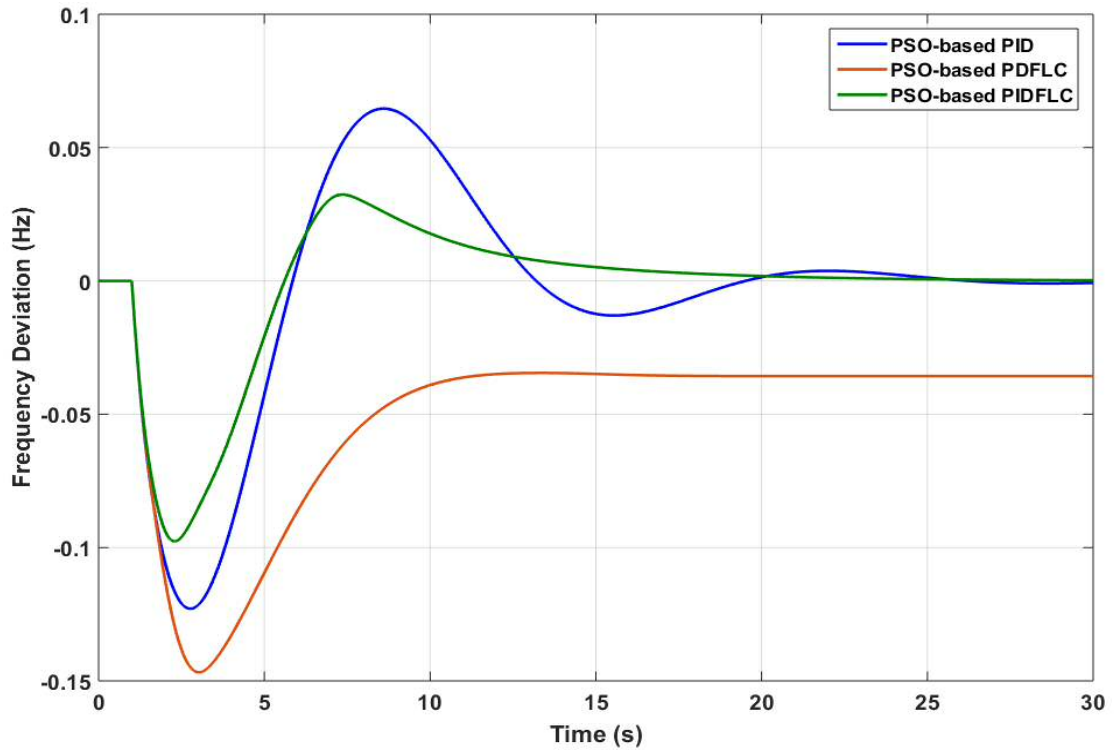


Figure 3.13. A comparison of controllers with case 1 parameters uncertainties and 9 fuzzy rules.

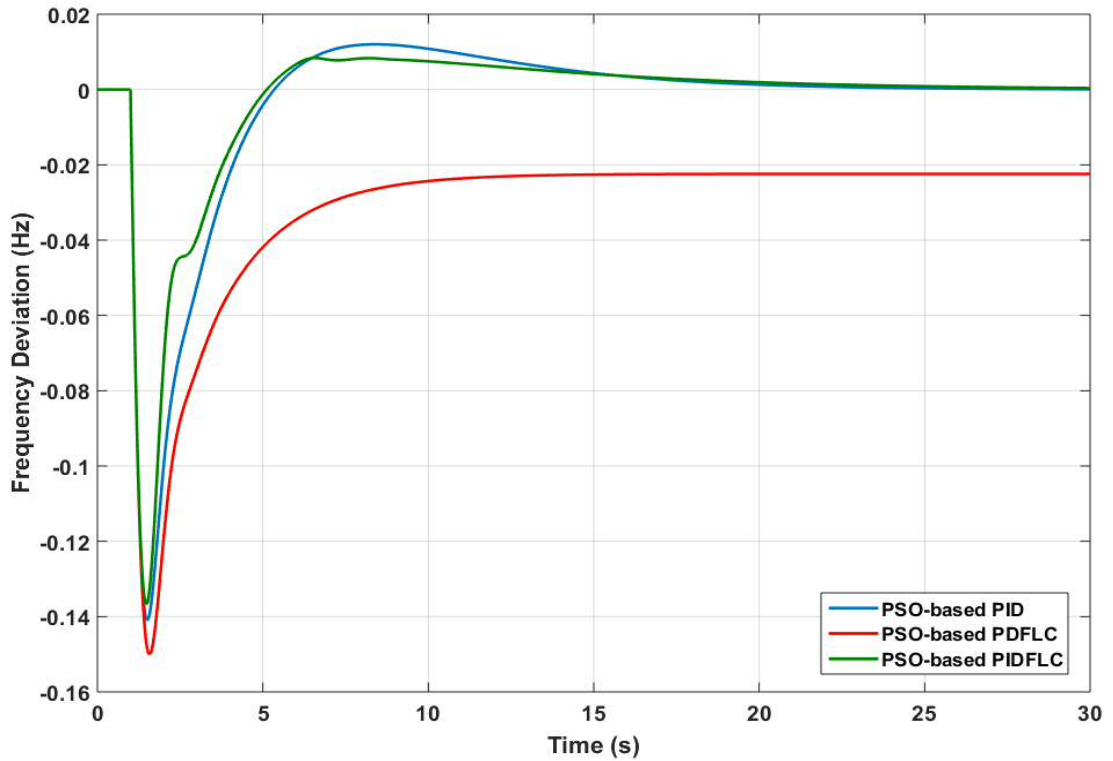


Figure 3.14. A comparison of controllers with case 2 parameters uncertainties and 9 fuzzy rules.

Table 3.9. Performances comparison of parameters uncertainties for frequency response using fuzzy controllers with 9 rules

		ΔF (Hz)		Settling time (s)		Error (Hz)	
		Case1	Case2	Case1	Case2	Case1	Case2
Controller type	PSO-PID	-0.125	-0.14	14	4	00	00
	PSO-PDFLC	-0.15	-0.15	8	6	-0.035	-0.025
	PSO-PIDFLC	-0.095	-0.13	11	3	00	00

3.5 Demonstration of the proposed control on a multi-machine power system

This section demonstrates the effectiveness of the proposed control method to supplement the local secondary frequency control rather than replacing it. The average overnight amount (0.023 p.u) of the secondary frequency capacity was used for January-2016 in the GB power system [145]. This amount was applied to the IEEE 10-machine benchmark power system. The IEEE 10-machine test system (see Figure 3.15) was widely used in the literature for testing new control techniques of the power system as it was explained in section 2.8.2 [127, 129]. Availability of this benchmark system is an opportunity to test the proposed controller using this time-domain power system to have more realistic frequency response behaviour.

3.5.1 Integrate the controller in Generator 9 with sudden load rise

The amount of the secondary frequency control (0.023 p.u = 23 MW) was applied at generator 9 (G9) for representing the MFR. A disturbance equal to 200 MW was applied and was represented as a sudden load rise on busbar 24 (see Figure 3.15). The proposed fuzzy controller showed a better response than classical PI secondary frequency controller. The absolute mean value (AMV) was obtained for each generator's frequency response to clarify the difference in the frequency responses (see Figure 3.16).

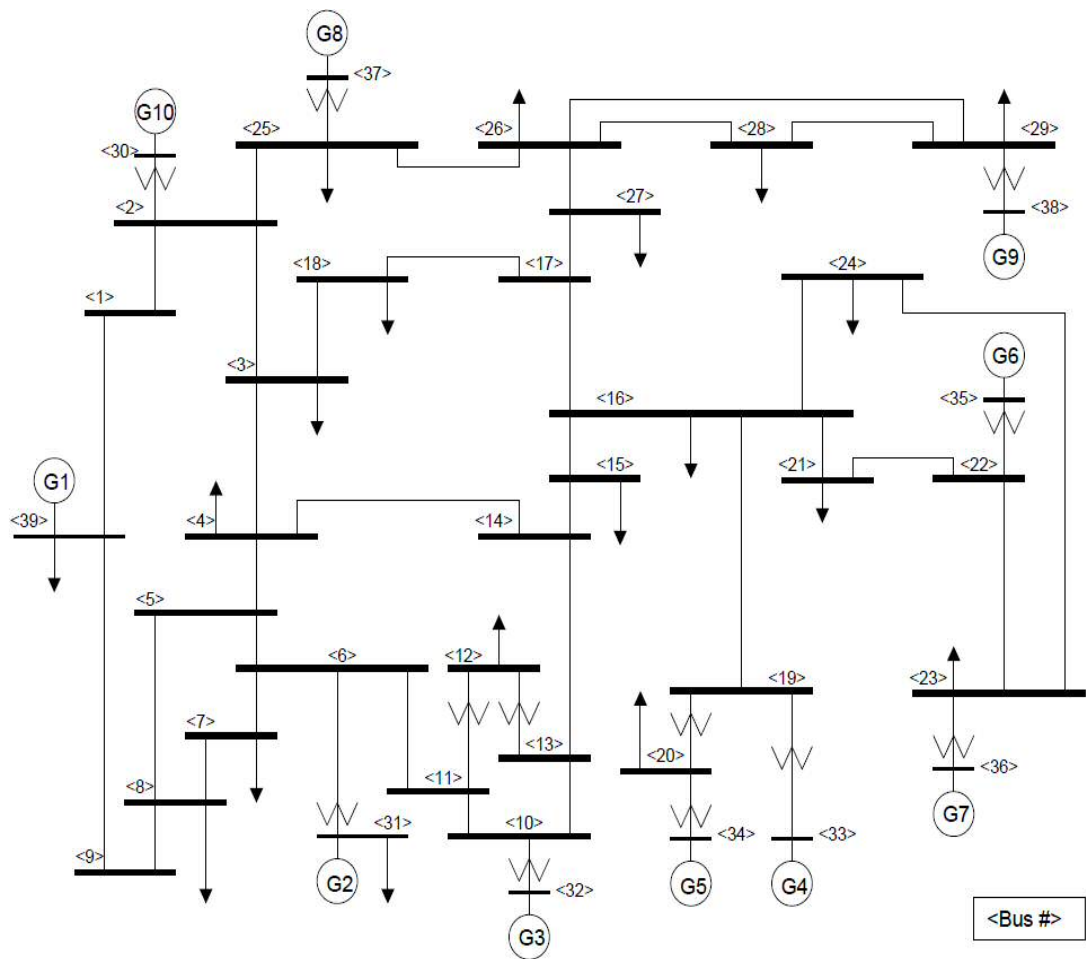


Figure 3.15. The 39-Bus, 10-machine New England test system (explained in section 2.7.2 [127, 129]).

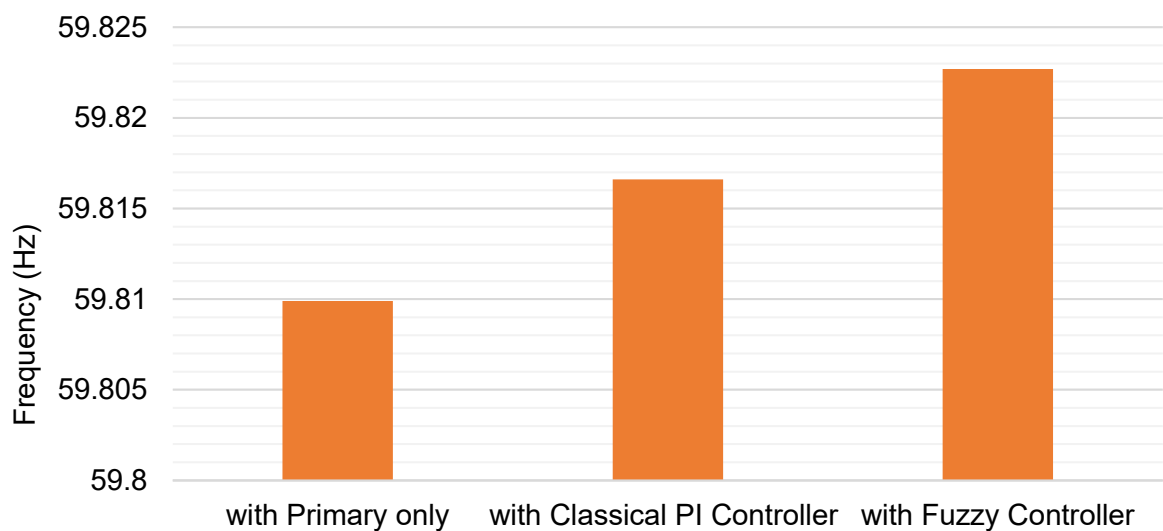


Figure 3.16. AMV of the frequency responses at generator G9 with and without the proposed controller (a disturbance equal to 200 MW).

3.5.2 Integrate the controller in generator 9 with three-phase fault

The same amount of the secondary frequency control (0.023 p.u = 23 MW) was applied at generator 9 (G9) to represent the MFR. The case study was done by applying a three-phase fault in the transmission lines between busbar16 and busbar 17 (see Figure 3.15). Figure 3.17 shows the AMV for the frequency responses comparison at generator G9.

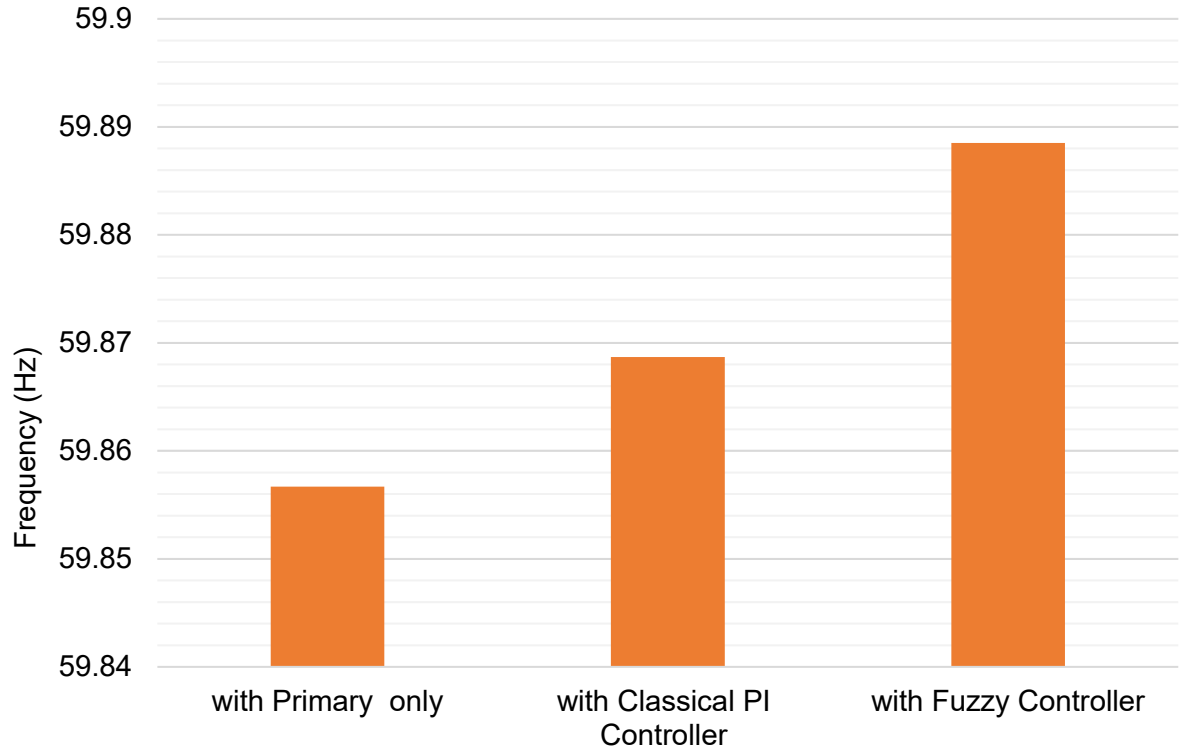


Figure 3.17. AMV of the frequency responses at generator G9 with and without the proposed controller (three-phase fault).

3.5.3 Integrate the controller in generator 10 with sudden load rise

The same amount (0.023 p.u = 23 MW) was applied at generator 10 (G10) to represent the MFR. A disturbance equal to 200 MW was applied and was represented as a sudden load rise in busbar 24 (see Figure 3.15). Figure 3.18 shows the AMV for the frequency response comparison at generator G10.

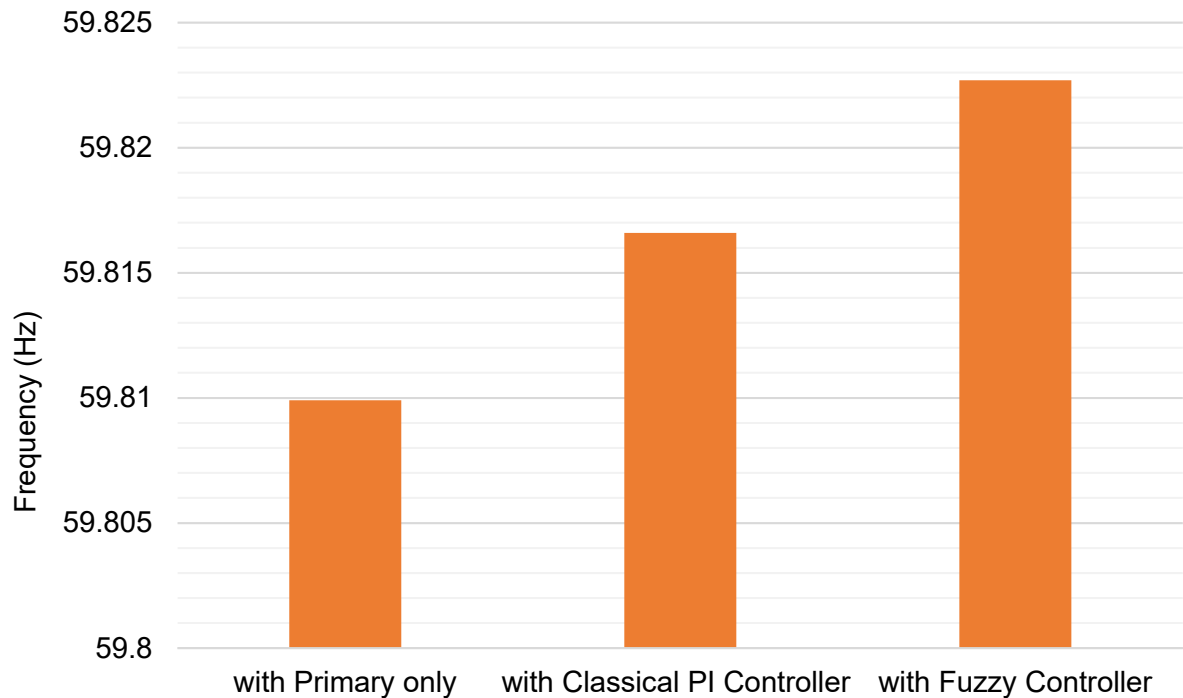


Figure 3.18. AMV of the frequency responses at generator G10 with and without the proposed controller (a disturbance equal to 200 MW).

3.5.4 Integrate the controller in generator 10 with three-phase fault

The amount of about 10% of the total generator capacity (≈ 1000 MW) was applied at generator 10 (G10) to represent the 10% increase in the secondary frequency capacity to represent the MFR. A three-phase fault in the transmission line of generator 1 (G1 in Figure 3.15) and the sudden load change in the previous cases were applied. This case is to display the power generated from G10 following the disturbance. Figure 3.19 shows the power generated from generator G10 following the disturbance at $t=4$ seconds.

Using the proposed fuzzy controller as a supplementary controller leads to an additional output power equal to 6.195 MW more than when only the classical PI controller was used. This improvement is equal to 1.7% following a disturbance (see Table 3.10). This improvement demonstrates that the developments in the controller's design can play an important role in future frequency control in the case when the MFR requirements are applied.

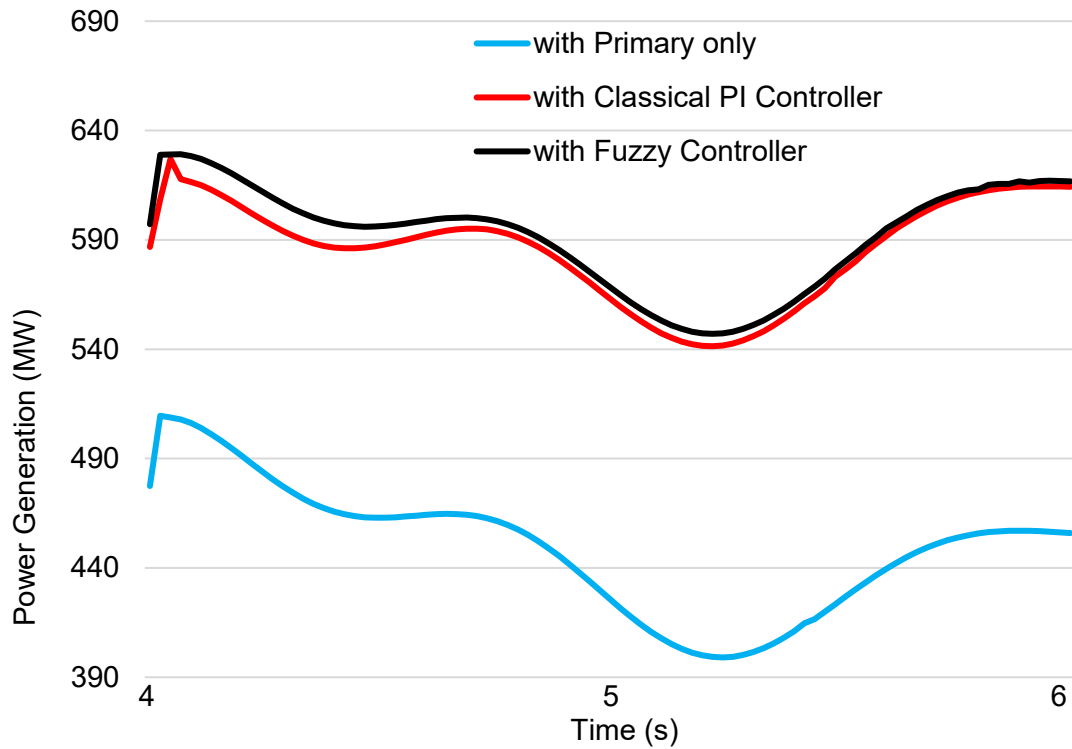


Figure 3.19. Comparison of power generated from generator G10 following a disturbance at $t = 4s$.

Table 3.10. Power generated by generator G10 following a disturbance considering secondary frequency controllers

	Power output (MW)	Improvements (%)
With the classical PI controller	585.692	0
With fuzzy controller	591.887	1.7

Recently, the development of the combined cycle gas turbine generators (CCGT) was carried out to get fast cycling and rapid start-up in the generated power to meet the requirements of MFR [132, 134]. The development of the CCGT was done by Siemens AG as explained in [132] to get Fast Cycling and Rapid Start-up in the generated power. The promising results, presented in [132], showed that +46 MW was obtained in 10 seconds and +66 MW in 30 seconds (see Figure 3.20). Therefore, the proposed frequency controller could be used in similar applications to get faster MFR and for generating faster power output in the CCGT or other technologies.

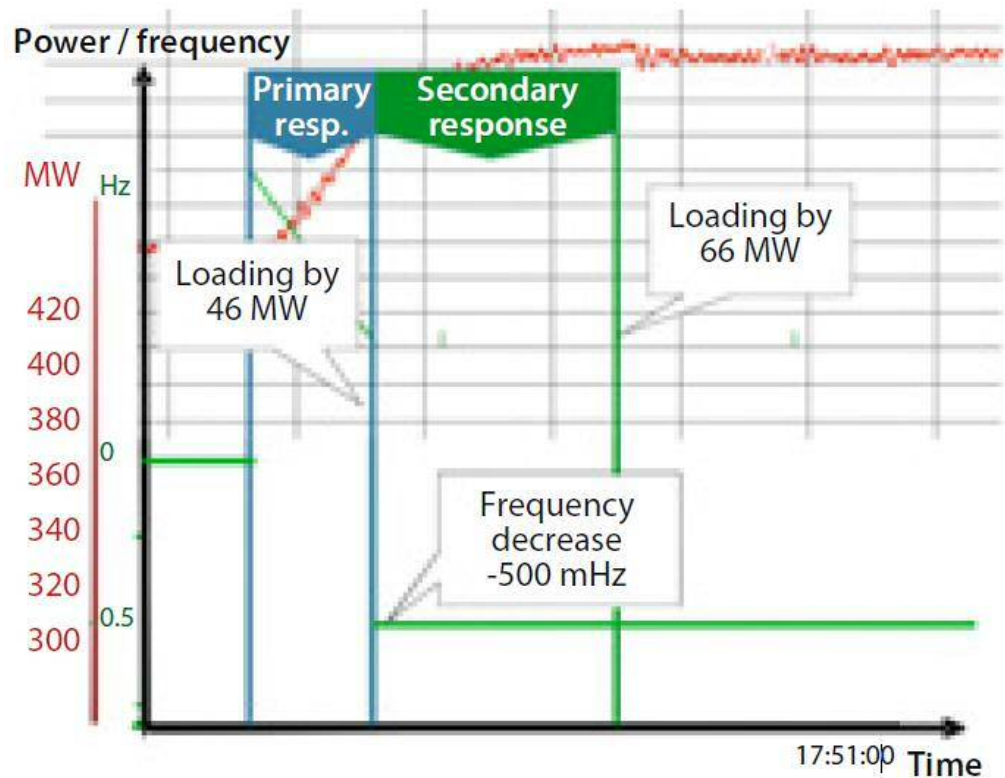


Figure 3.20. Results for the grid code support tests at the new Severn Power Station (CCGT), near Newport City, Wales, UK, by Siemens AG. The results for the MFR are: (i) Primary response achieved +46 MW (11%) in 10 seconds, (ii) Secondary response achieved +66 MW (15%) in 30 seconds [132].

3.6 Summary

A developed optimal fuzzy logic-based secondary frequency controller was presented to get fast and accurate mandatory frequency control in the GB power system. The proposed frequency controller supplemented the local control rather than replacing it and provided a superior frequency response than the conventional PI-controller. The proposed design could be used for the application of the LFC or AGC. In addition, it applies to both decentralised and centralised control methods. Furthermore, the controller could be applied to have a faster MFR in the application of, for example, CCGT.

CHAPTER 4

Control of a Population of Water Heater Devices for Frequency Response

4.1 Introduction

Due to the increasing need for RESs, performing frequency control using only generation side becomes not only expensive but also technically difficult, as explained in Section 2.2.1 [9-11]. By 2025/26, the fluctuation of the feed-in of the wind and solar leads to a sharp ramp in the total system demand during the day. In addition, the combination of high wind and PV output alongside with a low demand means that a significant number of interventions by the GB system operator should be taken for balancing and operability reasons.

Therefore, there are opportunities for demand-side services during both periods of low and high demand [8]. However, the uses of the emergency power amount from the load side for the frequency response services presents a new challenge. The challenge is associated with the control of large distributed loads such as WHs [24].

Controlling large distributed load was done using centralised and decentralised control methods [15, 35, 38]. The centralised control method reduced the uncertainty in the response of controllable units. However, the centralised method has a real challenge related to the communications such as the cost and latency [15]. In contrast, the decentralised control method removes this challenge, but it introduces an uncertainty due to the independent response of these large distributed loads [15, 35, 38].

However, to the best of the author knowledge, none of the previous work has considered providing a control method that compromises the advantages of both centralised

and decentralised control of WHs. Therefore, the problem of ‘smart management and control’ of the power consumption of controllable WHs are considered in this research.

A hierarchical control of a population of WHs is proposed to provide frequency response services when required. A model of a population of controllable WHs is developed based on Markov-chain. The model demonstrates the potential for a WHs aggregator to offer frequency response service and evaluates the effective population capacity during a frequency event.

4.2 Hierarchical control of water heaters

The electric WH is an important home appliance which can be controlled to provide frequency response services by turning ‘ON/OFF’ the device in response to a pre-set value of frequency deviation. Electric WHs are widely deployed in different buildings for different residential and non-residential uses in power systems [55]. There are two types of WHs, the ERWH and the HPWH as well as a hybrid type [53, 55, 60, 61].

The main aim of the proposed control is to use WHs devices to offer frequency response services when required. The aggregator aims to integrate a controller with each WH device to turn ‘ON/OFF’ the device after a pre-set value of frequency deviation. The proposed hierarchical control is based on two main decision layers; the aggregator layer and the device control layer as shown in Figure 4.1.

The aggregator control layer receives the states of WHs and enables/disables the device control layer. A controller is integrated with each WH device to turn ‘ON/OFF’ the device according to the command signal received from the aggregator, the value of f , and the level of the water temperature. It enables the population to provide the desired frequency response as shown in Figure 4.2, and to provide frequency response services when required.

When the frequency drops, three frequency bands are considered, the priorities of the response of the device are in relation to their water temperature and the value of f .

Therefore, the response will be from devices with the highest to lowest water temperature when the frequency drops. As a result, the aggregated devices will not respond at the same time and the risk of a simultaneous power change of a large number of controllable loads will be reduced. Hence, the impact on the power system and end-users will be reduced. In addition, when there is no frequency event, the devices are usually switched 'ON', therefore, for the frequency rise, the number of responsive devices is much lower than when it drops. As a results, for the high frequency service, one frequency band is considered.

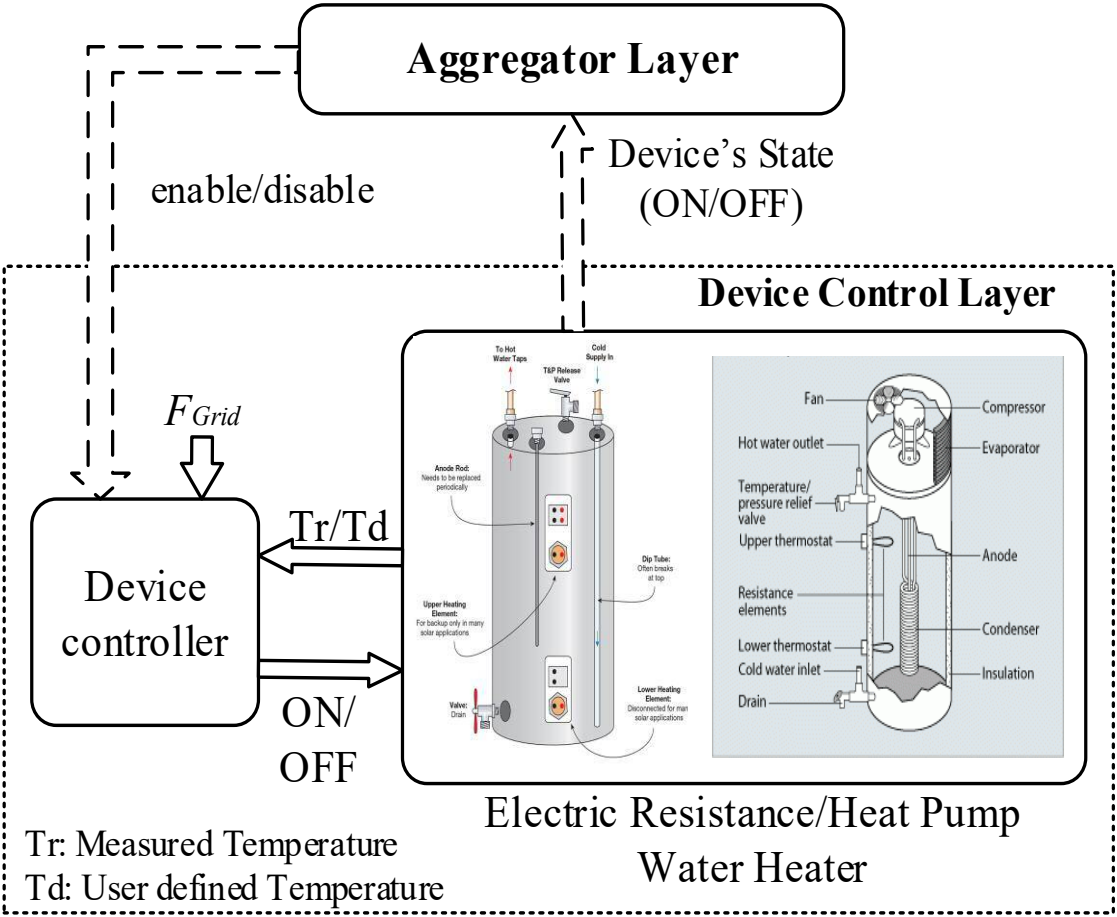


Figure 4.1. Block diagram of the proposed hierarchical control of WHs.

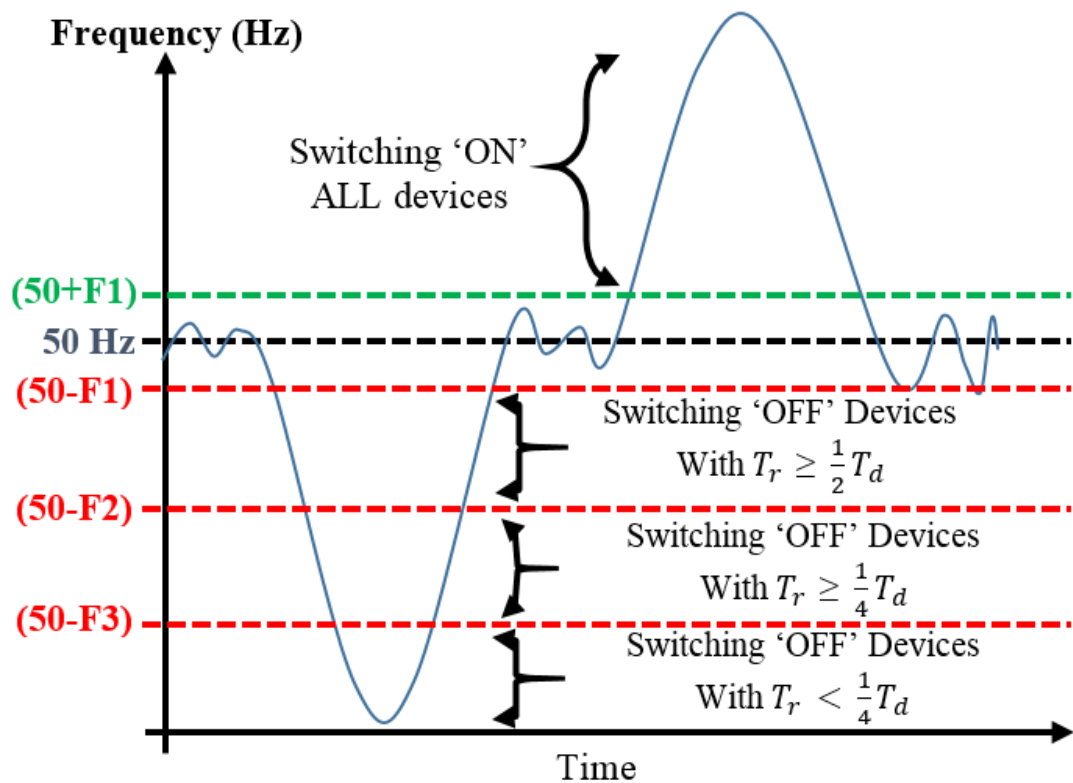


Figure 4.2. The desired response of the WHs population, where T_r = Measured temperature and T_d = User defined temperature.

4.3 Structure of the proposed device controller

To provide the desired frequency response shown in Figure 4.2 by using the device controller, it is assumed that this controller is installed in each WH and aims to control their 'ON/OFF' status. Therefore, the proposed water heater controller has three main components: (i) Measurements of frequency deviation, (ii) Measurements of water temperature and (iii) Logic gates. The latter is to control the device's 'ON/OFF' according to (i), (ii), and based on the command signal received from the aggregator (see Figure 4.3).

As shown in Figure 4.1, the aggregator collects the devices' state and initiate the control signal to enable/disable each controller. So, the aggregator control signal is either logic 1 to enable the device controller or logic 0 to disable it. Therefore the aggregator could decide the required population capacity or control the time of the device response.

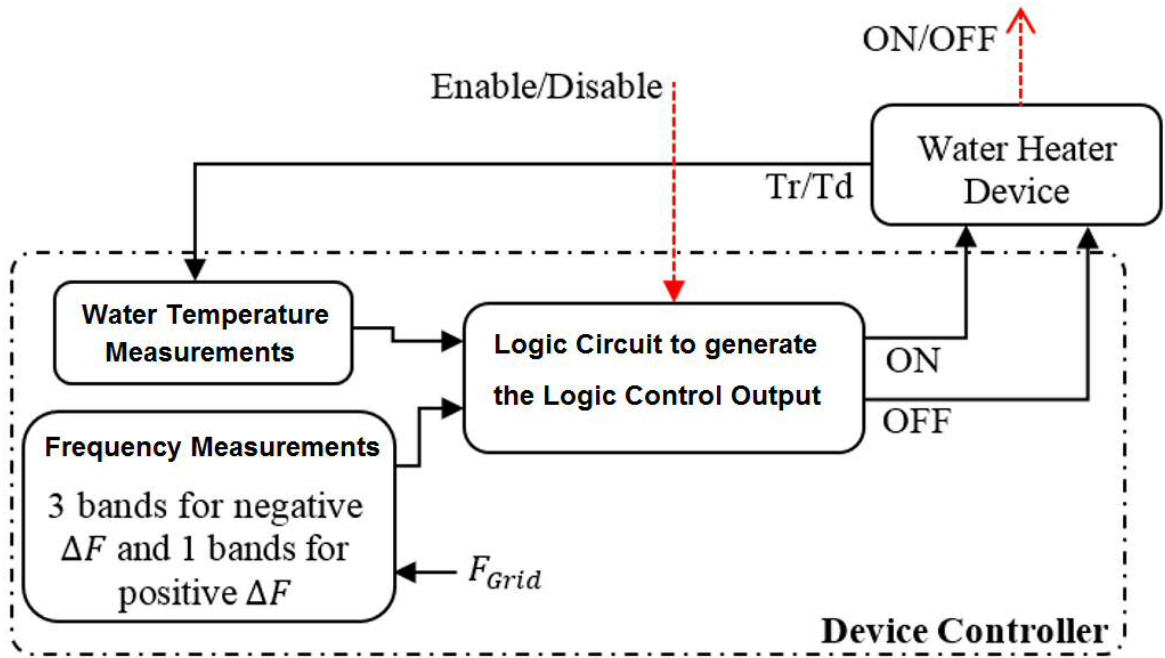


Figure 4.3. The block diagram of the proposed WH controller.

4.3.1 Measurements of frequency deviation

The frequency measurements contain three bands for the negative and one band for the positive (see Figure 4.4), these logic bands are represented by equations (4.1)-(4.4). These bands along with the temperature measurements (presented in the next section) are used to assign the priority for the device response reducing the impact on the system and maintain the end-user comfort level. However, the number of bands and their parameters (F_1 , F_2 , and F_3) are changeable and could be set according to the aggregator's preferences.

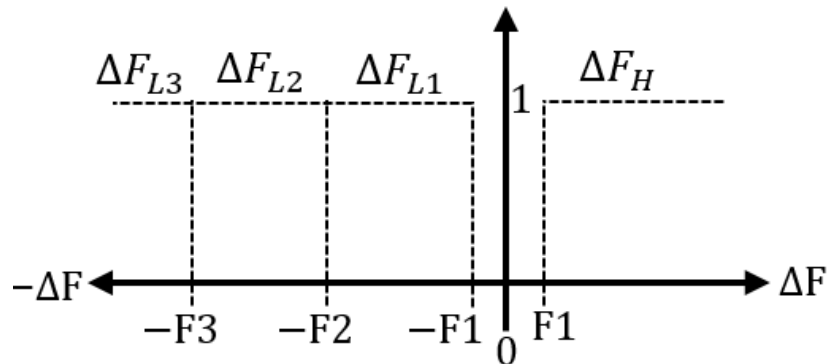


Figure 4.4. Logic indication groups of the frequency deviation levels.

(4.1)

(4.2)

(4.3)

(4.4)

4.3.2 Measurements of water temperature

The desired frequency response (see Figure 4.2) considers the water temperature alongside ΔF . The frequency response is achieved from devices with the highest to the lowest water temperature when the frequency falls. The proposed water temperature measurements are based on four levels (see Figure 4.5) by comparing the User-defined Temperature () with the Measured Water Temperature (). The resulted function ' ' is shown in equation (4.5) by dividing the over the . The logic indicators for these levels are implemented by using equations (4.6) - (4.9). However, the levels could be changed according to the aggregator preferences.

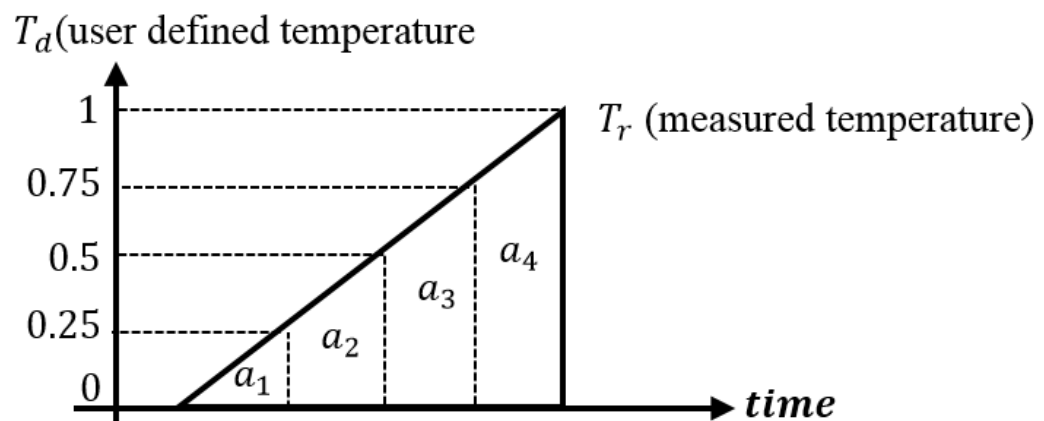


Figure 4.5. The proposed measurements levels for the water temperature.

— (4.5)

(4.6)

(4.7)

(4.8)

(4.9)

4.3.3 Structure of logic circuit and logic control output

The logic outputs of the bands (see Figure 4.4) and the water temperature levels (see Figure 4.5) are used as inputs to the logic gates in the WH controller to generate the logic control output as shown in Figure 4.3. The control output is a logic control signal to switch 'ON/OFF' the devices, where 1 is for 'ON' and 0 is for 'OFF' control output. The desired response of the aggregated devices is shown in Figure 4.2, to generate this response, the output of the device controller should be assigned with the state conditions shown in Table 4.1 when the aggregator command signal is logic 1. The state conditions presented in Table 4.1 are implemented using the complete logic circuit shown in Figure 4.6. The device controller will respond based on the last command signal received from the aggregator. Therefore, the WH will respond even when a failure occurs in the communication, the output of the controller is stored as a logic vector.

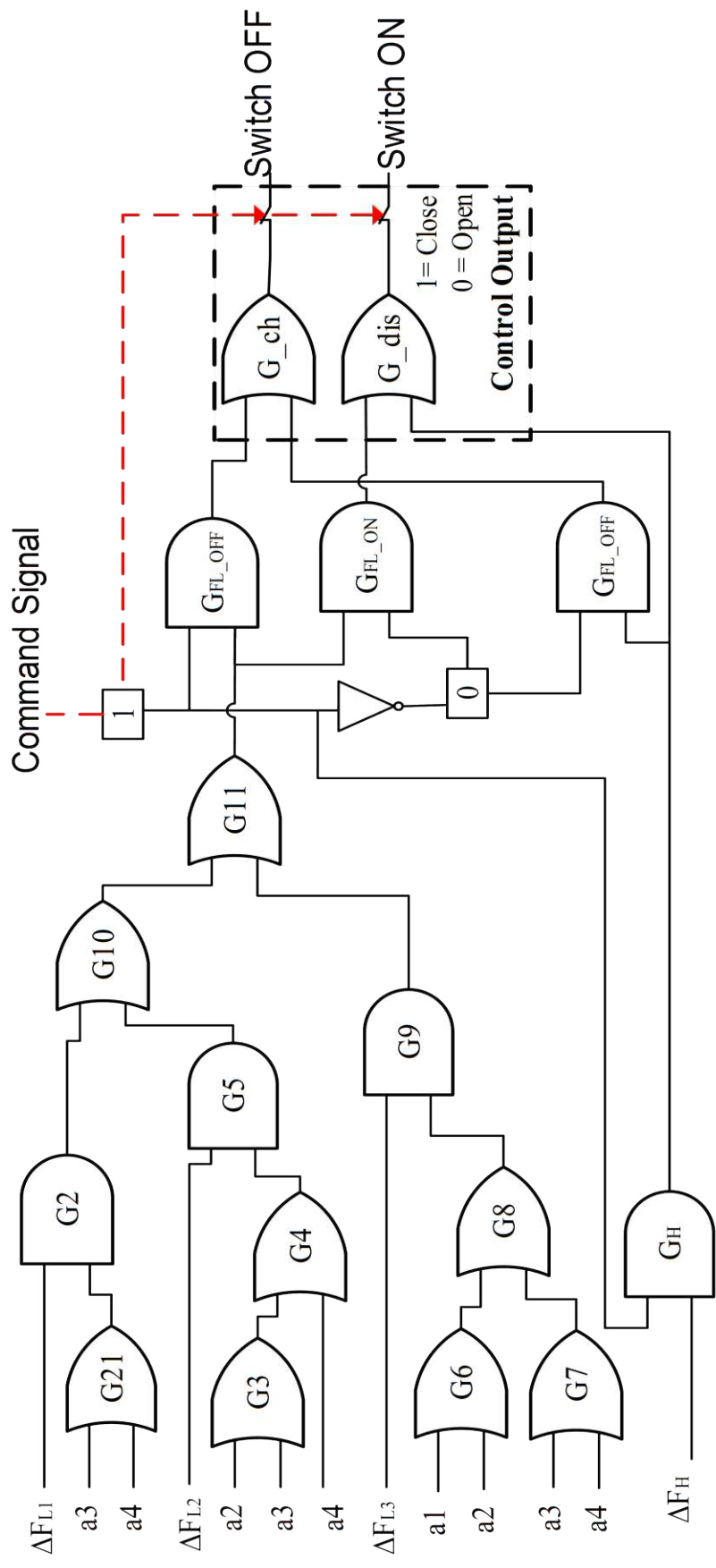


Figure 4.6. The logic circuits and logic control in the proposed water heater controller.

Table 4.1. States conditions³ of the switching in the device controller (NC= no change) for the negative .

	NC	NC	OFF=1 ON=0	NC
	NC	OFF=1 ON=0	OFF=1 ON=0	NC
	OFF=1 ON=0	OFF=1 ON=0	OFF=1 ON=0	NC
	OFF=1 ON=0	OFF=1 ON=0	OFF=1 ON=0	NC

4.4 Modelling of a population of controllable water heaters

It is assumed that all WHs devices receive logic 1 command signal from the aggregator to enable their controllers and provide frequency response services when required. Therefore, modelling the dynamic behaviour of the aggregated devices has two main parts: (i) Modelling the dynamic behaviour of devices' population just before the frequency event with their nominal power (initial condition), and (ii) Modelling the dynamic switching 'ON/OFF' for the devices' population during a frequency event. The latter is used to calculate the probability of the deviation of aggregated power from the nominal power of devices' population (of part (i)) during the frequency event. Markov model is a way to model overlapping sets of information to reflect our understanding of regions. It provides a

³ *For Example:* suppose that $F1=0.015$ Hz, $F2=0.05$ Hz, and $F3=0.1$ Hz (showed in Figure 4.4), and there is a frequency deviation Δ equal to -0.03 Hz. Therefore, the proposed controller will activate the device response by comparing value with the value of the device water temperature ' '. According to Figure 4.4, the logic output is 1. Hence, in Figure 4.6, the G2 gate logic output is 1 if the device is at or temperature level. Hence, GFL_OFF will give an output equal to 1 and activate the 'Switching OFF' device's response. A similar mechanism is applied to the rest of the levels. When a positive is indicated, the GH gate is multiplied by logic 1 to activate the 'Switching ON' device response.

stochastic model of diffusion which applies to individual objects. As a result, it gives us the foundation for diffusion we've studied. Therefore, Markov chain was used to represent the dynamic behaviour of the states of the population of water heaters [9-11, 52]. Hence, a developed Markov-based representation is used for the modelling work.

4.4.1 Modelling the dynamic behaviour of WHs population

The representation of the ERWHs and HPWHs was achieved based on Markov Chain states diagram (see Figure 4.7). The device model was implemented by Markov Chain matrices to represent the deviation of the power consumption of the aggregated load. The HPWH was modelled using four operation states: 'ON', 'OFF-Locked', 'OFF', and 'ON-Locked'. To represent the nature of the compressor in HPWH, it was assumed that when the device is switched to 'ON-Locked' or 'OFF-Locked', it will remain in this state during the control period. The ERWH was modelled according to only two states 'ON' and 'OFF' because it has no compressor. The μ_1 and μ_0 (see Figure 4.7) are the switching probability factors from one state to another. The state diagram of the ERWH is modelled in the state transition matrix shown in equation (4.10), and for the HPWH the state diagram is modelled in equation (4.11) [62, 64].

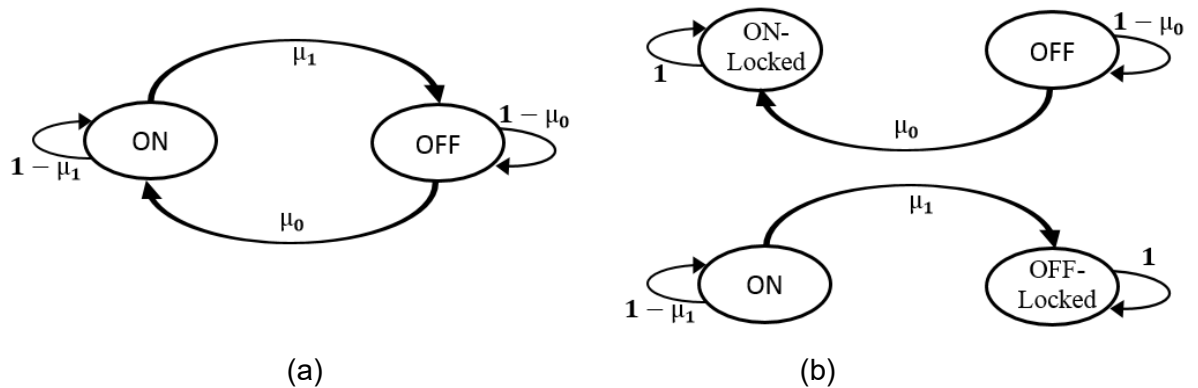


Figure 4.7. Markov-based state transition diagram of the dynamic load behaviour, (a) A population of ERWHs, (b) A population of HPWHs (adapted from [62]).

$$= \tag{4.10}$$

$$= \tag{4.11}$$

Each state shown in Figure 4.7 has an initial condition which represents the capacity (represented by the nominal power) at the moment just before the frequency event. For example, 'ON' is the group of the devices which they are in 'ON' operation condition, and if they have a capacity, for example, equal to 0.1 p.u of the total population. It means that this group is representing 10% of the total summation of initial conditions of all states. The total initial condition (represented by the nominal power) of the ERWH is modelled by the matrix shown in equation (4.12) and for the HPWH in equation (4.13).

$$= \tag{4.12}$$

$$= \tag{4.13}$$

4.4.2 Modelling the dynamic switching of devices during a frequency event

The device control layer can measure the non-zero frequency deviation and probabilistically change their power consumption by switching 'ON/OFF' their controllable amount of power. The amount of the probabilistically switching factors is set according to the value of f and Δf , as shown in Figure 4.7. The value of the α and β are between 0 and 1 according to the basic concepts of the Markov Chain. The value is dynamically linked with the value of the f whether it is positive or negative. When a negative f is measured, this indicates that there is a rise in load or fall in the generation. Therefore, the population will start to turn 'OFF' the controllable end-user loads. Hence, will start to increase the value of α and decrease the value of β , and vice versa when a positive f occurs.

In addition, the devices will not be directly turned 'OFF' at the same, this process will be done by a gradual sequence according to the amount of f , and reach its maximum

amount after a pre-set value. Therefore, fuzzy MSF was proposed to provide this gradual rise or fall in the switching process. The fuzzy membership functions are shown in Figure 4.8 to model the dynamic switching behaviour of the switching probabilities and , showed in Figure 4.7.

These membership functions can dynamically update the value of the switching probabilities (and with respect to the using the switching rules shown in equations (4.14) and (4.15). The proposed MSF are implemented by equations (4.16) - (4.19). The start/end values ($F1$, and $F3$) are similar to the values of the frequency bands in the device controller. This process is simulating the population response to provide a frequency response services starting/ending at a pre-set value of ⁴.

$$\text{---} \tag{4.14}$$

$$\text{---} \tag{4.15}$$

$$\text{-----} \tag{4.16}$$

$$\text{-----} \tag{4.17}$$

$$\text{---} \quad \text{-----} \tag{4.18}$$

⁴ The value of 'F1' is related to the beginning of the service and the dead band value, for example, it is assumed to be 0.015 Hz.

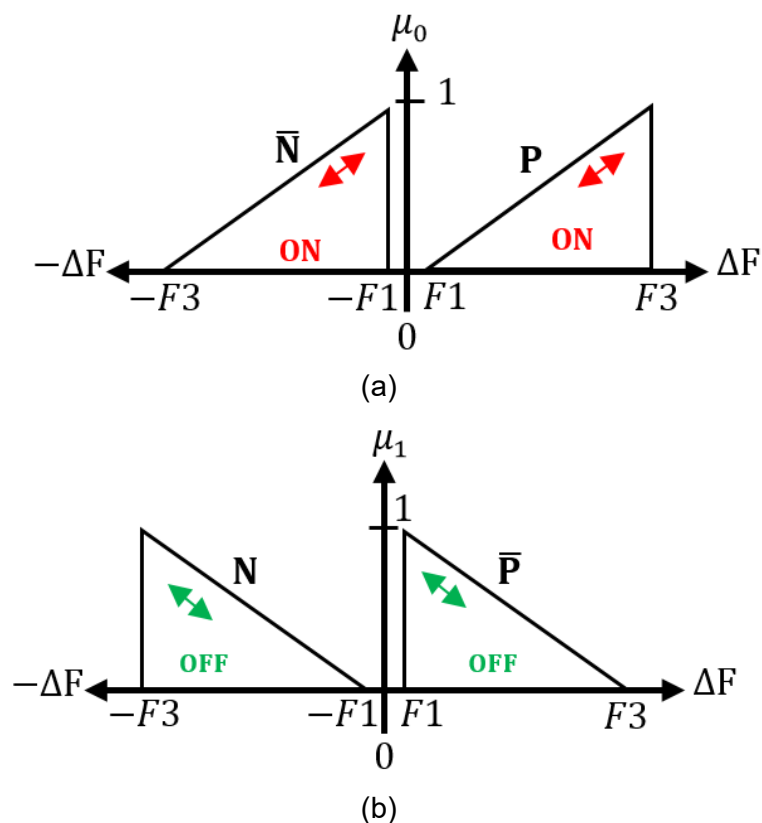


Figure 4.8. Proposed MSF to represent the dynamic switching conditions in a population of WHs, (a) the switching into ‘ON’ state, (b) the switching into ‘OFF’ state.

The updated values of the switching probabilities (μ_0 and μ_1) are used to dynamically re-update the state transition matrix showed in equations (4.10) and (4.11). After updating (μ_0 and μ_1), the initial condition (the nominal power) of the states is dynamically updated during a frequency event using equation (4.20). Equation (4.21) is used to aggregate the total power capacity of the population, (where: P_{ON} and P_{OFF} for ERWH and HPWH, respectively [62, 64]).

$$(4.20)$$

$$(4.21)$$

The value of $F1$, $F2$, and $F3$ (shown in Figures 4.8) are important to have a good frequency response. The start ($F1$) is the value when start switching 'OFF' the devices while the end ($F3$) is the value when all devices should be switched 'OFF'. Therefore, in the proposed model, the PSO was used to get the optimal value of ' $F1$ ' and ' $F3$ ' of Figure 4.8 with a constrained optimisation algorithm between 0.01 and 0.25 Hz. The algorithm was run by using the disturbance of 2008 event sequence in the GB power system (shown in Figure 4.10) which was approximately equal to 0.03 p.u. The optimal values are equal to ' $F1=0.015$ ', and ' $F3=0.248$ ' by minimising the ISE of the during the disturbance. The modeling process of the proposed controllable WHs is shown in Figure 4.9.

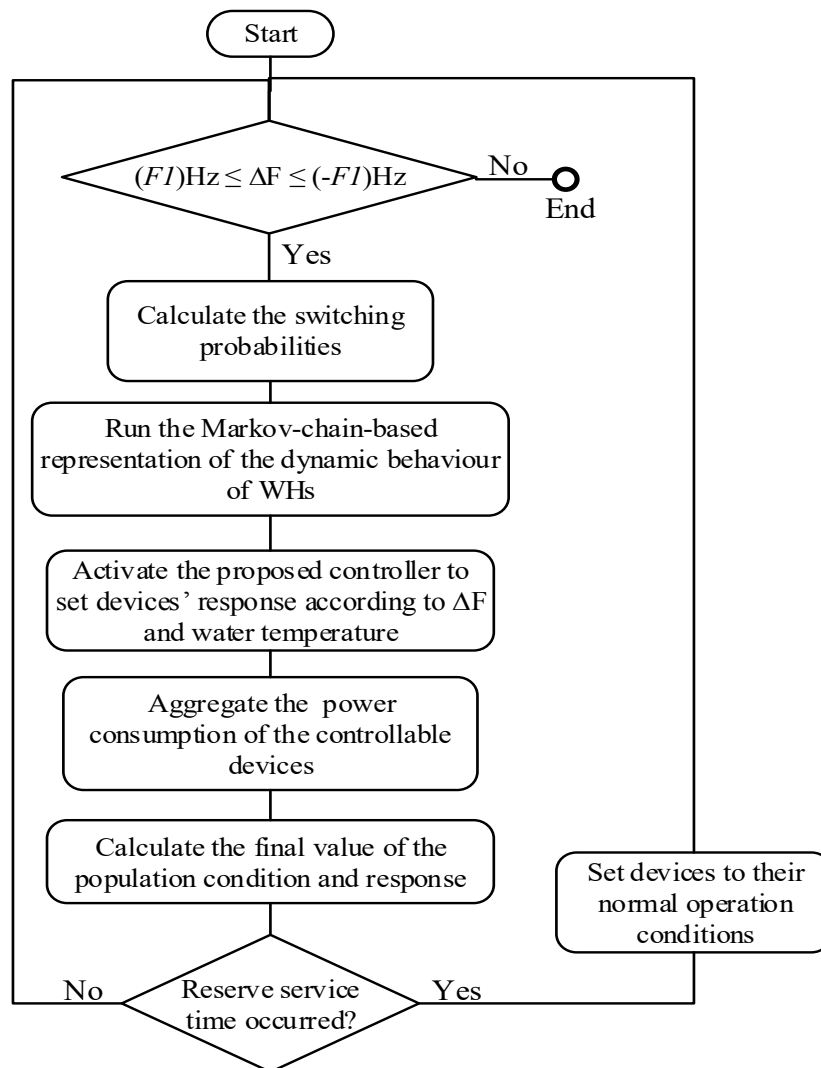


Figure 4.9. Flowchart of the modelling process of the control of a population of WHs.

4.5 Demonstration of the proposed control of WHs

The Markov-based model presented in section 4.4 is developed to demonstrate the proposed hierarchical control of WHs. The following assumptions were considered for the initial values: for HPWH 30% in 'ON' state, 10% in 'OFF-Locked' state, 50% in 'OFF' state, 10% in 'ON-Locked' state, and for ERWH 30% in 'ON', 70% in 'OFF' state.

The water temperature measurement, as shown in Figure 4.5 and equation (5), is considered for the 20 seconds' simulation period. Realistic water temperature demand profile of a water heater was considered from [146], covering: two bathing events, one in the morning and another in the evening. It also takes care of the hot water required for the washing and the cleaning purpose during noontime. The load profile showed that the change of the water temperature takes longer than the service time in the simulation period. Therefore, no noticeable change in T_w in equation (4.5) is observed of the temperature measurements during the frequency event in the simulation period. Hence, the value of T_w was assumed to be equal to 0.2 in all cases.

It is assumed that the frequency service from the controllable WHs is available for 24 hours. The aggregators provide the full power of their controllable devices for frequency response services (i.e. primary + secondary). The modelling of the controllable WHs population and the simulation results were carried out in MATLAB PowerSim, and designs code is shown Appendix A4. The results were stored as vectors for visualising the comparison of the results.

4.5.1 Simplified GB power system

The simplified GB power system model (see Figure 4.10) is used for the aggregation of various generation units. The disturbance of 2008 event in the GB power system was applied and is equal to 0.03 p.u [71, 136, 147-149]. The Markov-based model of the controllable WHs was implemented in the block of controllable WHs shown in Figure 4.10.

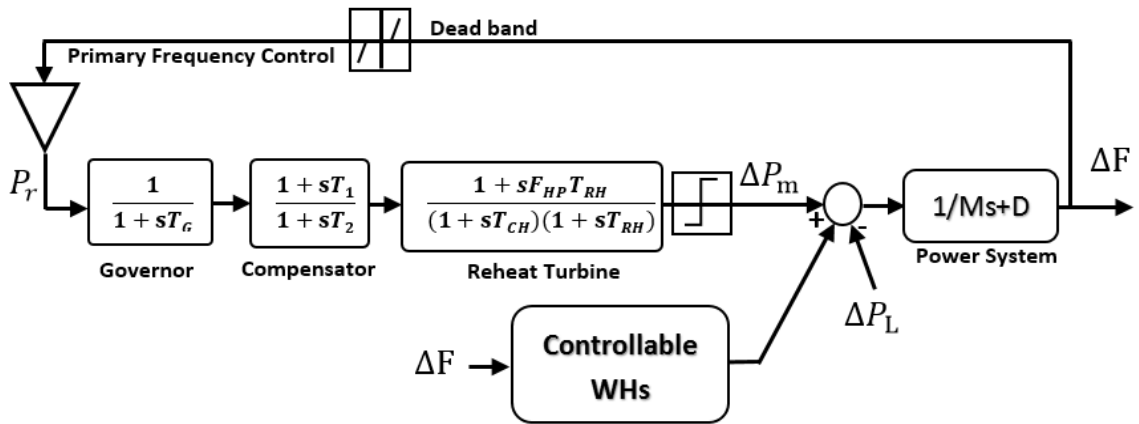


Figure 4.10. Simplified GB frequency control model with controllable WHs.

The simulation results using the simplified GB power system showed that the aggregation of controllable WHs reduced the frequency deviation and error to a lower value than without using controllable WHs. (see Figure 4.11).

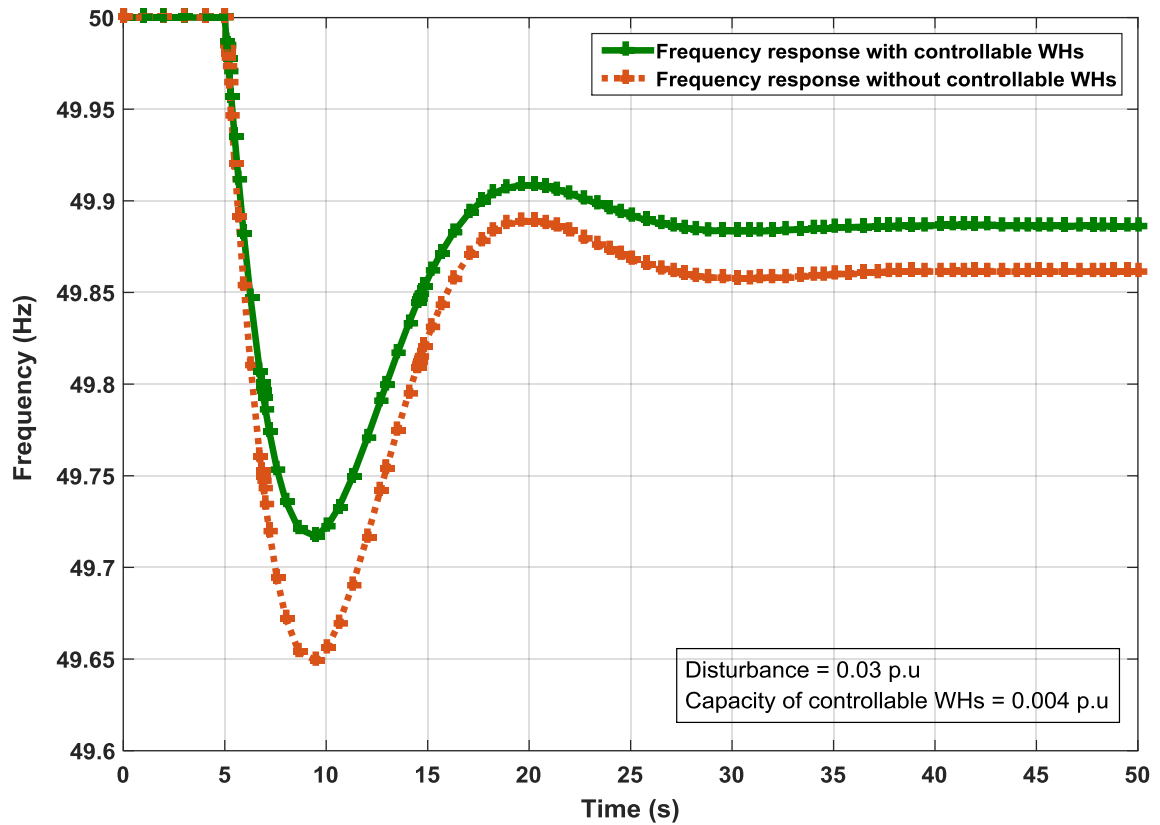


Figure 4.11. The frequency response of the simplified GB power system following a disturbance.

4.5.2 The South-East Australian power system

It is important to test the proposed model of controllable WHs in a multi-machine large power system. The South-East Australian model (IEEE 14-machine 59-bus, 5-area, and see Figure 4.12) was used for testing new control techniques (further details in section 2.7.3 [130, 131]). The model was developed in SimPower Systems, which is a MATLAB/Simulink package [130]. Each controllable load represents an aggregator with different size of controllable devices. Three different aggregators connected in different areas were implemented as shown in Table 4.2 and Figure 4.12.

Table 4.2. The assumption of controllable WHs types for each aggregator.

	Aggregation of ERWH (MW)	Aggregation of HPWH (MW)	Total (MW)
Aggregator 1	30	50	80
Aggregator 2	42	50	92
Aggregator 3	50	60	110

The disturbance occurred in 28\9\2016 in the South Australian power system was considered with a loss of wind generation units about 311 MW. The disturbance was applied at time $t=5s$ in the simulation study cases. This disturbance was considered as a sudden increase in the load at busbar 405 in area 4 (see Figure 4.12). Three study cases of aggregators are used, case X1 is for the use of one aggregator, case X2 is for the use of two aggregators, and case X3 is for the use of three aggregators as shown in Table 4.3.

Table 4.3. Study cases for the simulation results.

	Study cases		
aggregator at:	X1 (MW)	X2 (MW)	X3 (MW)
1-Bus 206 (area 2)	80	80	80
2-Bus 312 (area 3)	0	0	110
3-Bus 408 (area 4)	0	92	92
Total (MW)	80	172	282

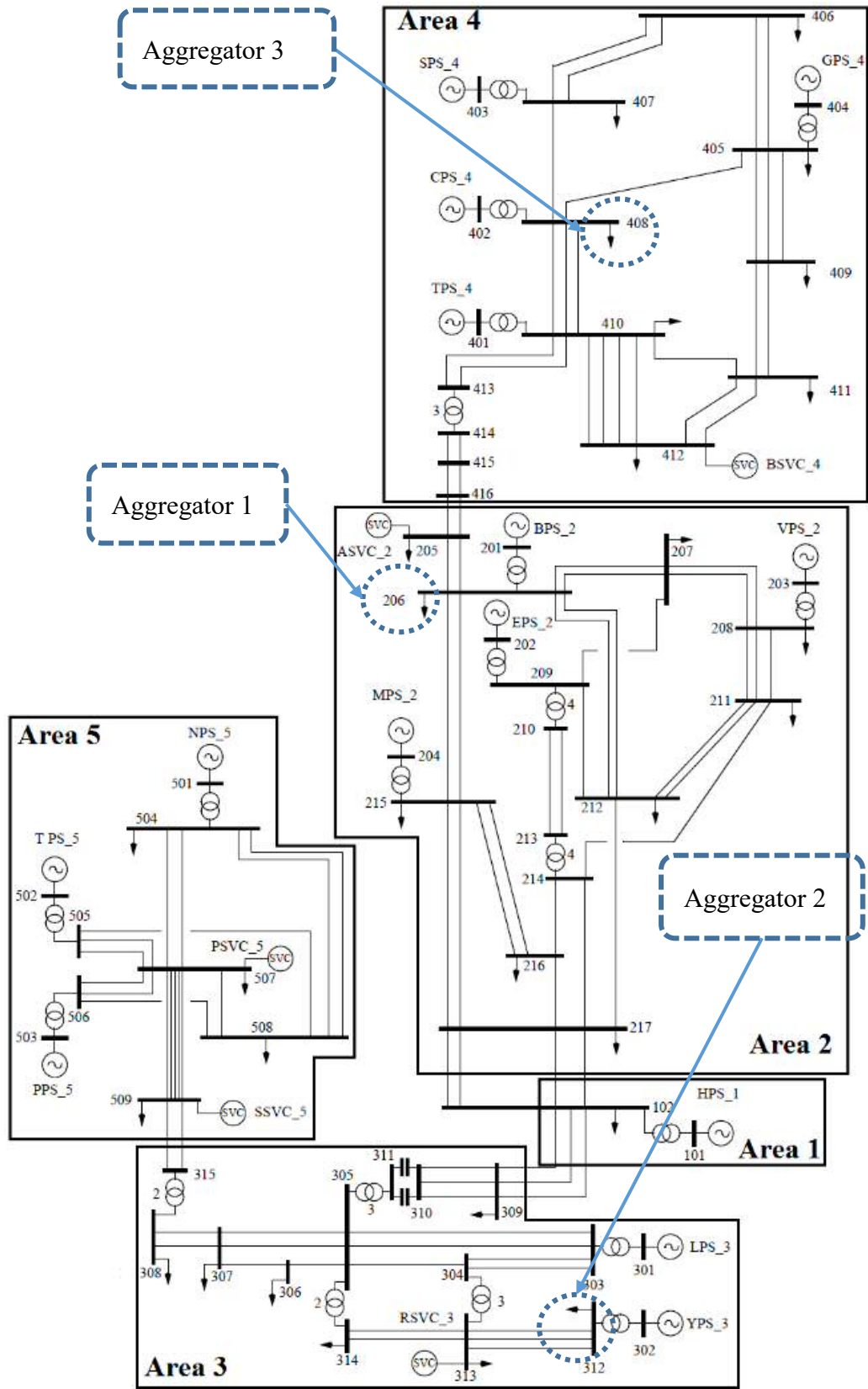


Figure 4.12. IEEE 14-machine 59-bus, 5-area, the South-East Australian power system [131, 150].

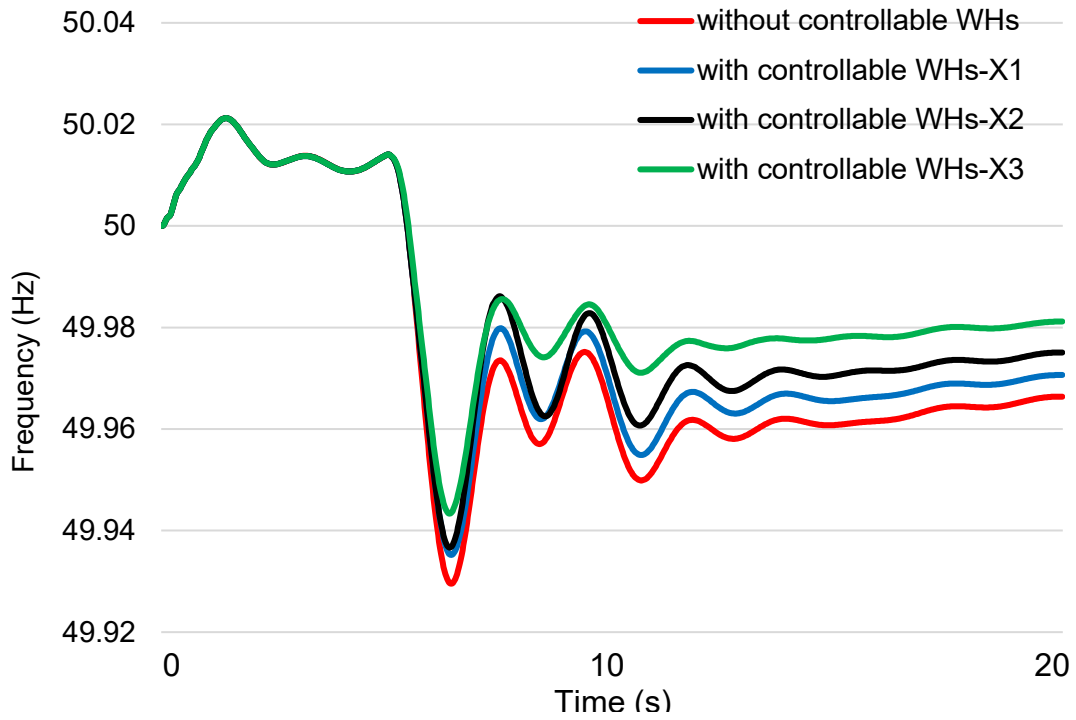


Figure 4.13. Frequency response comparison at the power generation unit of busbar 203-area 2.

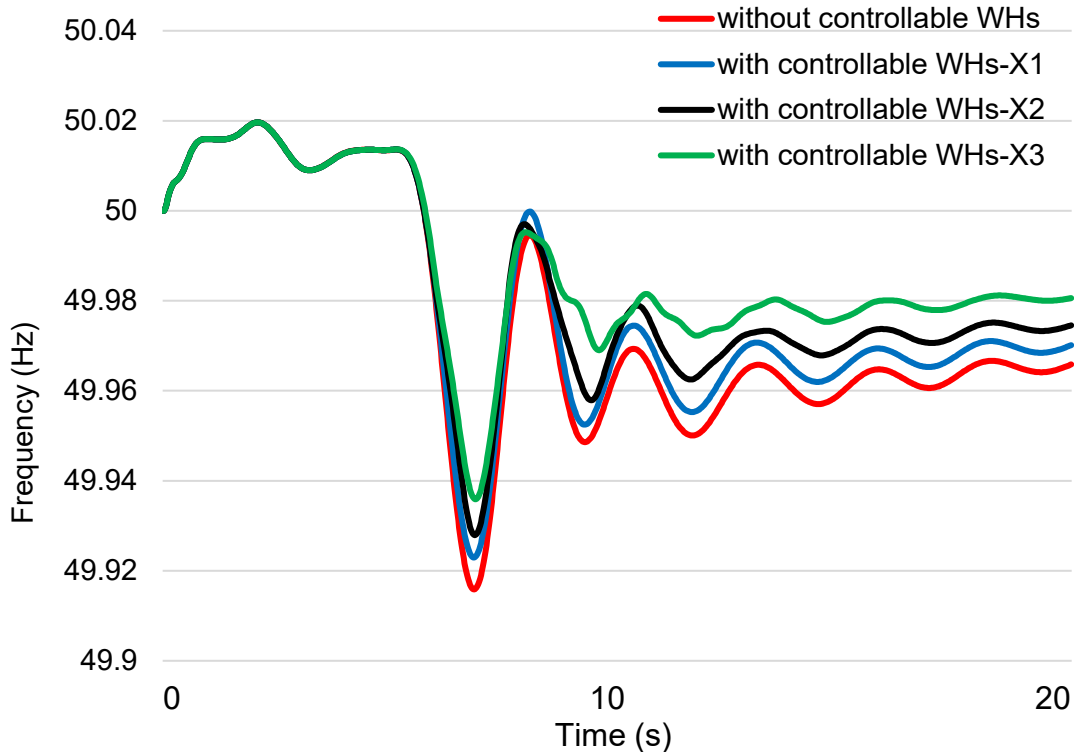


Figure 4.14. Frequency response comparison at the power generation unit of busbar 301-area 3.

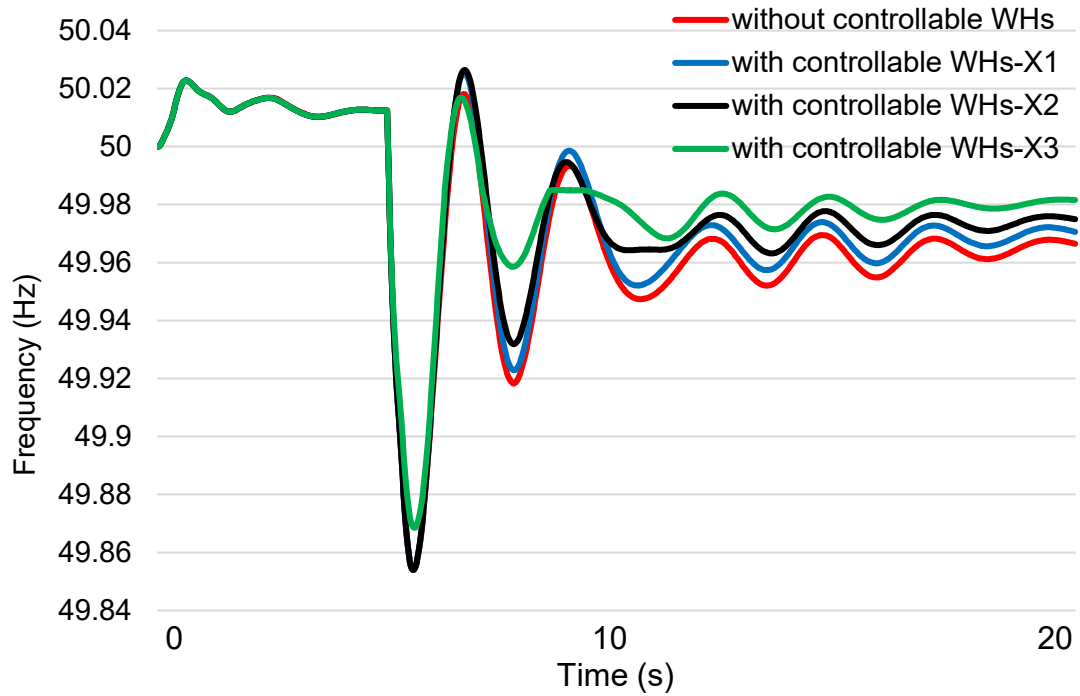


Figure 4.15. Frequency response comparison at the power generation unit of busbar 404-area 4.

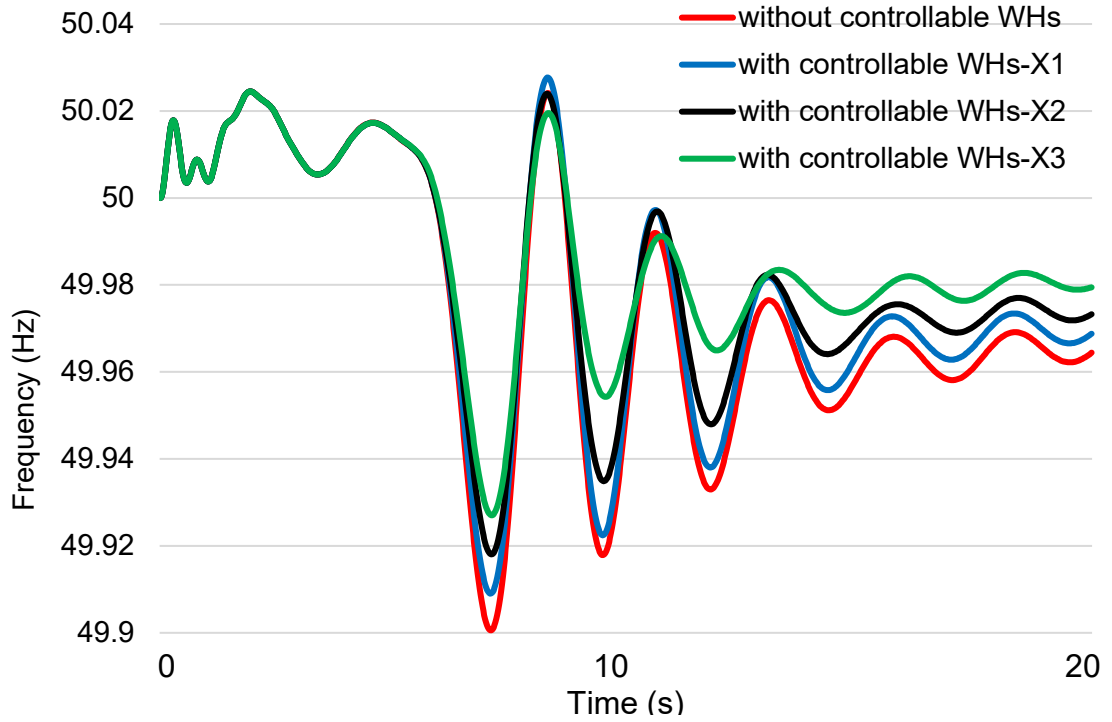


Figure 4.16. Frequency response comparison at the power generation unit of busbar 501-area 5.

The simulation results, with these study cases, are generated to display the comparison between the system frequency response with and without controllable WHs. Figure 4.13 – Figure 4.16 shows the simulation results at different generation units in the wide-area South-East Australian power system. The frequency deviation and the steady state error were improved by integrating the controllable WHs. Increasing the number of load aggregators (from case X1 to case X3), hence, increasing the controllable amount, leads to more frequency response improvement than without WHs aggregators.

4.6 Summary

A hierarchical control of WHs for frequency response was presented, and a WH controller was developed to provide frequency response services when required. A Markov-based model was used to simulate the behaviour of controllable WHs. The proposed control of a population of WHs can be applied in the future aggregation of large distributed WHs to provide frequency response services. The WHs controller provides a response based on the last command signal received from the aggregator, the value of ΔF , and the level of water temperature. However, it responds independently in the case of losing communications. Therefore, the proposed hierarchical control of WHs is not fully centralised or fully decentralised method for controlling large distributed controllable loads. In addition, the developed Markov-based representation of controllable WHs proved to be a useful tool to demonstrate the potential for a WHs aggregator and to evaluate the effective population capacity during the frequency service. With an initial of 30% 'ON', an aggregation of 280 MW of devices from different areas was effective in improving the frequency deviation and error following a disturbance in the South-East Australian power system with a system load base equal to 14.5 GW.

Chapter 5

Control of a Population of BESSs for Frequency Response

5.1 Introduction

It is estimated that the growth of electrical energy storage capacity in the GB power system by 2050 will be about 10.7 GW in one of system operator's future scenarios (for example, Consumer Power Scenario) [74]. The deployment of residential and non-residential BESSs is increasing due to the technical developments and cost reduction as well as high levels of PV panels' integration [73, 74]. A large number of these BESSs are connected to distribution networks and behind the meters [74, 76, 79, 80]. The capacity of BESSs is growing due to the improvements in their technologies as well as the cost reduction [151-153]. However, the efficient use of these systems for frequency response services is a new research field to explore. There are important challenges associated with the control of large distributed loads such as residential BESS [24].

Many previous work have considered the control of BESSs in either centralised or decentralised control methods [72, 76, 79, 80]. However, and to the author knowledge, none of them has considered to develop a control method that compromises the advantages of both centralised and decentralised control methods. Therefore, a developed control of large distributed residential and non-residential BESSs is considered in this chapter to provide frequency response services in future power systems.

5.2 Hierarchical control of BESSs

It is assumed that BESSs with different capacities are distributed throughout the power system. A demand aggregator, which is a third party company, aggregates these BESSs to offer frequency response services when required. This is done by integrating a controller into each BESS to control its charging/discharging processes. The demand

aggregator has a central controller, which is represented by the aggregator layer (see in Figure 5.1). The aggregator layer collects the SoC of BESSs and sends command signals to enable/disable each BESS controller in the BESS control layer.

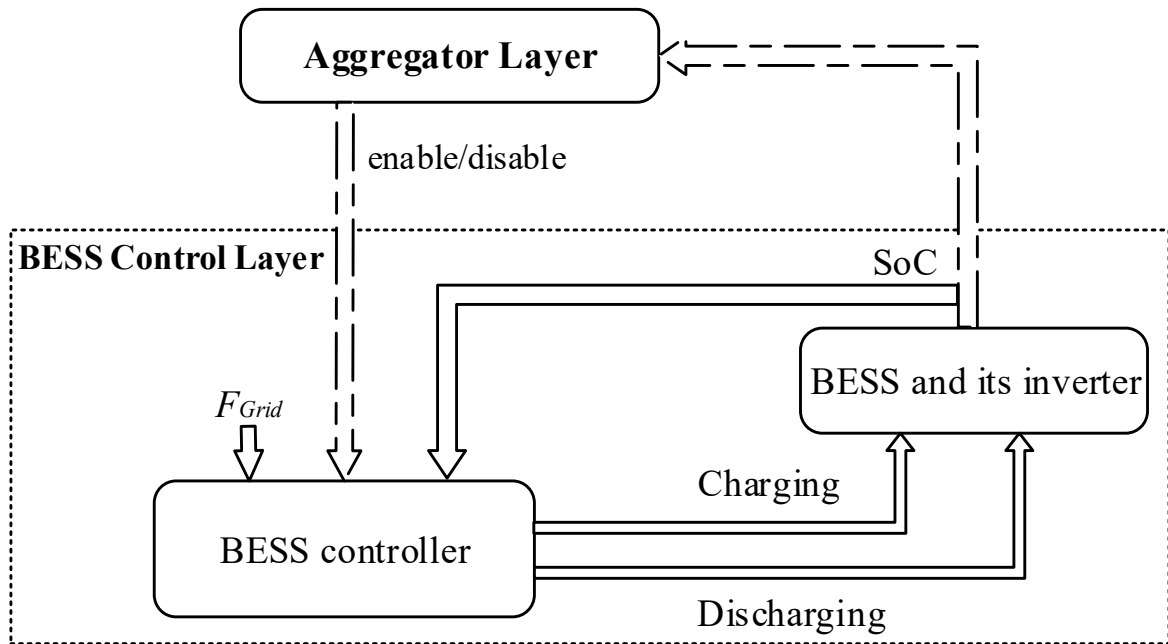


Figure 5.1. The block diagram of the hierarchical control of BESSs.

The relationship between the number of cycles and the depth of discharge of the battery has an impact on the degradation of the battery [154]. The lowest level of SoC is the lowest number of cycle, and therefore, the highest risk of reducing the life of the battery [153, 154]. Hence, considering the level of the SoC for the aggregated responsive BESSs is important as there may be hundreds of cycles each year when providing frequency response service.

Therefore, the BESS controller has pre-set frequency bands as shown in Figure 5.2. The response depends on the frequency deviation and the BESS SoC. This response depends on the ΔF and the BESS SoC. The, BESSs will respond starting from the highest SoC to the lowest SoC when the frequency drops below a nominal value. When a frequency rises above a nominal value, BESSs will respond starting from the lowest SoC to the highest SoC. As a result, the risk of a simultaneous power change of a large number of BESSs

during low-frequency is reduced. In addition, prioritising the BESSs SoC reduces battery degradation.

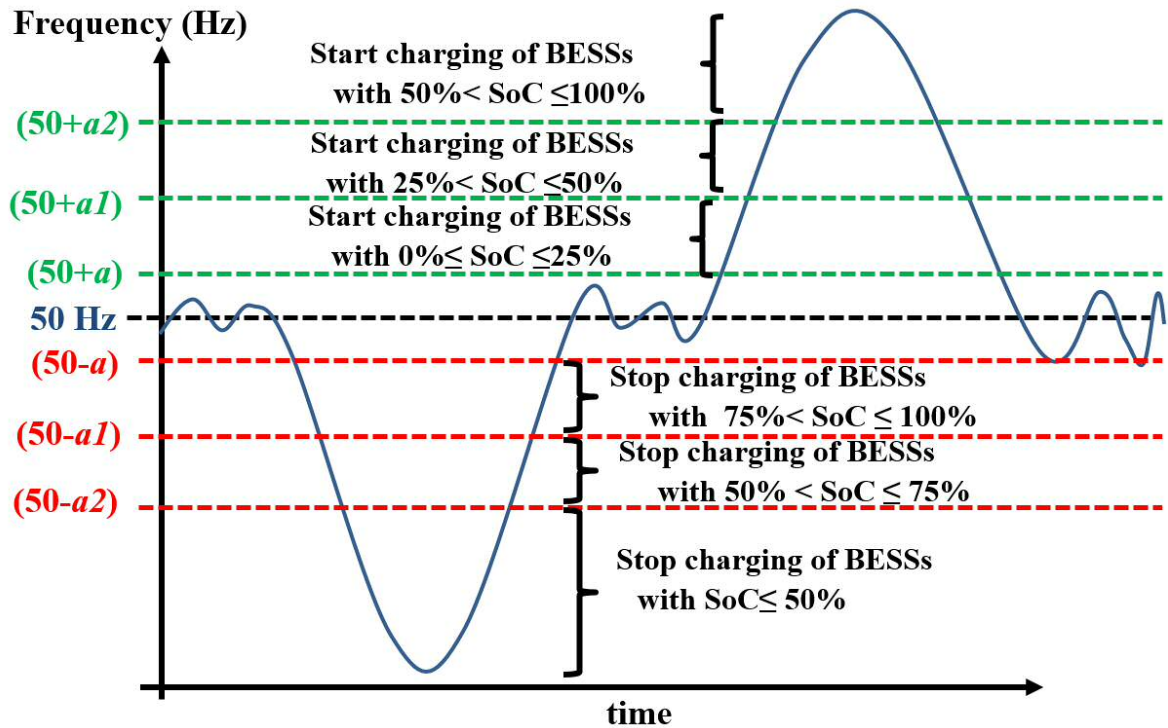


Figure 5.2. The desired response of a population of BESSs during a frequency event.

5.3 Structure of the proposed BESS controller

Figure 5.3 displays the BESS controller structure, which has three main components: (i) Measurement of SoC levels, (ii) Measurements of frequency deviation and (iii) The logic gates to control the BESS charging and discharging according to (i), (ii), and the aggregator enable/disable command signal. The command signals of the aggregator control layer are either logic 1 to enable the BESS controller or logic 0 to disable it.

Collecting the SoC values of all BESSs allows the aggregator to decide the available response capacity from the population of BESSs. In addition, in the case of discharging the BESSs and injecting power back to the grid, the proposed hierarchical control allows the aggregator to decide the response time of the BESSs according to their SoC levels. Therefore, the uncertainty in the response of the aggregated BESSs will be reduced during

the frequency service period. In this work, it assumed that that all BESSs receive logic 1 command signal to enable their controllers and provide frequency response when required. The design of each component is explained as follows:

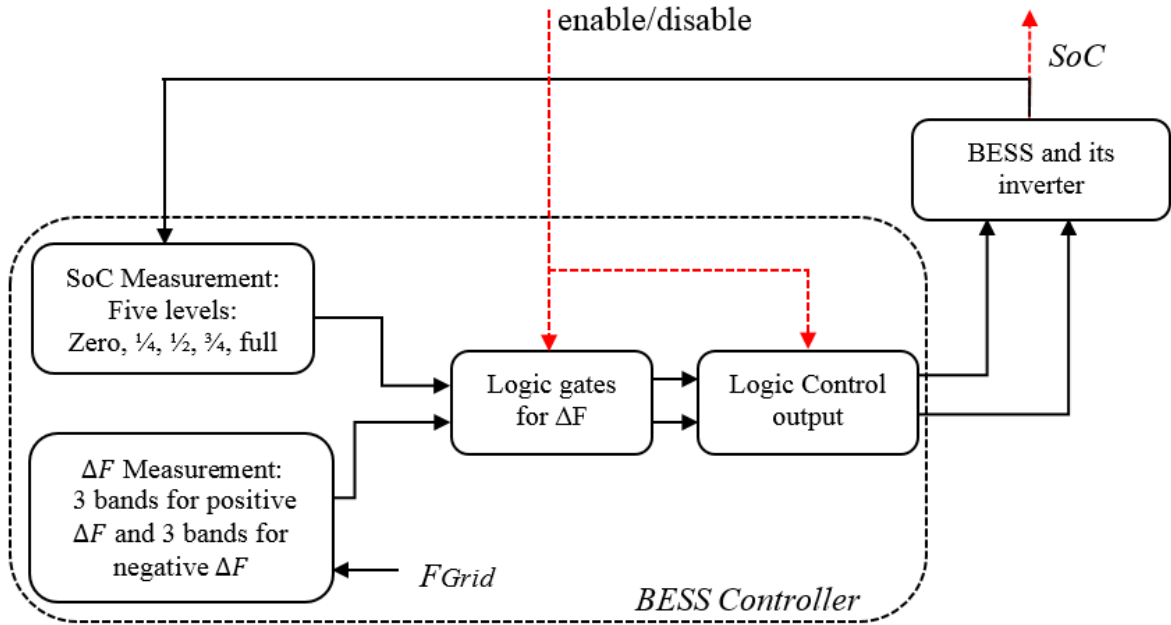


Figure 5.3. The block diagram of the BESS controller.

5.3.1 Measurements of SoC level

It is assumed that the SoC of a BESS lies within one of the following levels: 0%, 25%, 50%, 75%, and 100% SoC as shown in Figure 5.2. The logic outputs of the indicators of these levels are $C1$, $C2$, $C3$, $C4$, and $C5$ for 0% SoC, 25% SoC, 50% SoC, 75% SoC, and 100% SoC, respectively (see Figure 5.4). Equations (5.1) - (5.5) were used to categorise all BESS into one of these indicators. These indicators are the input to the logic gates of BESS charging/discharging control (see Figure 5.3).

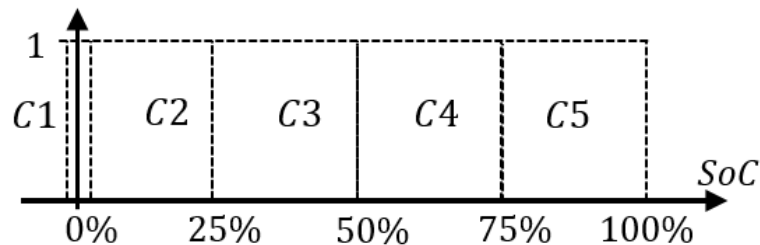


Figure 5.4. Logic bands for measurements of SoC level.

(5.1)

(5.2)

(5.3)

(5.4)

(5.5)

5.3.2 Measurements of frequency deviation

As shown in Figure 5.2, there are three levels of positive frequency deviations (i.e. $\Delta F_{H1,2,3}$) and three levels for negative frequency deviations (i.e. $\Delta F_{L1,2,3}$). These levels represent six bands of logic indicators as shown in Figure 5.5. The system frequency deviations are located within one of these bands using equations (5.6) - (5.11), where $\Delta F = F_{Grid} - 50$. The number of these bands is set according to the aggregators' preferences and the preferred degree of the frequency response smoothness. Hence, the higher the number of bands is the smoother the response of a population of BESSs. The value of the ΔF -axis parameters, (a , $a1$, and $a2$) are set by the aggregator and can be updated if necessary.

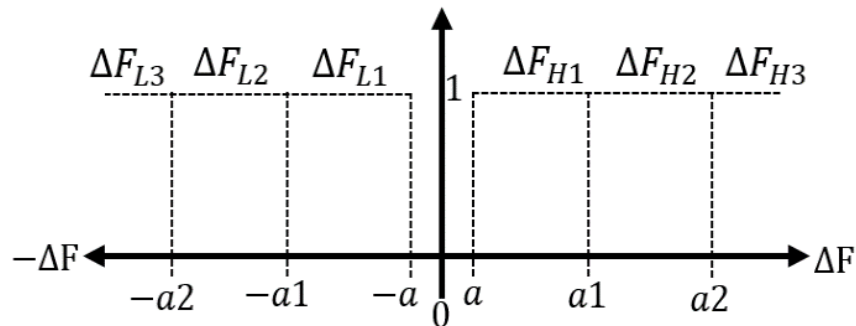


Figure 5.5. Six logic frequency bands in the BESS controller.

(5.6)

(5.7)

(5.8)

(5.9)

(5.10)

(5.11)

5.3.3 Structure of logic gates and logic control output

As shown in Figure 5.3, the output of the SoC measurements and frequency deviations measurements are used as inputs to the logic gates, the output of the logic gates and logic control output is either enable the charging /discharging of the battery when logic 1 or disable it when logic 0. Some of the logic gates and the control output's switches are controlled by the command signal received from the aggregator control layer. The command signal is either 1 to enable the BESSs controller or 0 to disable it. Therefore, when the command signal is logic 1, the BESS will provide a frequency response by charging/discharging the BESS as shown in the logic truth table in Table 5.1 and Table 5.2. As a result, the BESS controller provides a response based on the last command received from the aggregator control layer. Hence, the controller works independently when any failure occurs in the communication with the aggregator control layer. Therefore, the proposed control method is not fully centralised nor decentralised in controlling large distributed BESSs. The complete logic circuit of the BESS controller is shown in Figure 5.6.

Table 5.1. Truth table of the control output of the charging operation (NC=no change).

	0% SoC	25% SoC	50% SoC	75% SoC	100% SoC
	NC	NC	NC	NC	0
	NC	NC	NC	0	0
	0	0	0	0	0
	1	1	NC	NC	NC
	1	1	1	NC	NC
	1	1	1	1	1

Table 5.2. Truth table of the control output of the discharging operation (NC=no change).

	0% SoC	25% SoC	50% SoC	75% SoC	100% SoC
	NC	NC	NC	NC	1
	NC	NC	NC	1	1
	1	1	1	1	1
	0	0	NC	NC	NC
	0	0	0	NC	NC
	0	0	0	0	0

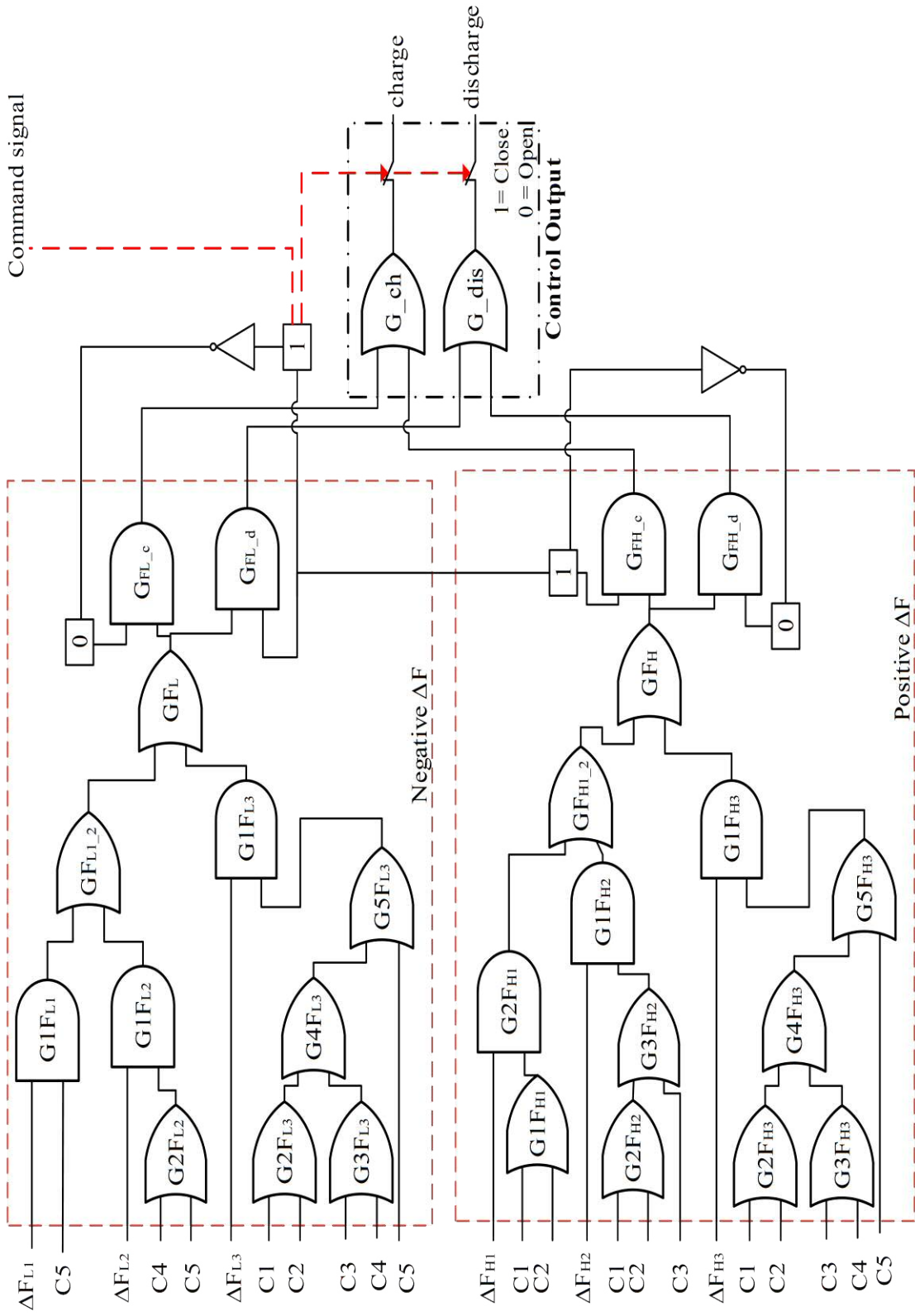


Figure 5. 6. Detailed logic Circuits in the proposed BESS controller.

5.4 Modelling of a population of controllable BESSs

A model of a population of controllable BESSs was designed to demonstrate the potential of the proposed hierarchical control scheme for an aggregator and to quantify the effective response capacity during the provision of the frequency service. As described in section 5.2 and Figure 5.2, the dynamic behaviour of the population of BESSs will be grouped into five different states according to their SoC levels: 0% SoC, 25% SoC, 50% SoC, 75% SoC, and 100% SoC. Therefore, modelling the dynamic behaviour of the population was divided into two parts. (i) Modelling the population of BESSs before the frequency event based on their nominal power (i.e. their initial condition of BESSs according to the SoC levels). (ii) Modelling the dynamic switching of controllable BESSs' charging/discharging operation during a frequency event.

In part (ii), the probability of the aggregated power deviation from the population's nominal power (i.e. of part (i)) during a frequency event is calculated. For example, if the population of BESSs is procured to provide the secondary frequency response service to the GB power system, its response could be sustained up to 30 minutes. Therefore, it is necessary to represent the dynamic behaviour of the aggregated power deviation of the BESS population during the event period. Markov-chain, in additions to the motivations explained in section 4.4, was previously used to represent dynamic behaviour of the battery SoC for electric vehicles batteries [77] or for PV charging-based batteries [77, 78]. Hence, a Markov-based model was developed to represent these two parts of the dynamic behaviour.

5.4.1 Modelling the dynamic behaviour of the BESSs population

A Markov-based state diagram representing the dynamic behaviour of the BESS's population is shown in Figure 5.7, this figure was drawn based on [78]. Each state represents one group of the population according to their SoC level. The dynamic transition from/to each state was represented by the transition probabilities P_1 , P_2 , and P_{-1} , P_{-2} , where $P_{1,2}$ and

$P_{-1,-2}$ represent the charging and discharging operations, respectively. The probabilities of the states to remain at zero SoC and full SoC in Figure 5.7 are K_{11} and K_{NN} .

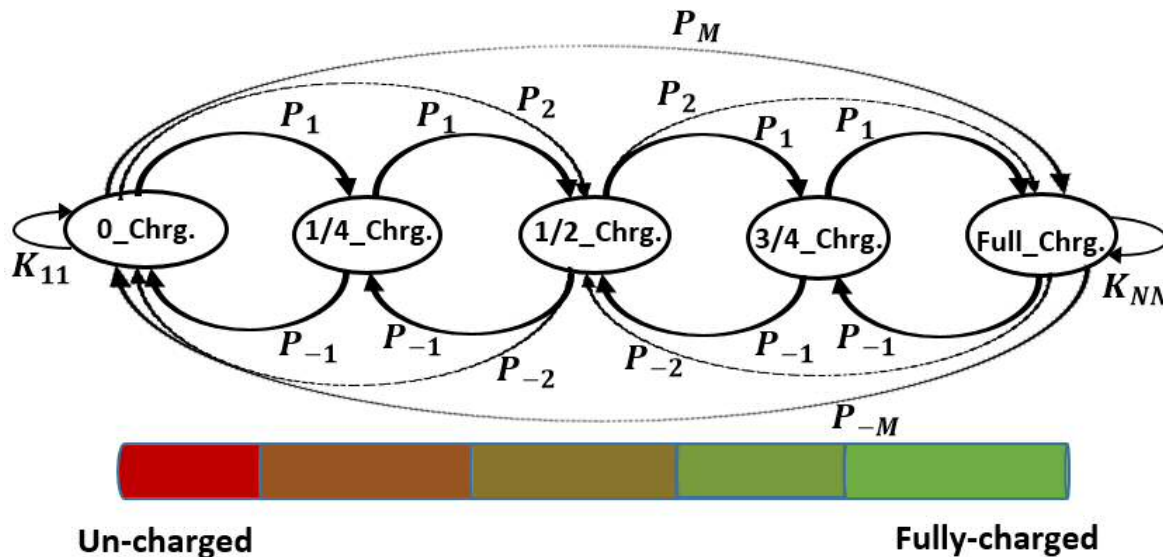


Figure 5.7. State diagram representing the dynamic behaviour of the BESSs population according to five levels of SoC (adapted from [78]).

The state diagram of Figure 5.7 was represented by a 5x5 state transition matrix as presented in equation (5.12) since the population of BESSs are divided into five groups according to the SoC level. Each state has an initial condition at the moment just before the frequency event⁵. The matrix in equation (5.15) represents initial conditions of the five states, where X_{10} represents the BESSs population with 0% SoC, and X_{N0} represents the BESSs population with 100% SoC.

$$(5.12)$$

⁵ For example, the state of 1/4_chrg shown in Figure 5.7 represents the group of BESSs with 25% SoC, if we assume this group has a capacity equal to 0.1 p.u of the total BESSs population. That mean the BESSs with 25% SoC represent 10% of the total capacity of BESSs at the moment just before the frequency event.

Where:

(5.13)

(5.14)

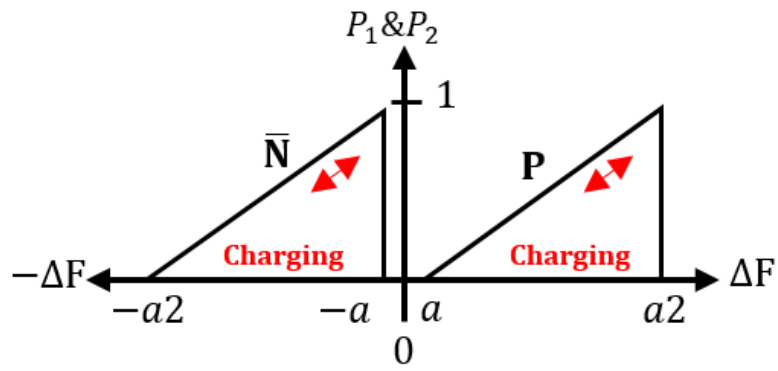
=

(5.15)

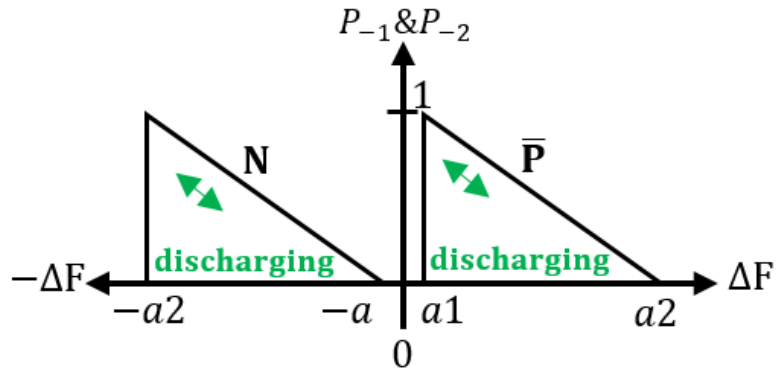
5.4.2 Modelling the dynamic switching of BESSs during a frequency event

The population of BESSs should start responding immediately after a nominal value of frequency deviation is achieved. Therefore, when switching 'OFF' charging of the population of BESSs, the switching probability (P_1, P_2) shown in Figure 5.7 will be set towards 0 to stop the charging. In contrast, the switching probability (P_{-1}, P_{-2}) of the population of BESSs will be set towards 1 to activate the discharging if necessary. Hence, the representation of the dynamic switching of (P_1, P_2) and (P_{-1}, P_{-2}) has a gradual transition from 0 to 1 during the frequency response provision period. This process is simulating the way a population of BESSs respond to a ΔF , which starts from a pre-set value and ends at a pre-set value (a and a_2 in Figure 5.2).

A triangle MSF has a gradual transition of its functions between 0 and 1 [136, 147-149, 155]. Therefore, this MSF was used to represent this gradual transition behaviour of the (P_1, P_2) and (P_{-1}, P_{-2}) between 0 and 1 (see Figure 5.8) similar to Chapter 4. The population response starts with 'a' value of the first frequency band and ends with 'a2' value where all BESSs should respond. The MSF can dynamically update the value of the switching probabilities (P_1, P_2) and (P_{-1}, P_{-2}) of the BESSs population using switching rules. These switching rules are implemented by the mathematical equations of (5.16) - (5.17). The updated values of (P_1, P_2) and (P_{-1}, P_{-2}) are used to dynamically re-update the state transition matrix of equation (5.12).



(a)



(b)

Figure 5.8. MSFs for the switching of the BESSs population, (a) switching probabilities into 'charging' state, (b) switching probabilities into 'discharging' state.

$$- \tag{5.16}$$

$$- \tag{5.17}$$

After updating the switching probabilities (P_1, P_2) and (P_{-1}, P_{-2}) , the initial condition of the five states are dynamically updated during a frequency event; this is done by using equation (5.18).

$$\tag{5.18}$$

Equation (5.19) is used to find the total responsive capacity of the population of BESSs after updating (P_1, P_2) and (P_{-1}, P_{-2}) and the states' initial conditions. Combining equations (5.19) and (5.20) results in equation (5.21), where $P(1)$ to $P(5)$ represent the updated initial condition of each state.

(5.19)

Where:

(5.20)

(5.21)

The matrix 'C' is also used to represent the dynamic response of the population of BESSs. This is implemented by assigning the value of the matrix's parameters (C_1, C_2, \dots) to either 0 or 1 according to the value of ΔF as shown in Figure 5.2. For example, to force the population of BESSs with 75% SoC and 100% SoC to respond during the second frequency band, i.e. between 'a1' and 'a2' (see Figure 5.2), parameters $C_1, C_2,$ and C_3 are equal to 0, while C_4 and C_5 are equal to 1. The power deviation of the BESSs population is calculated using equation (5.22), where the controllable BESSs in (5.21) is subtracted from the total load (). Figure 5.9 shows the flowchart of the proposed control of the population of BESSs. Figure 5.9 shows the control design for the negative ΔF bands explained earlier only. Similarly, the control design for the positive ΔF bands is implemented.

(5.22)

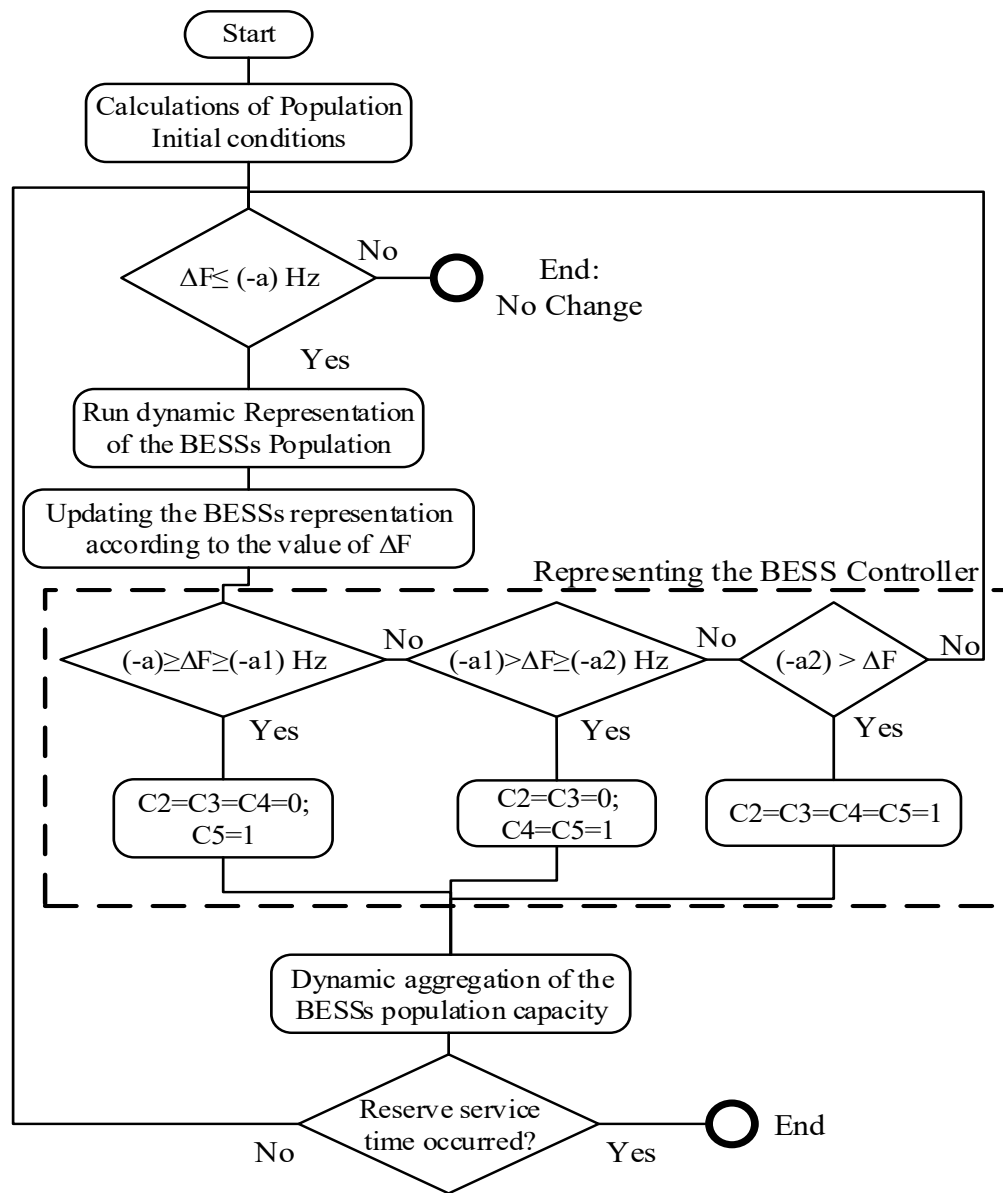


Figure 5.9. Flowchart of modelling process of the proposed control of a population of BESSs.

5.5 Demonstration of the proposed control of BESSs

The modelling and simulation results of the controllable BESSs are carried out using MATLAB® and MATLAB®/SimPowerSystems™. The results are stored as vectors to visualise and compare the results. The developed MATLAB code is presented in Appendix A5.

5.5.1 Simplified GB power system

The simplified model of the GB's power system (see Figure 5.10) was used (similar to the model in Chapter 4) to assess the performance of the controllable BESSs. This model captures the frequency response for different types of generation units. The operating generation capacity and the equivalent inertia (M) value were calculated according to the official reports from National Grid (the GB system operator).

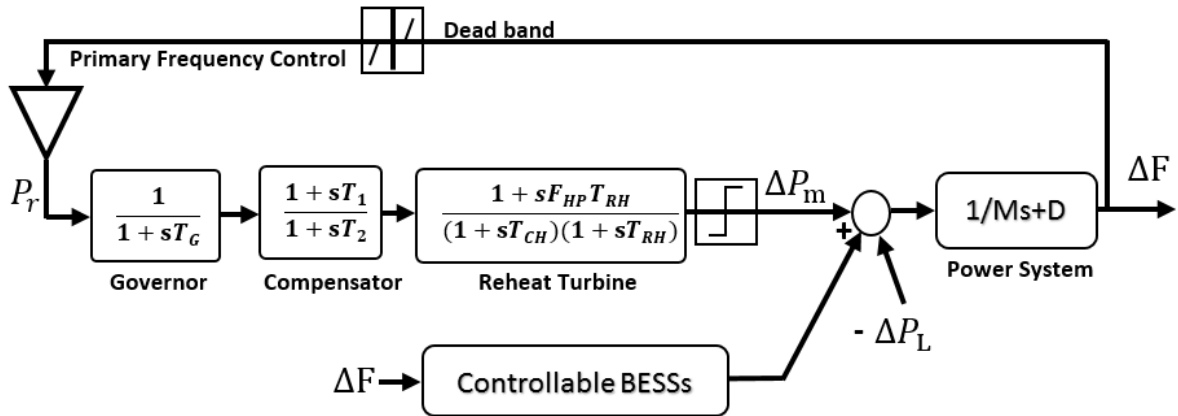


Figure 5.10. Simplified GB power system model for frequency control with controllable BESSs.

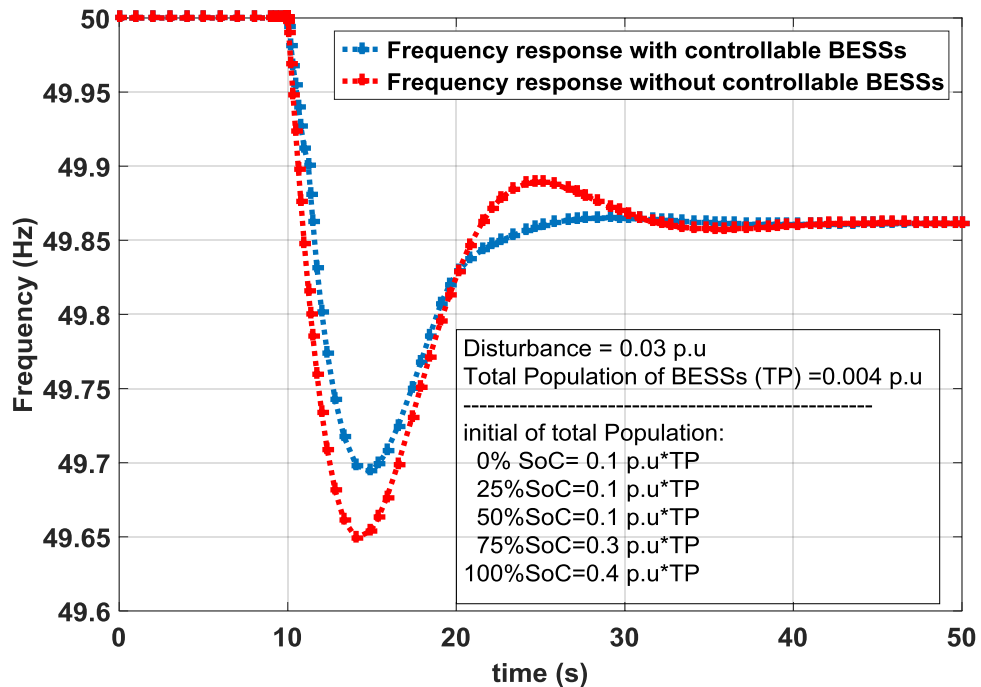


Figure 5.11. Frequency deviations of the simplified GB model after the loss of generation.

The large frequency disturbance, equal to 0.03 p.u., which took place in 2008 in the GB power system, was simulated [71, 136, 147-149]. The system frequency is shown in Figure 5.11. As shown in Figure 5.11, the frequency deviation was reduced due to the response from the population of BESSs through the proposed hierarchical control. The larger capacity of aggregated BESSs, the smoother system frequency response during a frequency even.

5.5.2 The South-Est Australian power system

The 14-machine South-East Australian power system was used to evaluate the proposed control scheme (see Figure 4.12 in Chapter 4). This model was used for testing new control techniques in a power system; further details were presented in section 2.7.3 based on [130, 131]. Each group of controllable loads represents an aggregator with different size of BESSs. Three different aggregators in different areas are considered as shown in Table 5.3 and Figure 5.12.

Table 5.3. Aggregators and their assumption of BESSs' population.

	Non-residential BESSs (MW)	Residential BESSs (MW)	Total (MW)
1-Bus 206 (area 2)	30	50	80
2-Bus 312 (area 3)	42	50	92
3-Bus 408 (area 4)	50	60	110

A large frequency disturbance was considered which recently took place on 28th of September 2016 in the south Australian power system to evaluate the proposed population control. The disturbance started when 123 MW of wind generation were lost followed by another loss of 192 MW wind generation after 6 seconds. This loss of approximately 311 MW generation led to 560 MW interconnector tripping. This event of generation and interconnectors loss sequence was modelled and applied to the test system at $t=5s$, $t=11s$, and $t=13s$, and the simulation results were captured. This disturbance was simulated as a

sudden increase in the load at busbar 405 near generator GPS_4 in area 4 (see Figure 4.12 in chapter 4). The load case 4 in reference [130, 131] was used as the base case of the system load which is approximately 14.5 GW.

Three case studies are considered to represent three realistic possibilities to integrate different aggregators with different capacities, case X1 for the use of one aggregator, X2 for two aggregators, and X3 for three aggregators (see Table 5.4). Also, the initial condition of BESSs according to the level of SoC is assumed as shown in Table 5.5. In addition, the frequency bands parameters, a , $a1$, and $a2$ also have an impact on the population response. Therefore, three different values were considered for the simulation comparison as shown in Table 5.6.

Table 5.4. Study cases for the South-East Australian power system (similar to the cases of capacities presented in Table 4.3).

aggregator at:	Study cases		
	X1 (MW)	X2 (MW)	X3 (MW)
1-Bus 206 (area 2)	80	80	80
2-Bus 312 (area 3)	0	0	110
3-Bus 408 (area 4)	0	92	92
Total (MW)	80	172	282

Table 5.5. Assumptions of initial conditions of the population of BESSs according to the level of SoC.

	0% SoC (C1)	25% SoC (C2)	50% SoC (C3)	75% SoC (C4)	100% SoC (C5)
	0.1	0.1	0.1	0.3	0.4

Table 5.6. Different values of frequency bands parameters.

	a	$a1$	$a2$
Value 1 (Hz)	0.015	0.05	0.1
Value 2 (Hz)	0.015	0.03	0.05
Value 3 (Hz)	0.015	0.02	0.04

5.5.2.1 Different cases of the aggregation capacity

In this section, the aggregators' cases shown in Table 5.4 and value 1 in Table 5.6 are considered. Increasing the number of aggregators and the amount of controllable BESSs leads to a significant reduction in the frequency deviation and frequency error (see Figure 5.12). In case of X3, there are 282 MW of controllable BESSs with high SoC levels, which reduces the highest frequency deviation from 0.23 Hz to 0.14 Hz for the last disturbance sequence at $t=13s$.

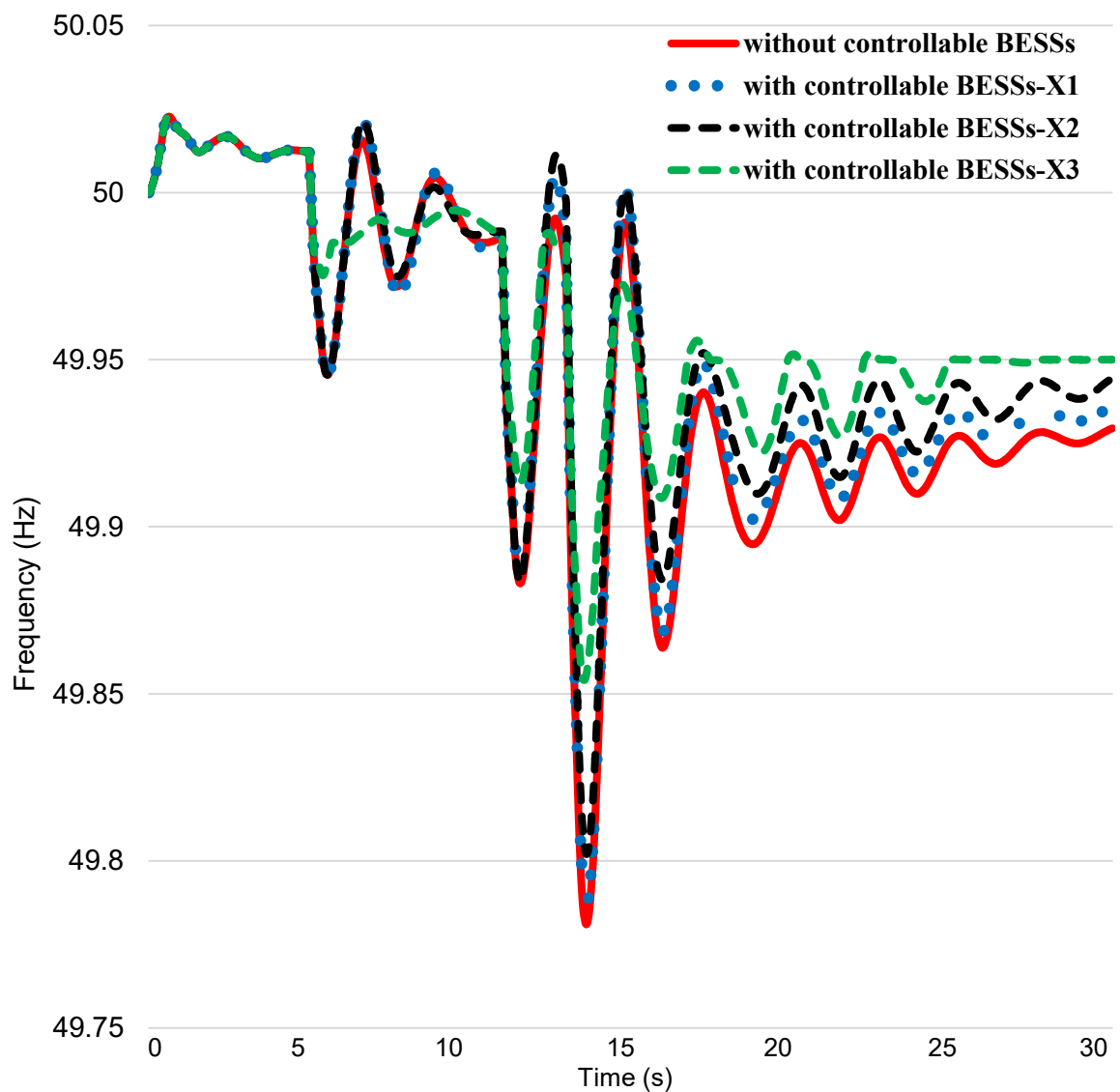


Figure 5.12. Frequency response at power unit (GPS_4) of busbar 404 using different aggregators' cases in Table 5.4.

5.5.2.2 Different value of frequency bands

In this section, different values of 'a, a1, a2' (Table 5.6) and case X1 in Table 5.4 (80 MW) were considered, these values are set by an aggregator and can be updated if necessary. Through these values, the BESS response can be controlled according to frequency bands and SoC. These values have an impact on the frequency response of the population of BESSs; the reduction in these values reduces the frequency deviations and vice versa (see Figure 5.13).



Figure 5.13. Frequency response at power unit of busbar 404 using a different value of frequency bands in Table 5.6.

5.6 Summary

A hierarchical control was proposed to aggregate different size of BESSs to provide frequency response services. Similar to the water heater controller presented in Chapter 4, the BESS controller can respond to either negative or positive frequency deviations. Hence, can participate in either high or low-frequency response services. However, the BESS controller has 3 different bands for the high frequency while the water heater controller in Chapter 4 has one band only. The BESS controller also enables BESS to work independently when any failure occurs in the communications with the aggregator.

A model of a population of BESSs was developed for the proposed hierarchical control to demonstrate the potential to provide frequency response service and to evaluate the effective capacity during a frequency event. The model divides the population of BESSs into five groups based on their SoC, and dynamically control the BESSs according to their SoC levels during the provision of frequency response services.

The control scheme was demonstrated using various case studies on the 14-machine South-East Australian power system. The response from an aggregation of 282 MW of controllable BESSs in the system with a system load base equal to 14.5 GW was effective in reducing frequency deviations following a disturbance.

The proposed control of BESSs can be applied to (i) Residential and non-residential BESSs, (ii) Large-scale BESSs, and (iii) V2G. Therefore, it demonstrates the potential for aggregators to offer different frequency response services and it can be used in the applications of VPP.

Chapter 6

Conclusions and Future Work

6.1 Conclusions

6.1.1 The development of a new secondary frequency control

An optimal secondary frequency control was designed based on fuzzy logic control to supplement conventional frequency control in future power systems. The fuzzy-based frequency controller was demonstrated on the simplified GB power system and the 10-machine New England power system. It was concluded that:

The secondary frequency controller provided an improved frequency response with reduced error and transient deviation compared to the conventional PI controller. In the 10-machine New England power system and following a disturbance, the output power of a generator with the fuzzy-based frequency controller was improved by 1.7%, which is 6.1 MW more than with the classical PI controller. In the simplified GB power system and following a disturbance, the fuzzy-based frequency controller provided high robustness against parameter uncertainties.

The fuzzy-based frequency controller offered a broad range of real-time applications in future power systems. It can be used by a system operator to supplement local frequency control rather than replacing it. It is suitable for the application of MFR in the GB power system. In addition, it can be used in the application of LFC/ AGC in future power systems.

6.1.2 Control of a population of water heaters and BESSs for frequency response

A hierarchical control for a large population of distributed WHs/BESSs was proposed, and a WH/BESS controller was designed to provide frequency response services. The population of controllable WHs/BESSs was modelled based on the Markov-chain to demonstrate the potential for WHs/BESSs aggregators to offer frequency response

services. The Markov-based model was demonstrated on the simplified GB power system and the South-East Australian power systems by applying real disturbances. It was concluded that:

The structure of the hierarchical control offered higher controllability and accuracy. This was based on two decision layers. The aggregator layer receives states and sends a command signal to enable/disable the WHs/BESSs control layer. Consequently, it reduces the uncertainty associated with the response of the aggregated WHs/BESSs during the service. The WHs/BESSs controller provides a response based on the last command signal from the aggregator, the value of frequency deviation and the level of water temperature or BESS SoC. However, it responds independently in the case of losing communications with the aggregator. Therefore, it is not fully centralised nor a fully decentralised method for controlling large distributed controllable loads.

The WHs/BESSs controller was designed based on simple logic gates and logic indicators for frequency deviation, level of water temperature and level of BESS SoC. The response from WHs is from the highest to lowest water temperature when the frequency falls, while the response from BESSs is from the highest to lowest SoC when the frequency drops and from the lowest to highest SoC when the frequency rises. Therefore, the WHs/BESSs controller reduces the impact on the power system and end-users. The BESS controller was designed with six frequency bands and five SoC levels, while the WHs controller was designed with four frequency bands and four water temperature levels. However, the number and values of frequency bands, water temperature levels and SoC levels could be changed according to the aggregator preferences. Therefore, the structure of the WHs/BESSs controller offers higher flexibility for the aggregator to assign different frequency services. In addition, the WHs/BESSs controller can deal with both high and low-frequency change. Hence, it can be used to provide primary, secondary, and high-frequency response services or to provide steady state frequency regulation.

The Markov-based model of a population of controllable WHs/BESSs demonstrated the potential for aggregators to offer frequency response services using the simplified GB power system and the large South-East Australian power system. The Markov-based model evaluated effective capacity during a frequency event in the large South-East Australian power system with a 14.5 GW system load base. Aggregation of 172 MW and 280 MW of controllable WHs/BESSs improved both the frequency deviation and frequency error following disturbances.

The hierarchical control offered a broad range of applications for the demand side response and VPPs in future power systems. It can be used in the aggregation of (i) Residential and non-residential water heaters, (ii) Residential and non-residential BESSs, (iii) Large-scale BESSs and (iv) V2G as a load.

6.2 Recommendations for future work

The control of large distributed loads is an important topic for future power systems. This topic was covered in Chapter 4 and Chapter 5 for controlling WHs and BESSs to provide frequency response services. However, the availability of controllable devices, such as WHs and BESSs, is uncertain due to many reasons. For example, an accurate number of devices that are required to respond to a frequency event is not accessible due to communication and data problems. Therefore, developing a model based on the Markov chain to predict the availability of these devices during a day/week/year by using a realistic data could be an important topic. In addition, the level of SoC of a BESS is a variable parameter, especially in batteries which are used to compensate the grid-side power supply. Therefore, developing a model based on the Markov-chain to study the behaviour of BESS SoC and to identify different levels of SoC during different uses and periods is an interesting field of research. In addition, the rate of charge/discharge was assumed to be constant in this thesis, therefore, using more realistic equation to represent this rate is an interesting topic for future work.

Integration of more RESs in a power system leads to an increase in the level of new oscillation modes. A PSS can be used to damp different types of these modes. However, PSS and POD have a real impact on reducing power system oscillations during disturbances, such as when a failure occurs in an AC system when it is connected to a DC system [122, 123]. Therefore, the coordination between PSSs and POD in future low inertia power systems is important. In addition, the PSS allocation on generators is also significant. Hence, an interesting research topic could be to study the impact of PSSs' allocation on damping different low-frequency oscillation modes applied to the GB power system.

The IEEE PSS4B (multi-band PSS) gains with its high value are more aggressive and, therefore, more effective in the inter-area frequencies between 0.1 and 1 Hz [102]. Moreover, higher PSS gains are required in case of local oscillation mode to achieve a desirable performance on a weak grid. However, the high gain has a risk of instability margins in the strong grids [102]. Hence, it is necessary to keep this trade-off in control limits. Therefore, the integration of adaptive techniques with the multi-band PSS will lead to a robust and modern design of PSS. In the case of power systems, such intelligent design can be considered as the key solution to RESs' penetration and the improvement of the power systems' efficiency [156], while the implementation of PMUs and PSSs reduces the risk of inter-area oscillation [156-158]. Therefore, studying the integration of modern adaptive PSS/POD with the PMUs is an important topic. In addition, discussing the stability assessment of the whole work is also an important topic for future work.

REFERENCES

- [1] National Grid, "*Future Energy Scenarios*", UK, 2017.
- [2] Energy and Climate Change Committee, "*2020 renewable heat and transport targets*", House of Commons, UK, 2016.
- [3] R. Harrabin, "Renewables provide more than half UK electricity for first time", *BBC News*, UK, 2017.
- [4] A. Vaughan, "Record levels of green energy in UK create strange new world for generators", *The Guardian Newspaper*, UK, 2017.
- [5] J. Zhu, "*Optimization of power system operation*", John Wiley & Sons, 2015.
- [6] National Grid, "System Operability Framework", National Grid, UK, 2015.
- [7] G. Strbac, A. Shakoor, M. Black, D. Pudjianto, and T. Bopp, "Impact of wind generation on the operation and development of the UK electricity systems", *Electric Power Systems Research*, vol. 77, no. 9, pp. 1214-1227, 2007.
- [8] National Grid, "System Operability Framework", National Grid, UK, 2016.
- [9] K. K. Marcelo A. Elizondo, Christian Moya Calderon and Wei Zhang, "Frequency Responsive Demand in U.S. Western Power System Model", in IEEE Power & Energy Society General Meeting, 26-30 July 2015, pp. 1 - 5.
- [10] J. H. K. Kalsi, J. Fuller, L. D. Marinovici, M. Elizondo, T. Williams, J. Lian, Y. Sun, "*Loads as a Resource Frequency Responsive Demand*" Prepared for the U.S. Department of Energy under Contract DE-AC05-76RL01830, Pacific Northwest National Laboratory Richland, Washington 99352, December 2015.
- [11] J. L. K. Kalsi, L. D. Marinovici, M. Elizondo, W. Zhang, and C. Moya, "*Loads as a Resource Frequency Responsive Demand*", Prepared for the U.S. Department of Energy under Contract DE-AC05-76RL01830, Pacific Northwest National Laboratory Richland, Washington 99352, September 2014.
- [12] National Grid, "NETS security and quality of supply standard", UK, 2017.
- [13] National Grid, "Frequency Response Services in the GB power system: General Descriptions", September, 2017.
- [14] N. Jenkins and J. Ekanayake, "*Renewable Energy Engineering*", Cambridge University Press, 2017.
- [15] S. S. Sami, "Virtual Energy Storage for Frequency and Voltage Control", PhD thesis, Institute of Energy, Cardiff University, UK, 2017.
- [16] National Infrastructure Commission, "*Smart power*", UK Government, UK, 2016.
- [17] National Grid, "Firm Frequency Response-FAQ", available online at: <http://www2.nationalgrid.com/UK/Services/Balancing-services/Frequency-response/Firm-Frequency-Response/>.
- [18] National Grid, "Firm Frequency Response-Services Reports", UK, 2017.
- [19] V. Trovato, I. M. Sanz, B. Chaudhuri, and G. Strbac, "Advanced Control of Thermostatic Loads for Rapid Frequency Response in Great Britain," *IEEE Transactions on Power Systems*, vol. 32, no. 3, pp. 2106-2117, 2017.
- [20] National Grid, "*Enhanced Frequency Control Capability (EFCC)*", UK, 2014.
- [21] National Grid, "*Future Energy Scenarios*", UK, 2015.
- [22] Y. Mu, J. Wu, J. Ekanayake, N. Jenkins, and H. Jia, "Primary Frequency Response From Electric Vehicles in the Great Britain Power System," *IEEE Transactions on Smart Grid*, vol. 4, no. 2, pp. 1142-1150, 2013.

- [23] W. Murrell, L. Ran, and J. Wang, "Modelling UK power system frequency response with increasing wind penetration", 2014 IEEE Innovative Smart Grid Technologies - Asia (ISGT ASIA), pp. 1-6, 20-23 May 2014.
- [24] A. C. Chapman, and G. Verbic, "Dynamic distributed energy resource allocation for load-side emergency reserve provision", 2016 IEEE Innovative Smart Grid Technologies - Asia (ISGT-Asia), pp. 1189-1194, Nov. 28 2016-Dec. 1 2016.
- [25] C. Wang, J. Wu, J. Ekanayake, and N. Jenkins, "*Smart Electricity Distribution Networks*", CRC Press, 2017.
- [26] B. Li, J. Shen, X. Wang, and C. Jiang, "From controllable loads to generalized demand-side resources: A review on developments of demand-side resources" *Renewable and Sustainable Energy Reviews*, vol. 53, pp. 936-944, 2016.
- [27] N. G. Paterakis, O. Erdinç, and J. P. Catalão, "An overview of Demand Response: Key-elements and international experience", *Renewable and Sustainable Energy Reviews*, vol. 69, pp. 871-891, 2017.
- [28] Western Power Distribution, "*Project FALCON: Commercial Trials Final Report*", Western Power Distribution Co., 2015.
- [29] G. Strbac, "Demand side management: Benefits and challenges", *Energy policy*, vol. 36, no. 12, pp. 4419-4426, 2008.
- [30] M. Cheng, J. Wu, S. J. Galsworthy, C. E. Ugalde-Loo, N. Gargov, W. W. Hung, and N. Jenkins, "Power system frequency response from the control of bitumen tanks", *IEEE Transactions on Power Systems*, vol. 31, no. 3, pp. 1769-1778, 2016.
- [31] Power Responsive, "*Demand Side Flexibility Annual Report*", 2016, available at: <http://powerresponsive.com/wp-content/uploads/2017/01/Power-Responsive-Annual-Report-2016-FINAL.pdf>.
- [32] The Energyst", "*Demand Side Response Report*", 2015, available at: <https://theenergyst.com/dsr/>.
- [33] Element Energy, "Demand side response in the non-domestic sector", *Prepared for Ofgem*, UK, 2012.
- [34] M. Cheng, J. Wu, J. Ekanayake, T. Coleman, W. Hung, and N. Jenkins, "Primary frequency response in the Great Britain power system from dynamically controlled refrigerators", 22nd International Conference and Exhibition on Electricity Distribution (CIRED 2013), Stockholm, Sweden, 2013.
- [35] J. A. Short, D. G. Infield, and L. L. Freris, "Stabilization of Grid Frequency Through Dynamic Demand Control", *IEEE Transactions on Power Systems*, vol. 22, no. 3, pp. 1284-1293, 2007.
- [36] M. T. Muhssin, L. M. Cipcigan, N. Jenkins, M. Cheng, and Z. A. Obaid, "Modelling of a population of Heat Pumps as a Source of load in the Great Britain power system." 2016 International Conference on Smart Systems and Technologies (SST), pp. 109-113.
- [37] S. Koch, M. Zima, and G. Andersson, "Active coordination of thermal household appliances for load management purposes", *IFAC Proceedings Volumes*, vol. 42, no. 9, pp. 149-154, 2009.
- [38] N. Lu, "An evaluation of the HVAC load potential for providing load balancing service", *IEEE Transactions on Smart Grid*, vol. 3, no. 3, pp. 1263-1270, 2012.
- [39] M. Cheng, J. Wu, S. J. Galsworthy, N. Gargov, W. H. Hung, and Y. Zhou, "Performance of industrial melting pots in the provision of dynamic frequency response in the Great Britain power system", *Applied Energy*, Vol. 201, 1 September, Pages 245-256, 2017.

- [40] M. Cheng, J. Wu, S. Galsworthy, N. Jenkins, and W. Hung, "Availability of load to provide frequency response in the Great Britain power system", Power Systems Computation Conference (PSCC), Wroclaw, Poland, pp. 1-7, 18-22 Aug. 2014.
- [41] E. Vrettos, J. L. Mathieu, and G. Andersson, "Demand response with moving horizon estimation of individual thermostatic load states from aggregate power measurements", American Control Conference (ACC), pp. 4846-4853, Portland, OR, USA, 4-6 June 2014.
- [42] A. M. Mathew, and R. Menon, "Assessment of demand response capability with thermostatic loads in residential sector", 2015 International Conference on Power, Instrumentation, Control and Computing (PICCC), Thrissur, India, pp. 1-5, 9-11 Dec. 2015.
- [43] J. L. Mathieu, M. Kamgarpour, J. Lygeros, G. Andersson, and D. S. Callaway, "Arbitraging Intraday Wholesale Energy Market Prices With Aggregations of Thermostatic Loads", *IEEE Transactions on Power Systems*, vol. 30, no. 2, pp. 763-772, 2015.
- [44] S. H. Tindemans, V. Trovato, and G. Strbac, "Decentralized Control of Thermostatic Loads for Flexible Demand Response", *IEEE Transactions on Control Systems Technology*, vol. 23, no. 5, pp. 1685-1700, 2015.
- [45] V. Trovato, I. M. Sanz, B. Chaudhuri, and G. Strbac, "Advanced Control of Thermostatic Loads for Rapid Frequency Response in Great Britain", *IEEE Transactions on Power Systems*, vol. PP, no. 99, pp. 1-1, 2016.
- [46] V. Trovato, F. Teng, and G. Strbac, "Value of thermostatic loads in future low-carbon Great Britain system", Power Systems Computation Conference (PSCC), pp. 1-7, Genoa, Italy, 20-24 June 2016.
- [47] V. Trovato, S. H. Tindemans, and G. Strbac, "Leaky storage model for optimal multi-service allocation of thermostatic loads", *IET Generation, Transmission & Distribution*, vol. 10, no. 3, pp. 585-593, 2016.
- [48] V. Trovato, I. Martinez-Sanz, B. Chaudhuri, and G. Strbac, "Advanced control of thermostatic loads for rapid frequency response in Great Britain", 2017 IEEE Manchester PowerTech, UK, pp. 1-1, 18-22 June 2017.
- [49] A. Latif, S. Khan, P. Palensky, and W. Gawlik, "Co-simulation based platform for thermostatically controlled loads as a frequency reserve", 2016 Workshop on Modeling and Simulation of Cyber-Physical Energy Systems (MSCPES), pp. 1-6, 11-11 April 2016.
- [50] V. Trovato, F. Teng, and G. Strbac, "Role and Benefits of Flexible Thermostatically Controlled Loads in Future Low-Carbon Systems", *IEEE Transactions on Smart Grid*, vol. PP, no. 99, pp. 1-1, 2017.
- [51] V. Trovato, S. H. Tindemans, and G. Strbac, "Demand response contribution to effective inertia for system security in the GB 2020 gone green scenario", IEEE PES ISGT Europe, pp. 1-5, 6-9 Oct. 2013.
- [52] W. Z. Christian Moya, Jianming Lian and Karanjit Kalsi, "A Hierarchical Framework for Demand-Side Frequency Control", in American Control Conference, Portland, OR, 4-6 June 2014, pp. 52 - 57.
- [53] Z. Xu, R. Diao, S. Lu, J. Lian, and Y. Zhang, "Modeling of Electric Water Heaters for Demand Response: A Baseline PDE Model", *IEEE Transactions on Smart Grid*, vol. 5, no. 5, pp. 2203-2210, 2014.
- [54] D. Cooper, and W. Cronje, "Autonomous water heater control for load regulation on Smart Grids", 2016 IEEE International Energy Conference (ENERGYCON), pp. 1-6, 4-8 April 2016.

- [55] T. Masuta, and A. Yokoyama, "Supplementary Load Frequency Control by Use of a Number of Both Electric Vehicles and Heat Pump Water Heaters", *IEEE Transactions on Smart Grid*, vol. 3, no. 3, pp. 1253-1262, 2012.
- [56] Y. J. Kim, E. Fuentes, and L. K. Norford, "Experimental Study of Grid Frequency Regulation Ancillary Service of a Variable Speed Heat Pump", *IEEE Transactions on Power Systems*, vol. 31, no. 4, pp. 3090-3099, 2016.
- [57] Y. J. Kim, L. K. Norford, and J. L. Kirtley, "Modeling and Analysis of a Variable Speed Heat Pump for Frequency Regulation Through Direct Load Control", *IEEE Transactions on Power Systems*, vol. 30, no. 1, pp. 397-408, 2015.
- [58] Home Power, "Water Heaters", 16 October, 2017, available at: <https://www.homepower.com/articles/solar-water-heating/domestic-hot-water>.
- [59] K. Youngjin, "Experimental study of grid frequency regulation ancillary service of a variable speed heat pump", IEEE Power and Energy Society General Meeting (PESGM), pp. 1-1, 17-21 July 2016.
- [60] E. Vrettos, S. Koch, and G. Andersson, "Load frequency control by aggregations of thermally stratified electric water heaters", 3rd IEEE PES Innovative Smart Grid Technologies Europe (ISGT Europe), pp. 1-8, 14-17 Oct. 2012.
- [61] T. Masuta, A. Yokoyama, and Y. Tada, "Modeling of a number of Heat Pump Water Heaters as control equipment for load frequency control in power systems", IEEE Trondheim PowerTech, pp. 1-7, 19-23 June 2011.
- [62] T. Williams, K. Kalsi, M. Elizondo, L. Marinovici, and R. Pratt, "Control and coordination of frequency responsive residential water heaters", IEEE Power and Energy Society General Meeting (PESGM), pp. 1-5, 17-21 July 2016.
- [63] W. Z. Christian Moya, Jianming Lian and Karanjit Kalsi, "A Hierarchical Framework for Demand-Side Frequency Control", in American Control Conference, Portland, OR, 2014, pp. 52 - 57.
- [64] J. L. K. Kalsi, L. D. Marinovici, M Elizondo, W Zhang and C Moya, "*Loads as a Resource Frequency Responsive Demand*", Prepared for the U.S. Department of Energy under Contract DE-AC05-76RL01830, Pacific Northwest National Laboratory Richland, Washington 99352, 2014.
- [65] E. L. Karfopoulos, and N. D. Hatziaargyriou, "A Multi-Agent System for Controlled Charging of a Large Population of Electric Vehicles", *IEEE Transactions on Power Systems*, vol. 28, no. 2, pp. 1196-1204, 2013.
- [66] H. W. Qazi, D. Flynn, and Z. H. Rather, "Impact of electric vehicle load response variation on frequency stability", IEEE PES Innovative Smart Grid Technologies Conference Europe (ISGT-Europe), pp. 1-6, 9-12 Oct. 2016.
- [67] M. R. V. Moghadam, R. Zhang, and R. T. B. Ma, "Distributed Frequency Control via Randomized Response of Electric Vehicles in Power Grid", *IEEE Transactions on Sustainable Energy*, vol. 7, no. 1, pp. 312-324, 2016.
- [68] M. Georgiev, R. Stanev, and A. Krusteva, "Flexible load control in electric power systems with distributed energy resources and electric vehicle charging", IEEE International Power Electronics and Motion Control Conference (PEMC), pp. 1034-1040, 25-28 Sept. 2016.
- [69] M. Cheng, S. S. Sami, and J. Wu, "Benefits of using virtual energy storage system for power system frequency response", *Applied Energy*, Volume 194, 15 May 2017, Pages 376-385.
- [70] J. Li, R. Xiong, Q. Yang, F. Liang, M. Zhang, and W. Yuan, "Design/test of a hybrid energy storage system for primary frequency control using a dynamic droop method

- in an isolated microgrid power system", *Applied Energy*, Vol. 201, 1 September 2017, Pages 257-269.
- [71] Z. A. Obaid, L. M. Cipcigan, and M. T. Muhsin, "Analysis of the Great Britain's power system with Electric Vehicles and Storage Systems", in 2015 18th International Conference on Intelligent System Application to Power Systems (ISAP), 2015, pp. 1-6.
- [72] S. J. Lee, J. H. Kim, C. H. Kim, S. K. Kim, E. S. Kim, D. U. Kim, K. K. Mehmood, and S. U. Khan, "Coordinated Control Algorithm for Distributed Battery Energy Storage Systems for Mitigating Voltage and Frequency Deviations", *IEEE Transactions on Smart Grid*, vol. 7, no. 3, pp. 1713-1722, May, 2016.
- [73] S. S. Sami, M. Cheng, and W. Jianzhong, "Modelling and control of multi-type grid-scale energy storage for power system frequency response", IEEE 8th International Power Electronics and Motion Control Conference (IPEMC-ECCE Asia), pp. 269-273, 22-26 May 2016.
- [74] National Grid, "*Future Energy Scenario*", UK, 2016.
- [75] Clean Energy. "Enel buys up lucrative battery storage project for £17 million", UK, 16 October, 2017.
- [76] Y. J. Kim, G. Del-Rosario-Calaf, and L. K. Norford, "Analysis and Experimental Implementation of Grid Frequency Regulation Using Behind-the-Meter Batteries Compensating for Fast Load Demand Variations", *IEEE Transactions on Power Systems*, vol. 32, no. 1, pp. 484-498, 2017.
- [77] E. B. Iversen, J. M. Morales, and H. Madsen, "Optimal charging of an electric vehicle using a Markov decision process", *Applied Energy*, vol. 123, pp. 1-12, Jun 15, 2014.
- [78] J. Song, V. Krishnamurthy, A. Kwasinski, and R. Sharma, "Development of a Markov-Chain-Based Energy Storage Model for Power Supply Availability Assessment of Photovoltaic Generation Plants", *IEEE Transactions on Sustainable Energy*, vol. 4, no. 2, pp. 491-500, April 2013.
- [79] Y. Tang, J. Zhong, and M. Bollen, "Aggregated optimal charging and vehicle-to-grid control for electric vehicles under large electric vehicle population", *IET Generation, Transmission & Distribution*, vol. 10, no. 8, pp. 2012-2018, 2016.
- [80] S. M. Alhejaj, and F. M. Gonzalez-Longatt, "Impact of inertia emulation control of grid-scale BESS on power system frequency response", International Conference for Students on Applied Engineering (ICSAE), pp. 254-258, 20-21 Oct. 2016.
- [81] N. Hatziargyriou, *MicroGrids*: wiley-IEEE press, 2014.
- [82] Clean Energy Initiative, "Why (and How) Microgrid Technology Is a Good Power Source", 6 November, 2017.
- [83] P. Lund, "The danish cell project-part 1: Background and general approach", IEEE Power Engineering Society General Meeting, pp. 1-6, USA, 24-28 June 2007.
- [84] J. B. Ekanayake, N. Jenkins, K. Liyanage, J. Wu, and A. Yokoyama, "*Smart grid: technology and applications*", John Wiley & Sons, 2012.
- [85] D. Pudjianto, C. Ramsay, and G. Strbac, "Virtual power plant and system integration of distributed energy resources", *IET Renewable Power Generation*, vol. 1, no. 1, pp. 10-16, 2007.
- [86] S. M. Hao Bai, X. Ran and Ch. Ye, "Optimal Dispatch Strategy of a Virtual Power Plant Containing Battery Switch Stations in a Unified Electricity Market", *Energies*, vol. 8(3), pp. 2268-2289, 2015.
- [87] C. Canizares, T. Fernandes, E. Galdi, L. Gerin-Lajoie, M. Gibbard, I. Hiskens, J. Kersulis, R. Kuiava, L. Lima, F. DeMarco, N. Martins, B. C. Pal, A. Piardi, R. Ramos, J. d. Santos, D. Silva, A. K. Singh, B. Tamimi, and D. Vowles, "Benchmark Models

- for the Analysis and Control of Small-Signal Oscillatory Dynamics in Power Systems", *IEEE Transactions on Power Systems*, vol. 32, no. 1, pp. 715-722, 2017.
- [88] D. Ke, and C. Y. Chung, "Design of Probabilistically-Robust Wide-Area Power System Stabilizers to Suppress Inter-Area Oscillations of Wind Integrated Power Systems", *IEEE Transactions on Power Systems*, vol. 31, no. 6, pp. 4297-4309, 2016.
- [89] A. Kumar, "Power System Stabilizers Design for Multimachine Power Systems Using Local Measurements", *IEEE Transactions on Power Systems*, vol. 31, no. 3, pp. 2163-2171, 2016.
- [90] L. Shi, K. Y. Lee, and F. Wu, "Robust ESS-Based Stabilizer Design for Damping Inter-Area Oscillations in Multimachine Power Systems", *IEEE Transactions on Power Systems*, vol. 31, no. 2, pp. 1395-1406, 2016.
- [91] A. I. Konara, and U. D. Annakkage, "Robust Power System Stabilizer Design Using Eigenstructure Assignment", *IEEE Transactions on Power Systems*, vol. 31, no. 3, pp. 1845-1853, 2016.
- [92] Y. Liu, Q. H. Wu, H. Kang, and X. Zhou, "Switching power system stabilizer and its coordination for enhancement of multi-machine power system stability", *CSEE Journal of Power and Energy Systems*, vol. 2, no. 2, pp. 98-106, 2016.
- [93] B. P. Padhy, S. C. Srivastava, and N. K. Verma, "A Wide-Area Damping Controller Considering Network Input and Output Delays and Packet Drop", *IEEE Transactions on Power Systems*, vol. 32, no. 1, pp. 166-176, 2017.
- [94] Excitation Committee, "IEEE Guide for Identification, Testing, and Evaluation of the Dynamic Performance of Excitation Control Systems", *IEEE Std 421.2-2014 (Revision of IEEE Std 421.2-1990)*, pp. 1-63, 2014.
- [95] Z. Kun, M. Chenine, L. Nordstrom, S. Holmstrom, and G. Ericsson, "Design Requirements of Wide-Area Damping Systems-Using Empirical Data From a Utility IP Network", *IEEE Transactions on Smart Grid*, vol. 5, no. 2, pp. 829-838, 2014.
- [96] Y. Yu, S. Grijalva, J. J. Thomas, L. Xiong, P. Ju, and Y. Min, "Oscillation Energy Analysis of Inter-Area Low-Frequency Oscillations in Power Systems", *IEEE Transactions on Power Systems*, vol. PP, no. 99, pp. 1-9, 2015.
- [97] L. Shi, K. Y. Lee, and F. Wu, "Robust ESS-Based Stabilizer Design for Damping Inter-Area Oscillations in Multimachine Power Systems", *IEEE Transactions on Power Systems*, vol. PP, no. 99, pp. 1-12, 2015.
- [98] M. S. Rawat, and R. N. Sharma, "The Effective Role of PSS in Damping Inter Area Mode of Oscillation Using MATLAB/Simulink", International Conference on Computational Intelligence and Communication Networks (CICN), pp. 732-736, 7-9 Oct. 2011.
- [99] J. P. Prabha Kundur, Venkat Ajjarapu, Göran Andersson, Anjan Bose, Claudio Canizares, Nikos Hatziargyriou, David Hill, Alex Stankovic, Carson Taylor, Thierry Van Cutsem, and Vijay Vittal, "Definition and Classification of Power System Stability", *IEEE Transactions on Power Systems*, vol. 19, no. 2, pp. 1387-1401, May 2004.
- [100] A. Paul, M. Bhadu, N. Senroy, and A. R. Abhyankar, "Study of effect of local PSS and WADC placement based on dominant inter-area paths", IEEE PES GM, pp. 1-5, 26-30 July 2015.
- [101] N. P. Patidar, M. L. Kolhe, N. P. Tripathy, B. Sahu, A. Sharma, L. K. Nagar, and A. N. Azmi, "Optimized design of wide-area PSS for damping of inter-area oscillations", IEEE 11th International Conference on Power Electronics and Drive Systems (PEDS), pp. 1172-1177, 9-12 June 2015.

- [102] I. Kamwa, R. Grondin, and G. Trudel, "IEEE PSS2B versus PSS4B: the limits of performance of modern power system stabilizers", *IEEE Transactions on Power Systems*, vol. 20, no. 2, pp. 903-915, 2005.
- [103] M. Ishimaru, R. Yokoyama, O. Neto, and K. Lee, "Allocation and design of power system stabilizers for mitigating low-frequency oscillations in the eastern interconnected power system in Japan", *International Journal of Electrical Power & Energy Systems*, vol. 26, no. 8, pp. 607-618, 2004.
- [104] K. Hashikura, and A. Kojima, "Delay-tolerant PSS with discrete-time Hinf observer-based predictor", 54th Annual Conference of the Society of Instrument and Control Engineers of Japan (SICE), pp. 884-887, 28-30 July 2015.
- [105] G. J. W. Dudgeon, W. E. Leithead, A. Dysko, J. O'Reilly, and J. R. McDonald, "The Effective Role of AVR and PSS in Power Systems: Frequency Response Analysis", *IEEE Transactions on Power Systems*, vol. 22, no. 4, pp. 1986-1994, 2007.
- [106] X. Y. Bian, Y. Geng, K. L. Lo, Y. Fu, and Q. B. Zhou, "Coordination of PSSs and SVC Damping Controller to Improve Probabilistic Small-Signal Stability of Power System With Wind Farm Integration", *IEEE Transactions on Power Systems*, vol. PP, no. 99, pp. 1-12, 2015.
- [107] A. Ajamal, M. Elthalathiny, and K. Ellithy, "PSSs design based on PMUs signals to enhance the stability of inter-area oscillations of interconnected power systems", IEEE Power and Energy Conference at Illinois (PECI), pp. 1-5, 20-21 Feb. 2015.
- [108] A. Dysko, W. E. Leithead, and J. O'Reilly, "Enhanced Power System Stability by Coordinated PSS Design", *IEEE Transactions on Power Systems*, vol. 25, no. 1, pp. 413-422, 2010.
- [109] L. Wenxin, G. K. Venayagamoorthy, and D. C. Wunsch, "A heuristic-dynamic-programming-based power system stabilizer for a turbogenerator in a single-machine power system", *IEEE Transactions on Industry Applications*, vol. 41, no. 5, pp. 1377-1385, 2005.
- [110] C. Deyu, P. Regulski, M. Osborne, and V. Terzija, "Wide Area Inter-Area Oscillation Monitoring Using Fast Nonlinear Estimation Algorithm", *IEEE Transactions on Smart Grid*, vol. 4, no. 3, pp. 1721-1731, 2013.
- [111] A. Stativa, M. Gavrilas, and O. Ivanov, "Optimal Power System Stabilizer design using multiple wide-area input signals", pp. 34-39.
- [112] M. Mokhtari, and F. Aminifar, "Toward Wide-Area Oscillation Control Through Doubly-Fed Induction Generator Wind Farms", *IEEE Transactions on Power Systems*, vol. 29, no. 6, pp. 2985-2992, 2014.
- [113] S. Lamichhane, and N. Mithulananthan, "Influence of wind energy integration on low frequency oscillatory instability of power system", 14th International Conference on Environment and Electrical Engineering (EEEIC), pp. 1-5, 10-12 May 2014.
- [114] N. Jiawei, S. A. N. Sarmadi, and V. Venkatasubramanian, "Two-Level Ambient Oscillation Modal Estimation From Synchrophasor Measurements", *IEEE Transactions on Power Systems*, vol. 30, no. 6, pp. 2913-2922, 2015.
- [115] L. H. Hassan, M. Moghavvemi, H. A. F. Almurib, K. M. Muttaqi, and V. G. Ganapathy, "Optimization of power system stabilizers using participation factor and genetic algorithm", *International Journal of Electrical Power & Energy Systems*, vol. 55, pp. 668-679, 2014.
- [116] B. Pal and B. Chaudhuri, "Power System Oscillations", *Robust Control in Power Systems*, 2, Springer US, 2005, pp. 5-12.

- [117] R. M. Hamouda, M. R. Iravani, and R. Hackam, "Torsional oscillations of series capacitor compensated AC/DC systems", *IEEE Transactions on Power Systems*, vol. 4, no. 3, pp. 889-896, 1989.
- [118] G. N. Pillai, A. Ghosh, and A. Joshi, "Torsional oscillation studies in an SSSC compensated power system", *Electric Power Systems Research*, vol. 55, no. 1, pp. 57-64, 2000.
- [119] T. N. Tuan, I. Erlich, and S. P. Teeuwsen, "Methods for utilization of MMC-VSC-HVDC for power oscillation dampin", IEEE PES General Meeting Conference & Exposition, pp. 1-5, 27-31 July 2014.
- [120] S. Golshannavaz, F. Aminifar, and D. Nazarpour, "Application of UPFC to Enhancing Oscillatory Response of Series-Compensated Wind Farm Integrations", *IEEE Transactions on Smart Grid*, vol. 5, no. 4, pp. 1961-1968, 2014.
- [121] Mitsubishi Electric, "Power System Stabilizer (PSS)", Marunouchi, Chiyoda-Ku, Tokyo 100-8310, Japan, 2010.
- [122] R. Rabbani, A. F. Zobaa, and G. A. Taylor, "Applications of simplified models to investigate oscillation damping control on the GB transmission system", 10th IET International Conference on AC and DC Power Transmission (ACDC 2012), pp. 1-6, 4-5 Dec. 2012.
- [123] L. Yong, J. R. Gracia, T. J. King, and L. Yilu, "Frequency Regulation and Oscillation Damping Contributions of Variable-Speed Wind Generators in the U.S. Eastern Interconnection (EI)", *IEEE Transactions on Sustainable Energy*, vol. 6, no. 3, pp. 951-958, 2015.
- [124] Y. Pipelzadeh, B. Chaudhuri, T. C. Green, and R. Adapa, "Role of western HVDC link in stability of future Great Britain (GB) transmission system", IEEE PES GM, pp. 1-5, USA, 26-30 July 2015.
- [125] R. F. B. MacLaren, "Application of power system stabilisers on the Anglo-Scottish interconnection. Testing of power system stabilisers", *IEE Proceedings, Generation, Transmission and Distribution*, , vol. 135, no. 3, pp. 251-254, 1988.
- [126] I. Kamwa, "*Performance of Three PSS for Interarea Oscillations*", SymPowerSystems Toolbox, 2015.
- [127] I. Hiskens, "*IEEE PES Task Force on Benchmark Systems for Stability Controls*", IEEE, 2013.
- [128] Power System Stability Subcommittee, "*IEEE PES Task Force on Benchmark Systems for Stability Controls*", IEEE, 2015.
- [129] I. K. A. Moeini, P. Brunelle and G. Sybille, "Open Data IEEE Test Systems Implemented in SimpowerSystems for Education and Research in Power Grid Dynamics and Control", in 50th International Universities Power Engineering Conference (UPEC), UK, pp. 1-6, 1-4 Sept. 2015.
- [130] A. Moeini, I. Kamwa, P. Brunelle, and G. Sybille, "Open data IEEE test systems implemented in SimPowerSystems for education and research in power grid dynamics and control", UPEC, Stoke, UK, 2015,.
- [131] R. Ramos and I. Hiskens, "*IEEE PES Task Force on Benchmark Systems for Stability Controls-Technical Report*", IEEE, 2015.
- [132] L. Balling, "*Fast cycling and rapid start-up: new generation of plants achieves impressive results*", Siemens AG, Erlangen, Germany, 2011.
- [133] National Grid, "*Guidance Notes –Synchronous Generating Units*", UK, 2012.
- [134] N. Henkel, "*Operational Flexibility Enhancements of Combined Cycle Power Plants*", Siemens AG, Energy Sector Germany, 2008.

- [135] Z. A. Obaid, L. M. Cipcigan, and M. T. Muhssin, "Design of a Hybrid Fuzzy/Markov Chain-based hierarchical Demand-side Frequency Control", in IEEE PES GM, 2017, Chicago. USA, 2017, pp. 1-5.
- [136] Z. A. Obaid, L. M. Cipcigan, and M. T. Muhssin, "Fuzzy hierarchical approach-based optimal frequency control in the Great Britain power system", *Electric Power Systems Research*, vol. 141, pp. 529-537, Dec, 2016.
- [137] D. Ke, F. Shen, C. Y. Chung, C. Zhang, J. Xu, and Y. Sun, "Application of Information Gap Decision Theory to the Design of Robust Wide-Area Power System Stabilizers Considering Uncertainties of Wind Power", *IEEE Transactions on Sustainable Energy*, vol. 9, no. 2, pp. 805-817, 2018.
- [138] J. Wang, H. Peng, M. Tu, J. M. P´erez-Jim´enez, and P. Shi, "A Fault Diagnosis Method of Power Systems Based on an Improved Adaptive Fuzzy Spiking Neural P Systems and PSO Algorithms", *Chinese Journal of Electronics*, vol. 25, no. 2, pp. 320-327, 2016.
- [139] M. A. Heidari, "Optimal network reconfiguration in distribution system for loss reduction and voltage-profile improvement using hybrid algorithm of PSO and ACO", *CIREN - Open Access Proceedings Journal*, vol. 2017, no. 1, pp. 2458-2461, 2017.
- [140] N. E. Y. Kouba, M. Mena, M. Hasni, and M. Boudour, "Load Frequency Control in multi-area power system based on Fuzzy Logic-PID Controller", IEEE International Conference on Smart Energy Grid Engineering (SEGE), pp. 1-6, 17-19 Aug. 2015.
- [141] N. E. Y. Kouba, M. Mena, M. Hasni, K. Tehrani, and M. Boudour, "A novel optimized fuzzy-PID controller in two-area power system with HVDC link connection", 2016 International Conference on Control, Decision and Information Technologies (CoDIT), pp. 204-209, 6-8 April 2016.
- [142] T. Mohammed, J. Momoh, and A. Shukla, "Single area load frequency control using fuzzy-tuned PI controller", North American Power Symposium (NAPS), pp. 1-6, 17-19 Sept. 2017.
- [143] K. Rana, and S. Kakran, "Improvement in dynamic performance of an interconnected power system in LFC using PID and fuzzy controller", International Conference on Emerging Trends in Electrical Electronics & Sustainable Energy Systems (ICETEESES), pp. 25-29, 11-12 March 2016.
- [144] H. N. Azadani, and R. Torkzadeh, "Design of GA optimized fuzzy logic-based PID controller for the two area non-reheat thermal power system", 2013 13th Iranian Conference on Fuzzy Systems (IFSC), pp. 1-6, 27-29 Aug. 2013.
- [145] National Grid, "FFR Market Information_Jan16_Tables", National Grid, UK, 2016.
- [146] V. Dwivedi, "Thermal Modelling and Control of Domestic Hot Water Tank", Master thesis, Department of Mechanical Engineering, University of Strathclyde Engineering, University of Strathclyde Engineering, 2009.
- [147] M. T. Muhssin, L. M. Cipcigan, N. Jenkins, M. Cheng, and Z. A. Obaid, "Modelling of a population of Heat Pumps as a Source of load in the Great Britain power system", International Conference on Smart Systems and Technologies (SST), pp. 109-113, 2016.
- [148] M. T. Muhssin, L. M. Cipcigan, Z. A. Obaid and W. F. AL-Ansari, "A novel adaptive deadbeat- based control for load frequency control of low inertia system in interconnected zones north and south of Scotland", *International Journal of Electrical Power & Energy Systems*, vol. 89, pp. 52-61, 2017.

- [149] M. T. Muhssin, L. M. Cipcigan, and Z. A. Obaid, "Small Microgrid stability and performance analysis in isolated island", 50th International Universities Power Engineering Conference (UPEC), pp. 1-6, 2015.
- [150] M. G. A. D. Vowles, "*Simplified 14-Generator Model of the South East Australian Power System*", School of Electrical & Electronic Engineering, The University of Adelaide, South Australia, 2014.
- [151] A. Urtasun, E. L. Barrios, P. Sanchis, and L. Marroyo, "Frequency-Based Energy-Management Strategy for Stand-Alone Systems With Distributed Battery Storage", *IEEE Transactions on Power Electronics*, vol. 30, no. 9, pp. 4794-4808, Sep, 2015.
- [152] J. M. Lujano-Rojas, R. Dufo-Lopez, J. L. Bernal-Agustin, and J. P. S. Catalao, "Optimizing Daily Operation of Battery Energy Storage Systems Under Real-Time Pricing Schemes", *IEEE Transactions on Smart Grid*, vol. 8, no. 1, pp. 316-330, 2017.
- [153] B. Lian, A. Sims, D. Yu, C. Wang, and R. W. Dunn, "Optimizing LiFePO₄ Battery Energy Storage Systems for Frequency Response in the UK System", *IEEE Transactions on Sustainable Energy*, vol. 8, no. 1, pp. 385-394, 2017.
- [154] B. Xu, A. Oudalov, A. Ulbig, G. Andersson, and D. S. Kirschen, "Modeling of Lithium-Ion Battery Degradation for Cell Life Assessment", *IEEE Transactions on Smart Grid*, vol. 9, no. 2, pp. 1131-1140, 2018.
- [155] Z. A. Obaid, N. Sulaiman, and M. N. Hamidon, "Design of fuzzy logic controller for AC motor based on field programmable gate array", , 2009 IEEE Student Conference on Research and Development (SCOReD), pp. 487-490, Malaysia, 16-18 Nov. 2009.
- [156] S. Kamalasan, and G. D. Swann, "A Novel System-Centric Intelligent Adaptive Control Architecture for Damping Interarea Mode Oscillations in Power System", *IEEE Transactions on Industry Applications*, vol. 47, no. 3, pp. 1487-1497, 2011.
- [157] C. Lin, C. Gang, G. Wenzhong, Z. Fang, and L. Gan, "Adaptive Time Delay Compensator (ATDC) Design for Wide-Area Power System Stabilizer", *IEEE Transactions on Smart Grid*, vol. 5, no. 6, pp. 2957-2966, 2014.
- [158] I. Kamwa, S. R. Samantaray, and G. Joos, "Optimal Integration of Disparate C37.118 PMUs in Wide-Area PSS With Electromagnetic Transients", *IEEE Transactions on Power Systems*, vol. 28, no. 4, pp. 4760-4770, 2013.

Appendix

A3. Design of Fuzzy-based secondary frequency controller

This section displays some of codes and design in MATLAB program for Chapter 3

A3.1 Design of Fuzzy Inference System (FIS) using MATLAB/Simulink Fuzzy Toolbox

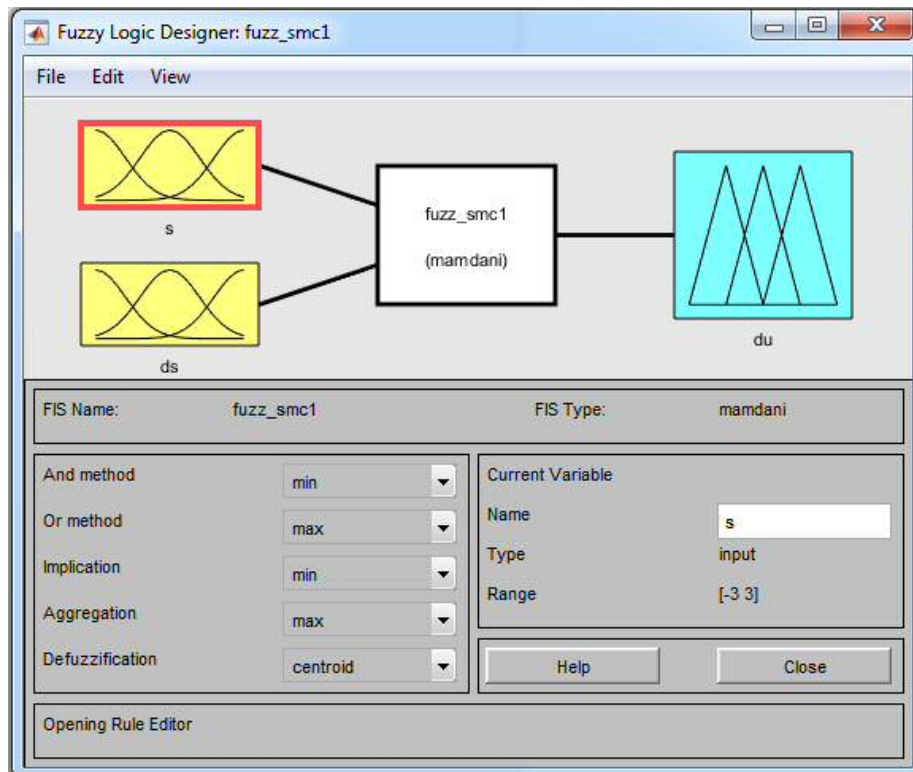


Figure A3.1.1. Fuzzy Inference System of Verion I in chapter 2 using MATLAB Fuzzy Toolbox.

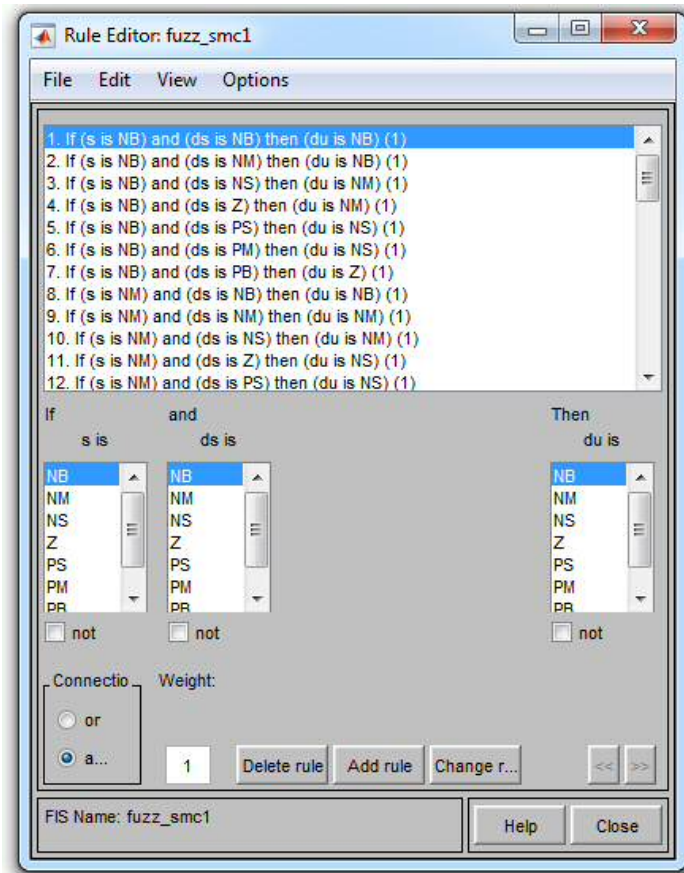


Figure A3.1.2 Deriving Fuzzy Rules in Matlab Fuzzy Toolbox for Version I FIS in

Chapter 3.

A3.2 PSO M-file code in Matlab for the optimisation of Classical PID controller.

```

close all
clear all
clc
%%%%%%%%%%%%%%%%%%%%%%%%%%%%%%%%%%%%%%%%%%%%%%%%%%%%%%%%%%%%%%%%%%%%%%%%
% IP SO parameters
popsize = 10; % Population size
wmax = 0.9; % Initial weights,
wmin = 0.4; % Final weights,
CR = 0.65; % Crossover rate
c1 = 2; % acceleration coefficient
c2 = 2; % acceleration coefficient
iter_max = 30; % Maximum iteration number
minPID = 0; % Minimum gain value
maxPID = 30; % Maximum PID gain
Vmax = 5; % Maximum velocity of particles
Vmin = -5; % Minimum velocity of particles
%%%%%%%%%%%%%%%%%%%%%%%%%%%%%%%%%%%%%%%%%%%%%%%%%%%%%%%%%%%%%%%%%%%%%%%%
% Initialize the population
iter = 0;
V = zeros(popsize,3);

```

```

PID = maxPID*rand(popsiz,3); % Initial population (PID gains)
PID = max(PID,minPID);
for k=1:popsiz
    P = PID(k,1);
    I = PID(k,2);
    D = PID(k,3);
    sim('PSO_PID') % Run the simulink file "Zeyad.sim"
    ISE(k,1) = error.signals.values(end); % Fitness alue of each particle
% ISE(k,1) = sum(error.signals.values); % Fitness alue of each particle
    ISE(k,1) = trapz(error.time,error.signals.values); % Fitness alue of each particle
    clc
end
[minISE,i_best] = min(ISE); % Find the best particleand the best ISE in the current swarm
Gbest = PID(i_best,:); % The best particle
Pbest = PID; % The best position of each particle so far
PbestISE = ISE; % The best experience of each particle so far
minISE1 = minISE;
Gbest1 = Gbest;
%%%%%%%%%%%%%%%%%%%%%%%%%%%%%%%%%%%%%%%%%%%%%%%%%%%%%%%%%%%%%%%%%%%%%%%%
for m = 1:iter_max
    X = PID;
    iter = iter+1;
    w = wmax - (wmax-wmin)*iter/iter_max;
    for i = 1:popsiz
        for j = 1:3
            V(i,j) = w*V(i,j) + c1*rand*( Pbest(i,j) - X(i,j) ) + c1*rand*( Gbest(1,j) - X(i,j) );
        end
    end
    V = min(Vmax,V);
    V = max(Vmin,V);
    X = X + V;
    X = max(X,minPID);
    X = min(X,maxPID);
    %%%%%%%%%%%%%%%%%%%%%%%%%%%%%%%%%%%%%%%%%%%%%%%%%%%%%%%%%%%%%%%%%%%%%%%%%
    % Implementation of crossover operation
    [r,c] = find(rand(popsiz,3)>CR);
    for k = 1:length(r)
        X(r(k),c(k)) = Pbest(r(k),c(k));
    end
    %%%%%%%%%%%%%%%%%%%%%%%%%%%%%%%%%%%%%%%%%%%%%%%%%%%%%%%%%%%%%%%%%%%%%%%%%
    PID = X;
    %%%%%%%%%%%%%%%%%%%%%%%%%%%%%%%%%%%%%%%%%%%%%%%%%%%%%%%%%%%%%%%%%%%%%%%%%
for k=1:popsiz
    P = PID(k,1);
    I = PID(k,2);
    D = PID(k,3);
    sim('PSO_PID') % Run the simulink file "Project_sim.sim"
% ISE(k,1) = error.signals.values(end); % Fitness alue of each particle
% ISE(k,1) = sum(error.signals.values); % Fitness alue of each particle
    ISE(k,1) = trapz(error.time,error.signals.values); % Fitness alue of each particle
    clc
    minISE
% Gbest1
end
%%%%%%%%%%%%%%%%%%%%%%%%%%%%%%%%%%%%%%%%%%%%%%%%%%%%%%%%%%%%%%%%%%%%%%%%
for i = 1:popsiz
    if ISE(i) < PbestISE
        PbestISE(i) = ISE(i);
        Pbest(i,:) = PID(i,:);
    end
end
%%%%%%%%%%%%%%%%%%%%%%%%%%%%%%%%%%%%%%%%%%%%%%%%%%%%%%%%%%%%%%%%%%%%%%%%
[minISE_s,i_best_s] = min(ISE); % Find the best particleand the best ISE in the current swarm
if minISE_s < minISE
    minISE = minISE_s; % The best ISE so far

```

```

Gbest = PID(i_best,:); % The best particle so far
end
%%%%%%%%%%%%%%%%%%%%%%%%%%%%%%%%%%%%%%%%%%%%%%%%%%%%%%%%%%%%%%%%%%%%%%%%
minISE1 = [ minISE1; minISE ];
Gbest1 = [ Gbest1; Gbest ];
%
% minISE
% Gbest
end
%%%%%%%%%%%%%%%%%%%%%%%%%%%%%%%%%%%%%%%%%%%%%%%%%%%%%%%%%%%%%%%%%%%%%%%%
clc
plot(minISE1)
grid on
P= Gbest(1);
I = Gbest(2);
D = Gbest(3);
figure
sim('PSO_PID') % Run the simulink file "Project_sim.sim"
plot(ef.time,ef.signals.values)
grid on
P
I
D
minISE

```

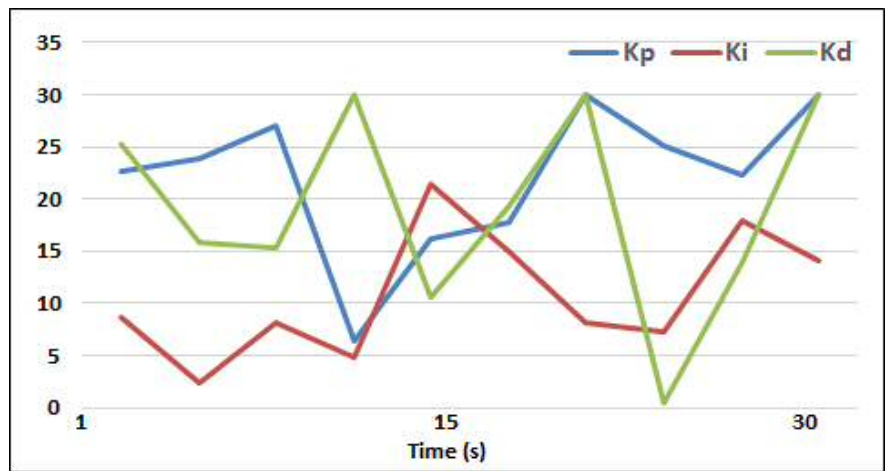


Figure A3.2.1. PSO-online optimization of the PID gains with the load disturbance for 30s iteration time.

A3.3 Impact of Parameters uncertainties in the simplified GB power system.

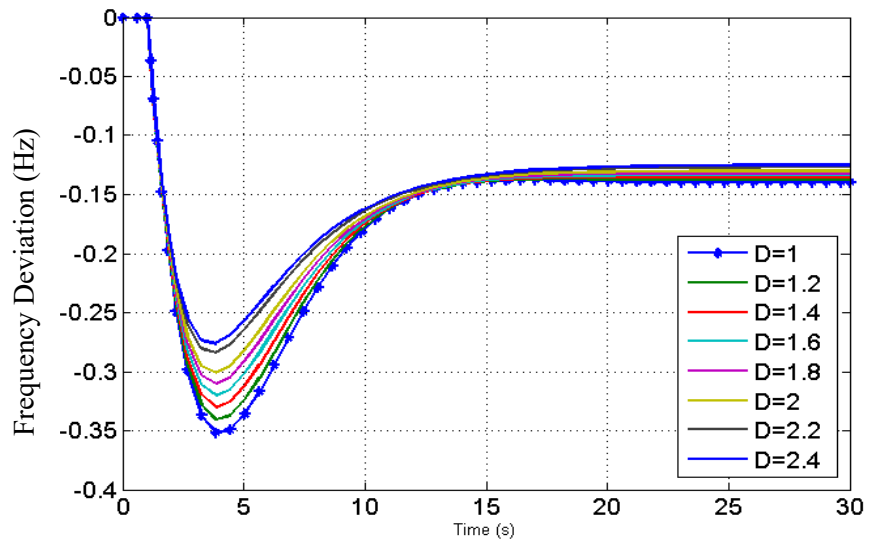


Figure A3.3.1 Frequency response of GB power system with different values of damping coefficient D without secondary frequency control.

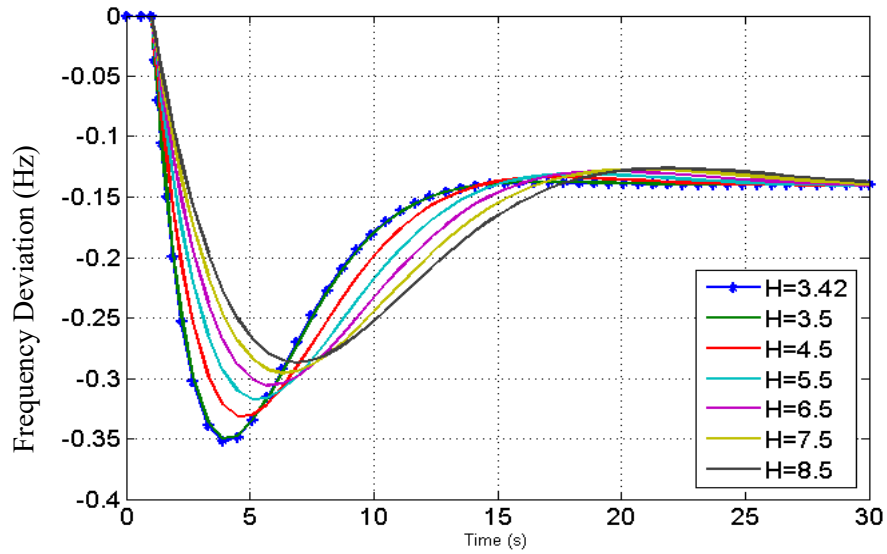


Figure A3.3.2 Frequency response of GB power system with different values of system inertia coefficient H without secondary frequency control.

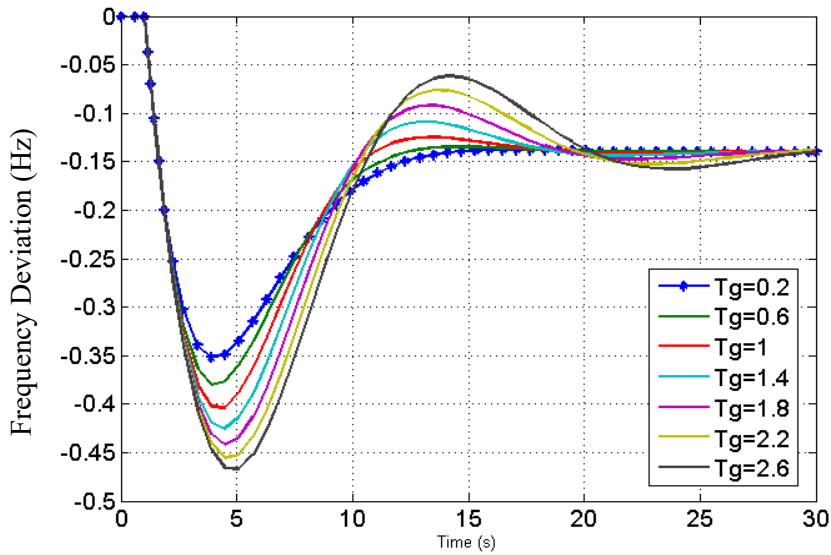


Figure A3.3.3 Frequency response of GB power system with different values of governor time constant T_g without secondary frequency control.

A4. Control of a Population of Water Heaters

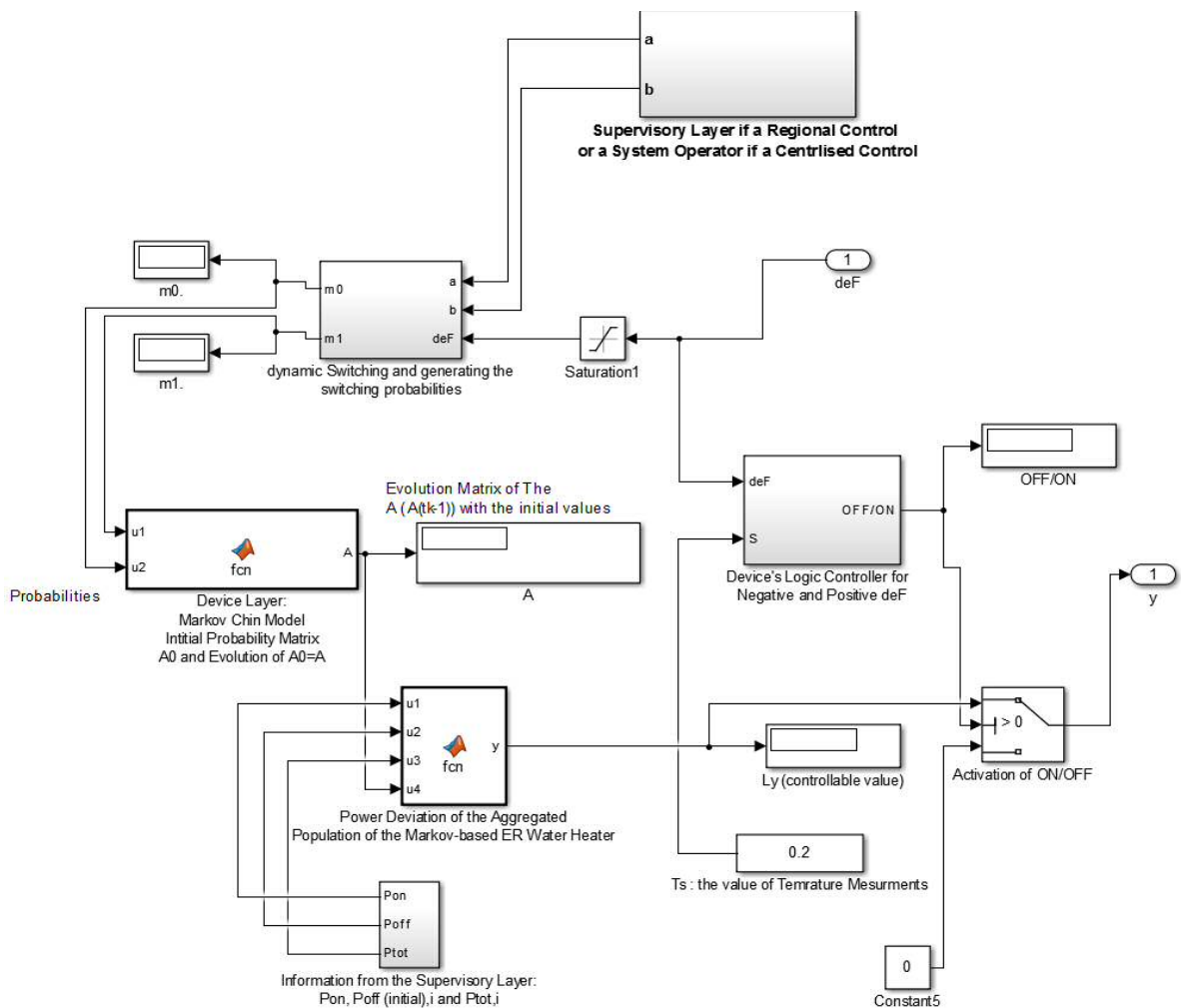


Figure A4.1. MATLAB design of a population of Water Heaters.

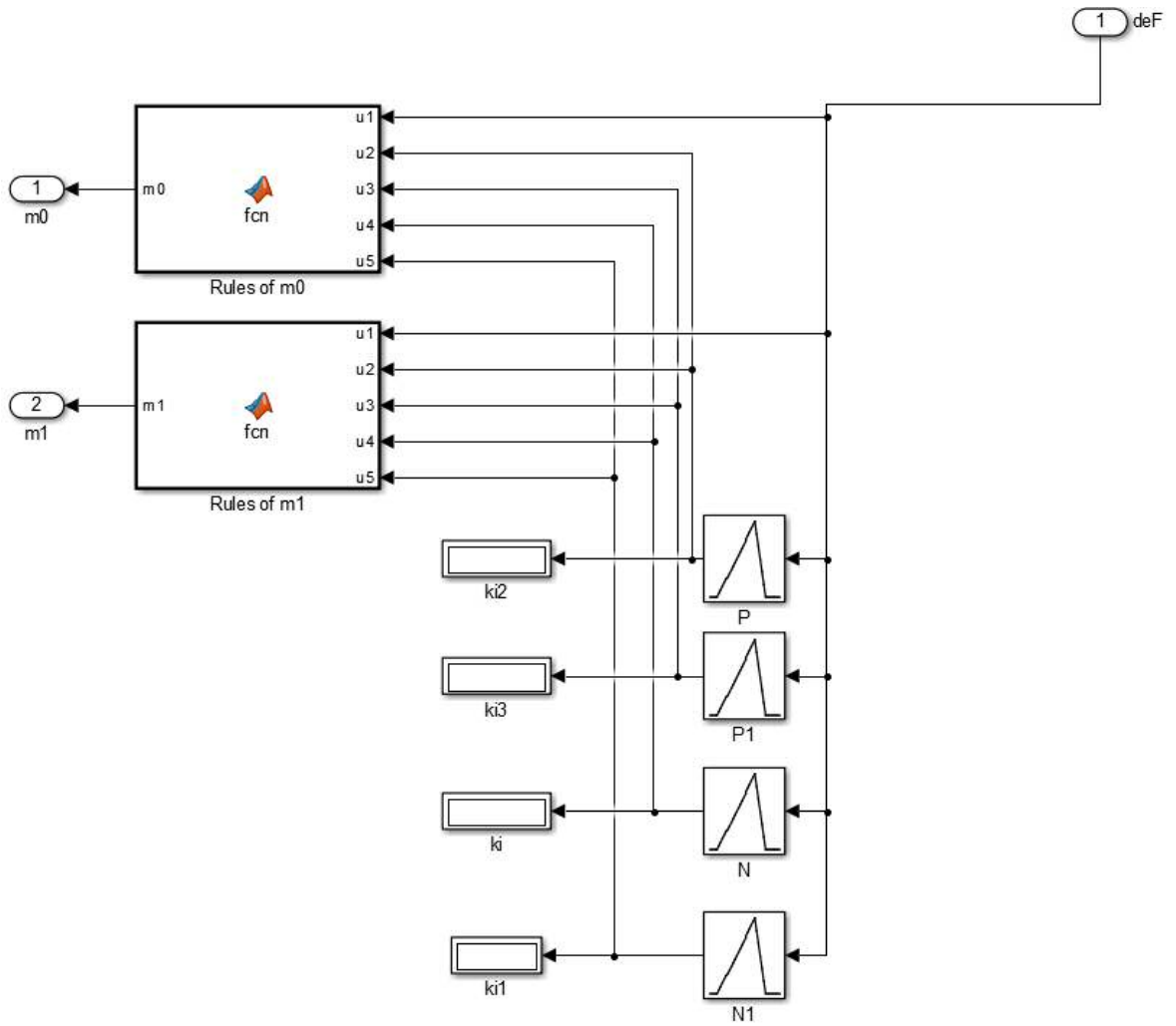


Figure A4.2. Dynamic switching of devices to generate the switching probabilities.

A5: Control of a population of BESSs

A5.1 The MATLAB code for modeling the switching of controllable BESSs during frequency event.

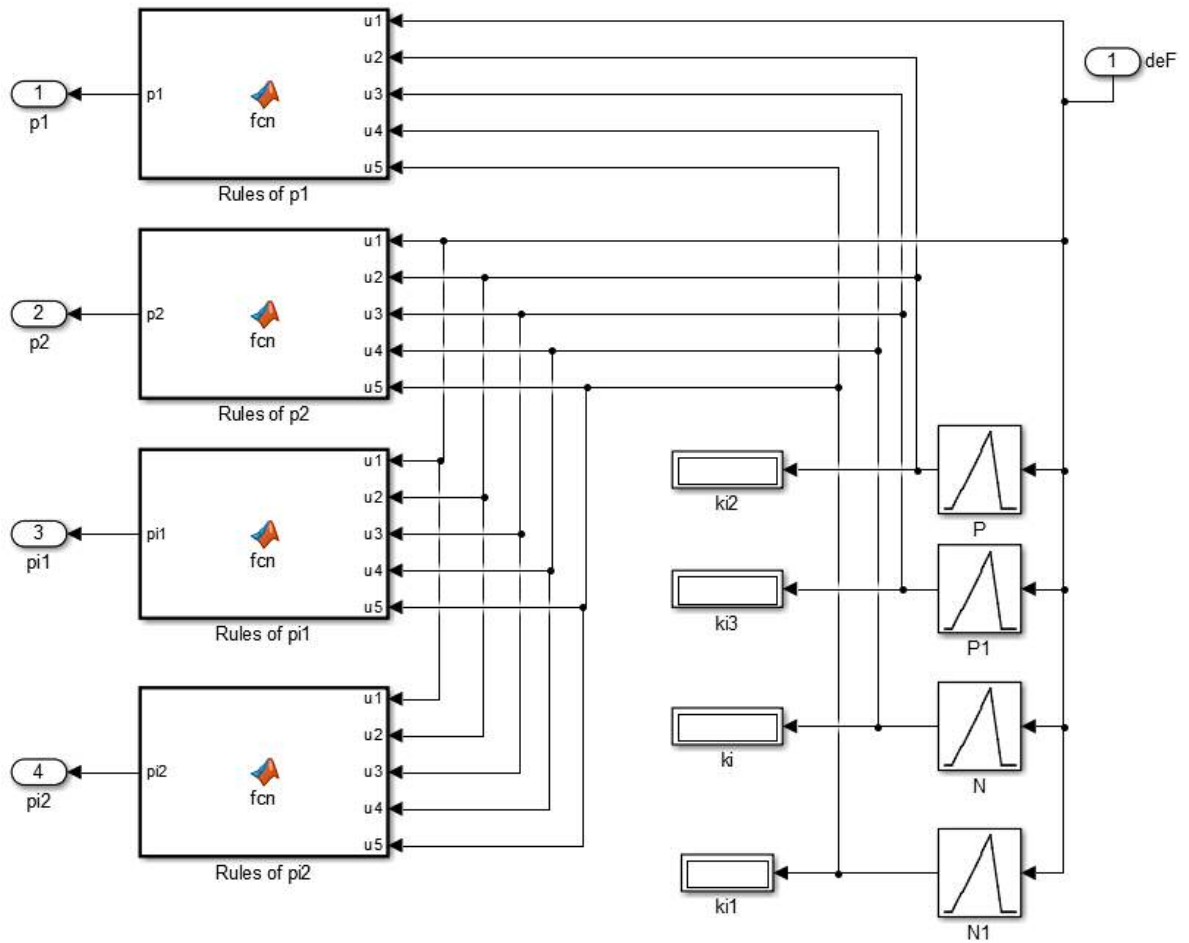


Figure A5.1. Dynamic switching of devices to generate the switching probabilities of controllable BESSs.

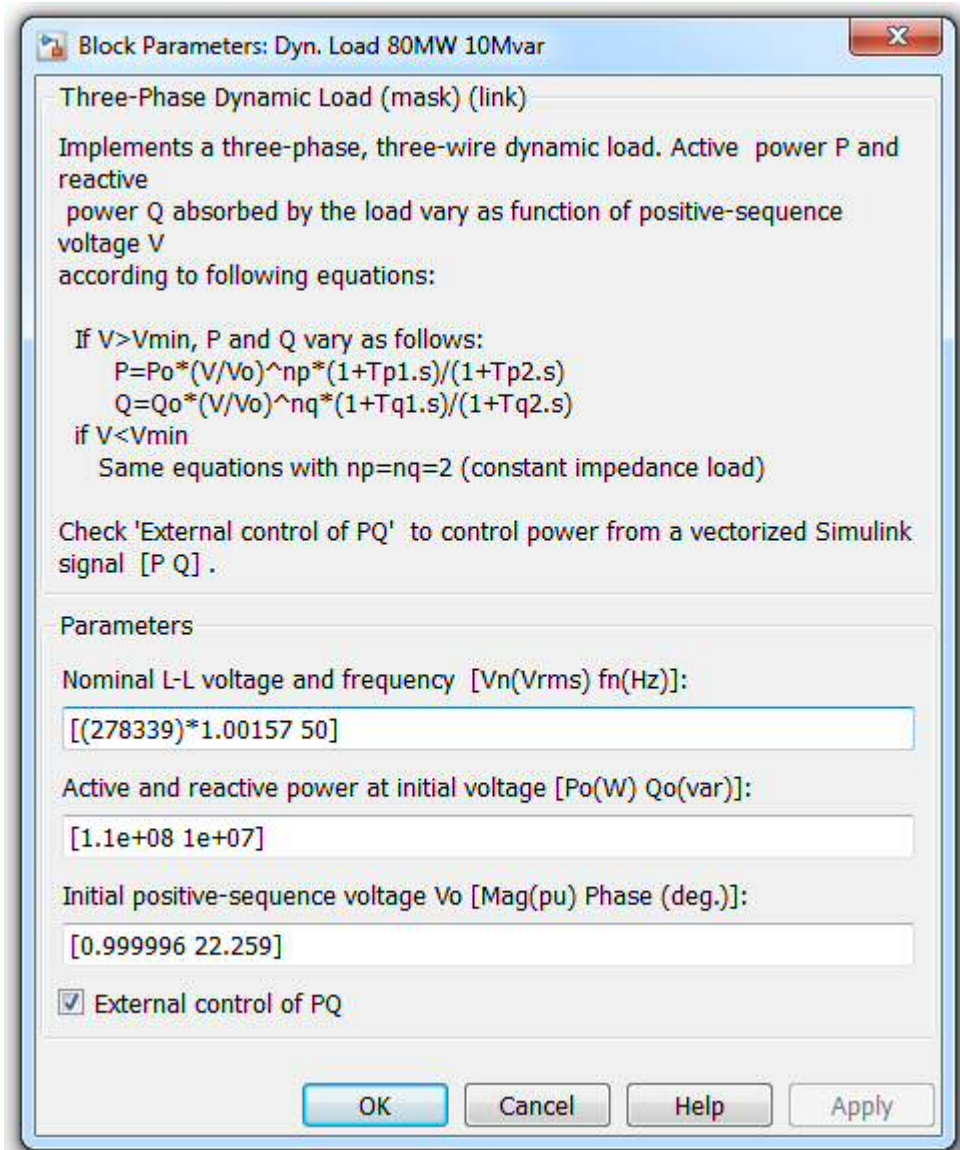


Figure A5.2. Showing the parameters threee-phase dynamic load with an eternal PQ control signal, it was used in Chapter 4 and Chapter 5 for the integration of controllable aggregated load.